DISSERTATION

AN ANALYSIS OF THE PHYSIOLOGY AND ENVIRONMENTAL INTERACTIONS THAT INFLUENCE SPECIES-SPECIFIC TRANSPIRATION ESTIMATES

Submitted by

David Michael Barnard

Department of Horticulture and Landscape Architecture

In partial fulfillment of the requirements

For the Degree of Doctor of Philosophy

Colorado State University

Fort Collins, Colorado

Fall 2014

Doctoral Committee:

Advisor: William L. Bauerle

Daniel Binkley
José L. Chávez
Patrick H. Martin

ABSTRACT

AN ANALYSIS OF THE PHYSIOLOGY AND ENVIRONMENTAL INTERACTIONS THAT INFLUENCE SPECIES-SPECIFIC TRANSPIRATION ESTIMATES

Transpirational water loss from vegetation constitutes a major component of the global hydrologic cycle; influencing energy balance and carbon cycling at multiple scales. At the leaf level, the control of transpiration is partitioned between environmental demand and physiological mechanisms that regulate water loss while allowing adequate carbon uptake for photosynthesis (A_n). Since the development of the Penman-Monteith potential evaporation equation, numerous research studies have focused on improving transpiration predictions over a range of spatial and temporal resolutions. Currently, efforts to predict transpiration must strike a balance between the predictive accuracy of complex models and the ease of implementation of generalized models. An example of a complex and accurate model is MAESTRA, a framework that uses an iterative leaf energy balance approach to simultaneously solve for A_n, stomatal conductance (g_s), and transpiration - linking g_s and A_n to account for the physiological mechanisms that regulate species specific water loss. The over-arching goal of this dissertation was to break MAESTRA down into its constituent physiological and environmental components while retaining transpiration predictive accuracy; distilling the large number of model inputs down to a few key parameters to reduce the time and labor of model parameterization.

In Chapter 2 of this dissertation, my first goal was to calibrate and validate MAESTRA on a species-specific basis for five tree species and then, using the range of physiology values measured among species, perform a sensitivity analysis to identify key parameters for

transpiration predictive accuracy. Two parameters from the Ball-Berry-Leuning g_s sub-model emerged as particularly important with a >20% influence on transpiration estimates: g_0, the minimum g_s as $A_n \rightarrow 0$ and g_1 the marginal cost of water per unit of carbon gain. I then illustrated how the influence of g_0 increases substantially under lower light conditions (up to a 70% effect) while never decreasing below 20% in high light conditions. Finally, I assessed the accuracy of the traditional method of obtaining g_0 (i.e. as an extrapolated intercept of a linear regression fit to A_n-g_s data collected in well-lit conditions) compared to g_0 values measured with a hand-held porometer in the absence of light. I found that regression derived g_0's underestimated leaf minimum g_s. Moreover, MAESTRA was more accurate, in comparison to measured transpiration, when parameterized with the observed values of g_0 instead of g_0 values obtained from the regressions (root mean square error from modeled-versus-measured regressions of 0.0067 and 0.0410 g m^{-2} s^{-1} respectively).

The third chapter of my dissertation focused on within canopy variation in wind speed and its influence on leaf energy balance, boundary layer conductance (g_{bV}) and transpiration estimates. I found that α, an exponential coefficient that ranges from 0-3 to describe the decrease in wind speed with depth into the canopy, varied among species and over the season. The development of canopy leaf area index (*LAI*) was closely linked with seasonal changes in α among species, but a simple empirical model that also included leaf width (L_w) and canopy height was a better predictor (R^2 = 0.77 and 0.92 for LAI and the empirical model respectively). Maximum g_{bV} in the early season ranged from ~2 to 3.5 mol m^{-2} s^{-1} among the study species and declined steadily as the canopy *LAI* increased to ~0.5 to 1.0 mol m^{-2} s^{-1}. The resulting Ω values (a ratio between g_{bV} and g_s that describes how well vegetation is coupled to the environment) followed a similar albeit inverted parabolic trend to the evolution of g_{bV}. Finally, I completed a

theoretical exercise using the validated model sets from Chapter 2 to determine the influence of a discrete increase in wind speed (0.6 to 2.4m s^{-1}) over a variety of environmental conditions. The influence of wind speed on transpiration ranged from -30 to 20%, varying with other environmental conditions.

The third chapter of my dissertation served as a culmination of the first two chapters; implementing MAESTRA as a real-time irrigation scheduling tool in a container grown tree nursery. I compared the performance of trees irrigated by species-specific MAESTRA parameterization to trees that were irrigated with a substrate moisture sensing method. Trees grown with the MAESTRA based irrigation produced 11-53% greater leaf area and 3.4-11% greater stem caliper with 18-56% more water applied than the moisture sensing method. Irrigation application efficiency was lower in the MAESTRA based method (80.1% compared to 89.5% for the sensing-based method), but both methods were within the range of suggested best management practices. After the season of irrigation scheduling was completed, I performed post-hoc model runs to determine how much accuracy would have been lost from estimates of species-specific irrigation if generalized multi-species physiological parameter means were used instead. By limiting species-specific parameterization to g_0 and g_1 alone, transpiration estimates could be within 10% error > 65% of the time and within 20% error > 95% of the time.

Overall, my dissertation had three main conclusions: (1) g_0 and g_1 are the two most important parameters for predicting transpiration with linked A_n-g_s modeling schemes, and that the ease of obtaining g_0 using simple hand held equipment should facilitate improved species-specific parameter values for modeling efforts at multiple scales, (2) the influence of wind speed on transpiration ranges from -20 to 30% and accurate representation of within canopy wind variability is necessary for accurate representation of g_{bV} and leaf energy balance (3) the

complexity of MAESTRA transpiration estimates can be greatly reduced by focusing efforts on accurate representation of g_0 and g_1, which will possibly allow for MAESTRA to be an effective yet realistic and scalable irrigation scheduling tool.

ACKNOWLEDGMENTS

This dissertation was completed only with the substantial help and input from others. First, I would like to thank Bill Bauerle, my advisor, for his genuine concern for my education and a desire to provide me with an excellent experience in earning my Ph. D. Dan Binkley, Jose Chavez and Patrick Martin deserve special thanks for their involvement on my Ph. D. committee. I am also grateful to Tom Demaline, the owner of Willoway Nursery for providing ample work space and nursery resources and to Tim Cullinan for his tireless assistance. Elsewhere in Ohio, the Great Lakes Brewery is owed thanks for how motivational the anticipation of a cold Burning River can be to get through a long hot day under the Ohio sun. I also owe thanks to David Kohanbash at Carnegie Melon for helping with computer automation and to the folks at Decagon Devices for technical support. Here at CSU I owe a large thanks to Dan Banks for his dedication to the art of field work and endless enthusiasm for the mundane tasks it entails. I also want to thank Alex Daniels for assistance with automating large numbers of model runs in MAESTRA. I have much appreciation and love for my mother and father both for their bottomless well of love and support and to my uncle Chuck, for his insightful, if not entirely cynical, advice. I also would like to thank my climbing partners Blake Miner, John Pedrosa and John Klooster whom have all provided days of needed relief through the voluntary self-flagellation that is alpine climbing and ski mountaineering. Finally, to my wife Becky I am the most grateful. The magnitude of your love and support is without comparison.

TABLE OF CONTENTS

Chapter 1: Introduction

"What we observe is not nature itself, but nature exposed to our method of questioning."

-Werner Heisenberg, Physics and Philosophy: The Revolution in Modern Science

Background

The exchange of mass and energy between vegetation and the atmosphere follows a suite of biophysical and physiological principles that can be assembled into mathematical models. One such assemblage is MAESTRA, a spatially-explicit and semi-mechanistic model capable of resolving flux estimates in three dimensions (Wang and Jarvis, 1990; Medlyn, 2004). The MAESTRA model follows an iterative procedure that uses estimates of leaf level energy balance, net photosynthesis (A_n), stomatal conductance (g_s), and measured meteorology to scale up to estimates of canopy fluxes of mass and energy exchange (Wang and Jarvis, 1990). The A_n predictions are derived from the mechanistic biochemical sub model developed by Farquhar and von-Caemmerer (1980) and input in the Ball-Berry-Leuning (BBL) g_s model (1995) for predictions of stomatal conductance defined as:

$$g_s = g_0 + \frac{g_1 A_n}{(c_s - \Gamma)\left(1 + \frac{VPD}{D_0}\right)} \tag{1}$$

where g_0 is the minimum g_s value defined as g_s as $A_n \rightarrow 0$ as leaf absorbed light $\rightarrow 0$, g_1 is the marginal water cost per unit carbon gain, c_s and VPD are the [CO_2] and vapor pressure deficit at the leaf surface respectively, Γ is the CO_2 compensation point (where CO_2 production from cellular respiration is equal to that fixed by photosynthesis), and D_0 is an empirical coefficient. The BBL model has been subjected to decades of validation, and is often deployed in other

model assemblages that predict water and carbon flux at scales from the leaf to the globe (e.g., Ball et al., 1987; Leuning, 1995; Sellers et al., 1996; Bauerle et al., 2004; Oleson et al., 2013).

Integral to accurate model predictions is accurate characterization of input parameters and a thorough understanding of their function and impact within the model (Reynolds and Acock, 1985). However, due to the time and resources involved in acquiring each parameter, there is a need to understand which parameters have the greatest impact on model output and how their influence varies with regard to changes in environmental conditions. The purpose of this dissertation was to investigate MAESTRA model formulation and identify key parameters that influence transpiration predictions. The linked A_n-g_s formulation of MAESTRA is similar to larger scale models (e.g., SiB2 or CLM; Sellers et al., 1996; Oleson et al., 2013 respectively) making the results of this dissertation applicable at larger scales. Additionally, the strength of the MAESTRA model lies in its predictive and semi-mechanistic formulation that can account for changes in environmental conditions in real time. For example, wind speeds can vary greatly over the day and with depth into the canopy. Hence, the second goal of this dissertation was to characterize the vertical gradient in wind speed in tree canopies and to quantify the influence that wind has on leaf boundary layer conductance, heat exchange and transpiration. Finally, the knowledge gained in executing the first two goals of this dissertation was used to initiate a real-time irrigation scheduling tool that uses MAESTRA estimates of transpiration to automatically determine irrigation volumes among tree species.

General research methodology

This research was undertaken as part of a five year grant awarded from the USDA, Specialty Crops Research Initiative (SCRI). The majority of this research was completed at

Willoway Nurseries Inc. located near Avon, OH, USA. Willoway is a large nursery (ca. 900 acres) and utilizes a pot-in-pot production system for the majority of their ornamental tree production. The owner of Willoway has also implemented a successful waste water recapture system and is invested in water resource conservation. Supplemental studies have been completed at the Colorado State University Horticulture Field Research Lab, campus greenhouses, and at USDA research greenhouses.

The first summer of research (2010) was devoted to characterizing the physiology, morphology and canopy aerodynamics of 10 tree species with economic and ecological significance. Canopy aerodynamic measurements were carried over into the second growing season with the intent of improving the spatial resolution of the canopy wind profile. The second year was also devoted to utilizing knowledge gained through modeling exercises to calibrate and validate MAESTRA for five of the ten species physiologically characterized in the first year. Calibration and validation were accomplished by the use of the water balance method (water used per tree = water applied – water leached). A thorough description of this large-container water balance research site is available in Zhu et al. (2005). Once validated, I implemented MAESTRA in the third summer (2012) to control irrigation in real time for five tree species. The fourth summer involved minor studies to supplement present data and post-hoc model runs and data analysis.

References

Ball, J., Woodrow, I. and Berry, J., 1987. A model predicting stomatal conductance and its contribution to the control of photosynthesis under different environmental conditions. In: J. Biggins (Editor), Progress in Photosynthesis Research. Martinus Niijhoff, Dordrecht, Netherlands, pp. 221-224.

Bauerle, W.L., Bowden, J.D., McLeod, M.F. and Toler, J.E., 2004. Modeling intra-crown and intra-canopy interactions in red maple: assessment of light transfer on carbon dioxide and water vapor exchange. Tree Physiology, 24(5): 589-597.

Farquhar, G.D., Caemmerer, S. and Berry, J., 1980. A biochemical model of photosynthetic CO_2 assimilation in leaves of C_3 species. Planta, 149(1): 78-90.

Leuning, R., 1995. A critical appraisal of a combined stomatal-photosynthesis model for C_3 plants. Plant, Cell & Environment, 18(4): 339-355.

Medlyn, B., 2004. A maestro retrospective. Forests at the Land–Atmosphere Interface. CAB International: 105-121.

Oleson, K. et al., 2013. Technical description of version 4.5 of the Community Land Model (CLM), NCAR Technical Note NCAR/TN-503+STR, pp. 420.

Reynolds, J.F. and Acock, B., 1985. Predicting the response of plants to increasing carbon dioxide: a critique of plant growth models. Ecological Modelling, 29(1): 107-129.

Sellers, P. et al., 1996. A revised land surface parameterization (SiB2) for atmospheric GCMs. Part I: Model formulation. Journal of Climate, 9(4): 676-705.

Wang, Y. and Jarvis, P., 1990. Description and validation of an array model—MAESTRO. Agricultural and Forest Meteorology, 51(3): 257-280.

Zhu, H. et al., 2005. A new system to monitor water and nutrient use in pot-in-pot nursery production systems. Journal of Environmental Horticulture, 23(1): 47-53.

Chapter 2: The implications of minimum stomatal conductance on modeling water flux in forest canopies

Overview

Stomatal conductance (g_s) models are widely used at a variety of scales to predict fluxes of mass and energy between vegetation and the atmosphere. Several g_s models contain a parameter that specifies the minimum g_s estimate (g_0). Sensitivity analyses with a canopy flux model (MAESTRA) identified g_0 to have the greatest influence on transpiration estimates (seasonal mean of 40%). A spatial analysis revealed the influence of g_0 to vary (30-80%) with the amount of light absorbed by the foliage and to increase in importance as absorbed light decreased. The parameter g_0 is typically estimated by extrapolating the linear regression fit between observed g_s and net photosynthesis (A_n). However, our measurements demonstrate that the g_s-A_n relationship may become nonlinear at low light levels and thus, extrapolating values from data collected over a range of light conditions resulted in an underestimation of g_0 in *Malus domestica* when compared to measured values (20.4 versus 49.7 mmol m^{-2} s^{-1} respectively). In addition, extrapolation resulted in negative g_0 values for three other woody species. We assert that g_0 can be measured directly with diffusion porometers (as g_s when $A_n \leq 0$), reducing both the time required to characterize g_0 and the potential error from statistical approximation. Incorporating measured g_0 into MAESTRA significantly improved transpiration predictions versus extrapolated values (6% overestimation versus 45% underestimation respectively), demonstrating the benefit in g_s models. Diffusion porometer measurements offer a viable means to quantify the g_0 parameter, circumventing errors associated with linear extrapolation of the g_s-A_n relationship.

Introduction

Leaf stomatal conductance (g_s) changes in response to physiological signals and environmental conditions to balance carbon assimilation with water loss (e.g. Wong et al., 1979). Hence, the ability to accurately predict the g_s response to changes in environmental conditions is central to estimating carbon and water flux at multiple scales. Damour et al. (2010) recently compared 35 g_s models that ranged from phenomenological to semi-mechanistic. Of the 35 models, the Ball, Woodrow and Berry (1987) model (BWB), later modified by Leuning (1995) (BBL), has been subjected to decades of testing and validation (e.g., Ball et al., 1987; Leuning, 1990; Leuning, 1995; Nijs et al., 1997; Medlyn et al., 2001; Katul et al., 2010; Way et al., 2011). Relative to other g_s models, the BWB is easier to apply and requires only four input parameters. The ease of parameterization and predictive accuracy under variable environments make the BWB g_s model commonly used at a variety of scales (e.g., Baldocchi and Meyers, 1998; Cox et al., 1998; Battaglia et al., 2004; Hanson et al., 2004; Sato et al., 2007; Friend et al., 2009; Damour et al., 2010; Landsberg and Sands, 2010), including large scale land surface schemes (e.g. Sellers et al., 1996; Oleson et al., 2010).

The BWB, and more recent BBL model, have semi-mechanistic predictive capabilities that scale g_s linearly with foliage net photosynthesis (A_n) in lieu of a direct response of the stomata to absorbed solar radiation at the leaf-level (PAR_L) (Zeiger, 1983; Pieruschka et al., 2010). For this study, we opted to use the BBL model because it has been shown to be more effective at closing the carbon budget when compared to the BWB (Way et al., 2011). The Leuning (1995) modification to the BWB model substituted vapor pressure deficit (VPD) for humidity, accounting for air temperature, and added the CO_2 compensation point (Γ), to estimate g_s as:

$$g_s = g_0 + \frac{g_1 A_n}{(c_s - \Gamma)\left(1 + \frac{VPD}{D_0}\right)} \quad (1)$$

where c_s and VPD are [CO_2] and vapor pressure deficit at the leaf surface respectively, D_0 and g_1 are empirical coefficients and g_0 characterizes the basal g_s prediction. It is common to see g_0 defined in one of two ways: (1) as a "fit" parameter – an extrapolated intercept from the least squares regression between g_s and model parameters (e.g., Ball et al., 1987; Ball, 1988; Collatz et al., 1991; Medlyn et al., 2011; Way et al., 2011) or (2) as the value of g_s when $A_n \leq 0$ (e.g., Leuning, 1990; Leuning, 1995; Dewar, 2002; Lombardozzi et al., 2012). Although these two definitions are similar, it is the second description that links a physiological significance to g_0 and implies that the parameter can be measured directly. Curiously, even the studies that define g_0 by the second definition have estimated the parameter value from the relationship between g_s and model parameters. Because model parameters vary among formulations (Ball et al., 1987; Leuning, 1995; Medlyn et al., 2011) and become irrelevant when $A_n \leq 0$, we use the term g_s-A_n as a surrogate for the relationship between g_s and model parameters. Nevertheless, no study that we are aware of has compared observed and extrapolated values of g_0 when parameterizing the BWB or BBL models or the effect of the two different parameterization methods on the accuracy of model estimates.

Several potential sources of error can underlie statistical estimations of g_0. First, data for the g_s-A_n regression are often collected mostly under well-lit conditions with a well-stirred cuvette that disrupts boundary layer conditions (Ball, 1988; Leuning, 1990; Collatz et al., 1991; Leuning, 1995; Dewar, 2002; Medlyn et al., 2011; Way et al., 2011). Second, in the original BWB description, Ball (1988) acknowledged that the g_s-A_n relationship, in low light, may deviate from the linear relationship. Despite this observation, Ball used an extrapolated g_0 that

was “not statistically different from zero” for parameterizing the C_3 species *Glycine max* while noting higher observed values. Likewise, Collatz et al. (1992) reported that observed g_0 was greater than extrapolated values in the C_4 species *Zea mays*. Third, it is common to see extrapolated values of g_0 that are not biophysically possible (i.e. negative values) (Ball and Farquhar, 1984; Schulze et al., 1987; Shimono et al., 2010; Medlyn et al., 2011). Fourth, when the same data set is used to parameterize different g_s models (e.g., the BWB versus the BLB) the resulting extrapolated values of g_0 can differ significantly (Way et al., 2011). Lastly, least squares estimates can be greatly influenced by the quantity and/or quality of data points used to perform the regression. This can be particularly vexing in studies of the g_s-A_n relationship as data collection can be time-consuming due to the stomatal equilibration period (up to 15 minutes per data point (Franks and Farquhar, 1998; Woods and Turner, 2006)), and the need for multiple data points to extrapolate a single g_0 estimate with acceptable error.

A growing consensus in the literature acknowledges nighttime g_s across species (e.g., Donovan et al., 2003; Barbour and Buckley, 2007; Howard and Donovan, 2007; Seibt et al., 2007; Christman et al., 2008) and plant functional types (PFTs) (reviewed in Caird et al., 2007), whereas a consistent g_0 response to water stress has been lacking. The use of observed nighttime g_s for g_0 parameterization in g_s models has not yet been recognized and may represent a significant disconnect between plant physiology studies and ecological modeling efforts. Currently, when not extrapolated from g_s-A_n data, g_0 values in g_s models are assumed to be constant and/or unrealistically low (e.g., Sellers et al., 1996; Wang and Leuning, 1998; Tuzet et al., 2003; Oleson et al., 2010; Ono et al., 2013). The relative ease of measuring g_s under dark conditions (i.e. when $A_n \leq 0$) with a diffusion porometer may improve on g_0 estimates,

warranting a reexamination of how g_0 is characterized, how g_0 may respond to seasonal drought episodes and the extent to which observations of g_0 affect whole canopy transpiration estimates.

In this study we set out to characterize g_0 at the leaf-level, using nighttime *in-situ* observations, in response to season and water stress. We hypothesized that the g_0 parameter could be measured and used to improve predictions of canopy transpiration in deciduous species. We scaled up observed g_0 values from the leaf to the canopy with MAESTRA, a 3-dimensional process based canopy transpiration model that can successfully predict forest canopy transpiration (Bauerle et al., 2004a; Hanson et al., 2004; Medlyn et al., 2005; Medlyn et al., 2007; Bowden and Bauerle, 2008). We used MAESTRA, validated on a species-specific basis, as a tool to spatially investigate how g_0 influences canopy transpiration estimates and responds to changes in the environment.

Materials and Methods

Site characteristics and plant material

The main design of this study included two separate research sites (Table 2.1). One, located in Avon, OH, was utilized to parameterize and validate MAESTRA and the other, located in Fort Collins, CO, was constructed to monitor the drought and seasonal response of g_0 (growing season was day of year 167-271). A third, supplemental glass house study, took place in Fort Collins, CO (see description below). A full description of the site design for the OH site can be found in Zhu et al. (2005). Briefly, the OH site was subdivided into six plots, each containing 25 subsurface 57 L socket containers (a pot-in-pot production system). Five sockets comprised each row (five rows per plot), connected in series via PVC to channel container leachate into a tipping bucket (FC525, Texas Electronics Inc., Dallas, TX, USA). Tipping bucket

tips were continuously counted and recorded at 1 minute intervals (model CR23X, Campbell Scientific, Logan UT, USA). Additionally, one socket per row was equipped with a Theta Probe substrate moisture sensor (model ML2x, Dynamax Inc. Houston, TX, USA) to determine bulk container substrate electric permittivity (ε_a). A two-point calibration, specific to the substrate used in this study, was completed to allow for ± 1% volumetric water content (VWC) measurement accuracy. Environmental variables (temperature, wind speed, relative humidity, precipitation and incident photosynthetically active radiation (PAR_I) were measured every minute and averages stored at 5-minute intervals (model EM50R, Decagon Devices Inc., Pullman, WA, USA).

In the OH study we used four tree species with broad ecological and commercial significance (*Acer rubrum* L. 'Red Sunset', *Betula nigra* 'Cully', *Carpinus betula* 'Columnaris' and *Cercis canadensis*) in 57 L containers. One year old whips were potted into a soil-less organic substrate consisting of a mixture of 64% pine bark, 21% peat moss, 7% Haydite, and 7% sterilized regrind. The remaining 1% was slow release fertilizer 12-0-42 (Agrozz Inc., Wooster, OH, USA). For irrigation, each container had two 180° spray stakes (PC Spray Stake, Netafim Inc., USA, Fresno, CA, USA) operating at a flow rate of 12 L h^{-1}. Substrate moisture status was continually monitored and kept within a VWC range of 35-42% (VWC >43% was predetermined to exceed the maximum container substrate water holding capacity).

The CO site consisted of eight rows of five replicates each in a pot-in-pot system. The same plant material was studied at the CO and OH site, except *Quercus rubra* replaced *Acer rubrum* L. 'Red Sunset' at the CO site to broaden the among-species range in growth rates and physiological properties. All else being equal, the CO trees were one year older than those in OH and were top-dressed with time release fertilizer (18-5-9, Osmocote Classic; The Scotts Co.,

Marysville, OH, USA) at the beginning of the season. For the CO water stress study, five replicates each per species were assigned randomly to either well-watered or water-stressed treatments and each treatment was randomly assigned to a uniformly irrigated row. Replicate trees assigned to the well-watered treatment were irrigated to maintain a VWC between the ranges of 35-42% – checked weekly with a hand-held Theta Probe. Water deficit irrigation amounts were calculated as a percentage of the well-watered treatment and consisted of the following irrigation amounts held for 10-14 days each: 100%, 80%, 60%, 40%, 20%, and 0%. This irrigation schedule included occasional returns to well-watered status (100%) in an effort to characterize the underlying effect that water deficits may have on g_0.

Measurements of g_0 and g_s

All g_s and g_0 measurements were collected with hand-held steady-state diffusion porometers (SC-1, Decagon Devices Inc., Pullman, WA, USA) on three randomly selected trees per treatment per species. The parameter g_0 in the BBL g_s models is defined by Leuning (1995) to be g_s as $A_n \rightarrow 0$ as $PAR_L \rightarrow 0$. Using this definition as justification, we sought to investigate the influence of observed g_0 (g_s measured under dark conditions – one h after nightfall) on model output as opposed to statistically derived estimates. Midday g_s measurements were collected on the same leaves as g_0 near solar noon on concurrent cloudless days. Both midday g_s and g_0 measurements at the CO site were collected ten times over the course of the season (day of year 167-271) from two leaves per tree and averaged. All leaves sampled were fully expanded and from south facing sun-exposed branches. At the OH site, g_0 was measured similar to the trees in CO (three times during the season - day of year 155, 208 and 235).

Model Parameterization

A full description of MAESTRA is beyond the scope of this paper, however, significant background information, as well as equations, may be found in Bowden and Bauerle (2008) and Bauerle and Bowden (2011), with a full description of the leaf to crown transpiration linkage given in Medlyn et al. (2007). Briefly, MAESTRA is a hierarchical and iterative computational framework that spatially integrates estimates of leaf energy balance, photosynthesis and g_s by computing grid-point-specific fluxes of mass and energy throughout the entire crown. For g_s specifically, photosynthesis estimates (derived from the Farquhar photosynthesis model) are combined with meteorological variables and static leaf-level estimates of g_0, g_1, Γ and D_0 to calculate a g_s prediction via the BBL g_s model. The g_s prediction is then combined with meteorological variables in an isothermal form of the Penman-Monteith equation to compute latent heat exchange and a transpiration estimate. Because latent heat loss alters the leaf energy balance, initial energy balance estimates are then adjusted and the process is repeated iteratively until estimates reach convergence. This approach has been successfully implemented to predict transpiration fluxes in various models (e.g., Meyers and Paw U, 1987; Collatz et al., 1991; Baldocchi et al., 2002; Medlyn et al., 2007; Staudt et al., 2010).

Leaf-level physiological input parameters were determined primarily by the use of gas exchange analysis with a CIRAS-2 portable photosynthesis system (PP Systems International Inc., Amesbury, MA, USA). Bauerle and Bowden (2011) reported six parameters of high importance (>5% impact) when estimating transpiration. Therefore, a strong emphasis was placed on the careful acquisition of these parameter values (Table 2.2). Five of the parameters (maximum rate of carboxylation (V_{cmax}), maximum rate of electron transport (J_{max}), dark respiration (R_d), quantum yield (α), and genotype stomatal response coefficient (g_1)) are

determined through the analysis of photosynthesis versus CO_2 and light response curves constructed with the CIRAS-2. A sixth parameter, leaf width (L_w), was measured every other week throughout the growing season. The D_0 parameter was assumed to be 1500 Pa (Leuning, 1995; Bauerle and Bowden, 2011). Canopy and tree physical characteristics (canopy width in the *x* and *y* axes, canopy and stem height and stem caliper) were collected at the same time. We measured canopy leaf area (on alternating weeks) throughout the growing season by counting the total number of leaves in individual crowns and multiplying by the average area per leaf – determined by image analysis (Image-J, NIH, Washington, D.C., USA) on 20 randomly selected leaves from three separate randomly selected trees per treatment. We determined genotype specific leaf transmittance, absorptance and reflectance with a SPAD meter (SPAD-502, Konica Minolta Global, Ramsey, NJ, USA) on the same leaves measured for gas exchange, following the procedure in Bauerle et al. (2004b).

Model validation

We ran MAESTRA for weather data collected at one minute intervals and recorded on a five-minute time-step from the OH site to compute species-specific water use estimates over the season. To calculate measured water use, we subtracted daily leachate volume from the volume of water applied per treatment (irrigation + precipitation – leachate). We then compared weekly simulated and measured water use averages.

Simulation experiments

Once validated, we simulated stands that were parameterized with physiology from leaf-level gas exchange (as described above) for *Acer rubrum* (Table 2.2). Representative forest

stands consisted of 5 m stem spacing, 7.5 m live crown length plus 2.5 m of stem height, and a 5 m crown width shaped as a half-ellipsoid. Simulations aimed to investigate the impact of g_0 on transpiration estimates of an individual canopy within a forest. To investigate gradients in the parameter effect of g_0 on transpiration along a canopy depth profile, the canopy was separated into a three dimensional grid of 36 cells with equal volumes, for which point estimates of A_n, g_s, and transpiration were calculated. Whole canopy estimates were calculated as the sum of point estimates from the 36 sub-volumes. To determine the g_0 parameter effect on transpiration estimates we held all other input parameters constant and varied the g_0 parameter input from the measured mean value (42.57 mmol m^{-2} s^{-1}) ± one standard deviation (20.47 - 64.67 mmol m^{-2} s^{-1}). The parameter effect was then calculated as the absolute value of the difference between transpiration output from MAESTRA parameterized with the upper and lower standard deviations normalized by output from the mean value and then multiplied by 100.

To simplify the BBL model for the purposes of this study, and convey the influence of each portion separately, we condense the dynamic portion of the model (to the right of the addition sign that encompasses the g_s-A_n linkage) with a single term (βg_s) expressed as:

$$\beta g_s = \frac{g_1 A_n}{(c_s - \Gamma)\left(1 + \frac{VPD}{D_0}\right)} \tag{2}$$

This allows the BBL model to be separated into two constituent parts as:

$$\Sigma g_s = g_0 + \beta g_s \tag{3}$$

where Σg_s represents the total g_s prediction. Equation 2 illustrates that the βg_s component in the simplified version (Equation 3) of the BBL model is coupled to A_n – derived from the mechanistic Farquhar photosynthesis model (Farquhar et al., 1980).

Comparison of observed and extrapolated g_0 values

To illustrate the difference in transpiration estimates between observed g_0 and those derived by statistical estimation with the least squares fit to the g_s-A_n relationship, we acclimated one year old *Malus domestica* (n = 4) trees planted in 38 L containers with a commercial potting mix in a climate controlled glass house for seven days. Once acclimated, we collected data to parameterize MAESTRA (see description above). To characterize the g_s-A_n relationship in well-lit conditions, we collected measurements at PAR_L levels ranging from 200 to 1000 μmol m^{-2} s^{-1}. Preliminary tests indicated that stomatal equilibration took a maximum of 11 minutes at each light level, thus we allowed 12 minutes for g_s acclimation at each step. Stabilized readings were taken at 13, 14, and 15 minutes and averaged. To illustrate the fine-scale departure from linearity in the g_s-A_n relationship under low-light conditions, we observed g_s and A_n at PAR_L levels of 0, 25, 50, 75 and 100 following the same stomata acclimation procedure outlined above. Both the high and low-light measurements were completed in sequence on the same leaf to produce one single g_s-A_n relationship per replicate. The individual replicates were then pooled to derive an estimate of g_0. Estimates were determined as the x-y intercept of a linear regression between observed g_s and BBL model input parameters calculated as:

$$\frac{A_n}{C_s - \Gamma}\left(1 + \frac{VPD}{D_0}\right)^{-1} \tag{4}$$

Together with g_s-A_n characterization, each container was irrigated daily to container capacity, wrapped in plastic (to eliminate water loss to evaporation) and monitored gravimetrically at minute intervals with a series of scales (Adam CBK, Adam Equipment Inc., Bletchley Milton Keynes, UK). Water use was computed from 30-minute averages. Gravimetric water use and glass house environmental conditions were recorded for four continuous days (Decagon EM50R, Decagon Devices Inc., USA). Immediately after four days of continuous

gravimetric measurements, individual crown physical dimensions were recorded and leaves were removed, bagged, and scanned (Model 3100, Li-Cor Biosciences, Inc., Lincoln, NE, USA). MAESTRA was parameterized on an individual replicate basis and simulations were conducted on a 30-minute time step. MAESTRA simulated whole tree transpiration estimates were compared to 30-minute averages of gravimetric water use.

Results

Species, seasonal and drought response of g_0 and midday g_s

Seasonal means of g_0 differed significantly among species (P = 0.009 one-way ANOVA). Figure 2.1 shows that observations of g_0 did not change significantly over the course of the growing season in *Acer rubrum*, *Carpinus betula* or *Cercis canadensis* (P > 0.1 for all, repeated measures ANOVA), whereas *Betula nigra* had a significant seasonal change (P = 0.01). However, when the final measurement time-point is removed from the analysis, the seasonal response of *Betula nigra* was no longer significant (P = 0.34). Whole-season means between the droughted and well-watered treatments did not differ significantly in any of the species (P > 0.1 for all analyses, two sample *t*-test). However, the drought treatment means were lower for every species except *Carpinus betula*, which had a higher g_0 under drought conditions. There was not a significant interaction between water stress level and season in any species (P > 0.05). When all species were pooled, g_0 averaged 38.4 mmol m^{-2} s^{-1} and showed no significant response to drought (P = 0.79); but a significant curvilinear response of midday g_s to drought was observed (Fig. 2.2, P = 0.0036).

MAESTRA validation and g_0 investigations

In comparison to measured weekly transpiration, MAESTRA accurately estimated species-specific whole tree water use (Fig. 2.3). Root Mean Square Error (RMSE) of measured versus predicted transpiration ranged from 0.014 kg m^{-2} d^{-1} in *Acer rubrum* to 0.031 kg m^{-2} d^{-1} in *Betula nigra*. There was a general trend towards a slight overestimation of model estimates, evident by a Mean Bias Error (MBE) ranging from 0.031 kg m^{-2} d^{-1} in *Cercis canadensis* to 0.074 kg m^{-2} d^{-1} in *Carpinus betula*, however, transpiration was slightly biased towards underestimation in *Betula nigra* (MBE of -0.01 kg m^{-2} d^{-1}).

A sensitivity analysis demonstrated that g_0 was the most significant parameter for estimating seasonal canopy transpiration (Fig. 2.4a). The mean seasonal parameter effect of g_0 was 43.4% with a standard deviation of 9.5%. The analysis also showed the g_1 parameter to be highly significant with a mean of 25.2% and standard deviation of 4.1%. Alpha, V_{cmax} and J_{max} had significant impacts (> 5%) on transpiration estimates as well (Fig. 2.4a). Seasonal estimates of transpiration varied significantly when MAESTRA was parameterized with upper or lower bounds (mean ± one standard deviation) of measured g_0 values for *Acer rubrum* (Fig. 2.4b), but the estimates appear to be influenced more by the lower as opposed to upper bound value. Figure 2.4c illustrates the parameter effect of g_0 on daily estimates of water flux changes throughout the season.

When the canopy was separated into a three dimensional *x*, *y*, and *z* grid of equal sub volumes, there was strong spatial variation in the within-canopy g_0 parameter effect (Fig. 2.5). In simulated canopies with relatively low total leaf area index (LAI) (e.g., LAI = 2 m^2 m^{-2}), the effect was less pronounced, but as LAI increased (e.g., LAI = 5 or 10 m^2 m^{-2}) there was a large increase in the parameter effect with increasing depth into the canopy (Fig. 2.5). Regression

analyses revealed the parameter effect of g_0 to be strongly correlated with leaf absorbed PAR_L ($R^2 = 0.93$) and temperature ($R^2 = 0.72$). However, when the effect of leaf temperature (T_{leaf}) was tested in the absence of light there was no change in the g_0 parameter effect, indicating that PAR_L was driving the variation in parameter effect, not T_{leaf}.

The influence of g_0 is the greatest under low-light conditions, but it can still have a substantial parameter effect (~30%) under sparse foliage conditions (e.g., LAI < 2) and in portions of the canopy that remain well-lit (e.g., Fig. 2.5 LAI 5 and 10). Likewise, g_0 can have 100% of the control on g_s predictions when $A_n \leq 0$, but the g_0 parameter effect on Σg_s decreases to ~30% at PAR_L levels above ~400 μmol m^{-2} s^{-1} (Fig. 2.6). At lower PAR_L levels, A_n is usually below light saturation for C_3 foliage and the g_0 component becomes larger than βg_s, thus contributing to the majority of Σg_s. However, as PAR_L and A_n increase, the influence of βg_s increases and g_0 and βg_s converge at a species-specific threshold PAR_L level (~125 μmol m^{-2} s^{-1}, in the case of red maple). At ~125 μmol m^{-2} s^{-1}, each contributes exactly 50% to Σg_s. As leaf PAR_L absorption continues to increase above the threshold light level, βg_s then has the majority of influence on Σg_s.

Comparison of observed and estimated g_0 values

For the trees measured in OH, estimates of g_0 from least squares fits were significantly different than observed values ($P < 0.005$). Three species had negative values of g_0 from statistical estimates and the error range of the fourth species included a negative intercept (Table 2.2). In the fine-scale studies with *Malus domestica*, observed values of g_0 were ~150% larger than those derived from least squares estimates (Fig. 2.7). The inset in Figure 2.7 shows that the

g_0 estimates extrapolated from observed versus BBL model parameters (Equation 4) was not different than g_s-A_n g_0 estimates (cf. Fig. 2.7 and inset).

Comparison of observed and estimated g_0 canopy transpiration estimates

The MAESTRA model was more accurate when parameterized with observed values of g_0 as compared to g_0 values obtained from a least squares fit to the g_s-A_n relationship (RMSE of 0.0067 and 0.0410 g m^{-2} s^{-1} respectively). Over a four day period, total observed values of g_0 resulted in a slight overestimation (mostly occurring at night, see below) of water flux (6%), whereas the least squares derived g_0 value resulted in a ~41% underestimation of transpiration (MBE of 0.0003 and -0.0021 g m^{-2} s^{-1} respectively; Fig. 2.8). When error and bias estimate statistics (i.e. RMSE and MBE respectively) are partitioned into daytime and nighttime components, we found predictions from observed values to be overestimated at night (RMSE and MBE of 0.0089 and 0.0015 g m^{-2} s^{-1} respectively) versus extrapolated g_0 values (RMSE and MBE of 0.0028 and -0.0005 g m^{-2} s^{-1} respectively). During the daytime, however, observed g_0 input resulted in smaller transpiration estimate error and slight negative bias statistics (RMSE and MBE of 0.0022 and -0.0006 g m^{-2} s^{-1} respectively) as compared to extrapolated g_0 input values (RMSE and MBE of 0.0382 and -0.011 g m^{-2} s^{-1} respectively).

Discussion

Typically, g_0 has not been measured directly but has instead been defined as a fit value, extrapolated from a linear regression. Other studies have forgone the data collection required to characterized the g_s-A_n relationship (and thus g_0) and have instead assumed constant and often unrealistically low values for g_0. In this paper, we challenge these paradigms by showing how

the linear fit estimates of g_0 can yield erroneous canopy transpiration predictions and small errors in g_0 can have a substantial effect on transpiration estimates. We designed this study to have four primary objectives: (1) to characterize observed g_0 changes over an entire growing season in droughted and well-watered deciduous trees, (2) to validate a canopy transpiration model parameterized with leaf-level g_0 measurements, (3) to use the validated model to investigate the spatial influence of the g_0 parameter on water flux estimates in forest canopies, and (4) to test the hypothesis that MAESTRA parameterized with directly observed g_0 values would produce more accurate estimates of transpiration than if it were parameterized with g_0 values from statistical estimation.

The lack of a consistent g_0 response to drought (Figs. 2.1 and 2.2) conflicts with the findings of several other studies that have shown a decrease in g_0 under drought stress (Running, 1976; Cavender-Bares et al., 2007; Zeppel et al., 2011). We did, however, find a midday g_s water stress response (Fig. 2.2), suggesting that the drought response mechanisms that control midday g_s versus g_0 may not be linked. In several desert species, Ogle et al. (2012) also found that midday g_s and g_0 decouple, whereas Mott and Peak (2010) reported a coupled response for g_0 and g_s in the herbaceous species *Tradescantia pallida*. These two studies highlight the inconsistencies amongst reports attempting to explain the g_0 response. Moreover, they emphasize that no one causative environmental factor seems to explain the observed differences. Pressure probe studies have attempted to implicate guard cell mechanics as the source of species difference in g_0 (Franks and Farquhar, 1998; 2007), while observed g_0 variation within species has often been attributed to environment (Matyssek et al., 1995; Cavender-Bares et al., 2007; Howard and Donovan, 2007; Scholz et al., 2007; Zeppel et al., 2011). Figure 2.2 supports the hypothesis that inter-specific differences may be governed by guard cell mechanics by showing

that drought-induced minimum midday g_s (0% applied irrigation) is similar to our observed g_s under dark conditions. Another study investigating the response of understory leaves to sun flecks (Allen and Pearcy, 2000) determined that leaves with a higher g_0 can reach maximum photosynthesis faster than leaves that began at a lower g_0. Unknown however, is whether g_0 is homogenous throughout a forest canopy (especially large and complex canopies), if it varies along a canopy depth profile, or if it differs between sun versus shade leaves. To further understand g_0, within canopy variability and driving mechanisms should be investigated.

Over the course of an entire growing season, g_0 was by far the most influential parameter on water flux estimates in simulated tree canopies (Fig. 2.4a). Our three-dimensional analysis revealed (1) an increase in the parameter effect of g_0 with increasing canopy LAI and (2) an increasing parameter effect towards the center of individual crowns and forest canopies (e.g., Fig. 2.5). The spatially-variable transpiration response to g_0 may be explained by a gradient in environmental variables. Even though MAESTRA is a three-dimensional canopy model, it is unable to resolve within-canopy CO_2 concentration gradients and wind speed attenuation is calculated at each vertical-layer (i.e. in 2-dimensions). However, T_{leaf} and PAR_L are both resolved three dimensionally. Regression analyses revealed that these two factors are correlated with the g_0 parameter effect on transpiration estimates. To isolate the influence of T_{leaf} and PAR_L from one another we held one constant and varied the other over a realistic range, finding that both were correlated with the g_0 parameter effect. We then analyzed the canopy transpiration response in the absence of within canopy light variation and found the parameter effect of g_0 was not influenced by changes in T_{leaf}. Instead, the parameter effect remained steady at approximately 80% across a range of T_{leaf}. The lack of a T_{leaf} effect can be attributed to the difference in transpiration estimates when βg_s is zero ($PAR_L = 0$), thus leaving Σg_s entirely dependent upon g_0

over the tested range of T_{leaf} (Fig. 2.6). The lack of a g_0 response to T_{leaf} may appear counter-intuitive, but it is important to note that the magnitude of the g_0 parameter effect is inversely proportional to the contribution of βg_s to Σg_s. As the contribution of βg_s is driven by the magnitude of A_n (thus PAR_L) lower PAR_L levels create an environment where g_0 has the maximum influence on transpiration estimates.

Typically, g_0 has been parameterized by a linear least squares fit to the g_s-A_n relationship or to a linear fit between model parameters (Equation 4) and observed g_s (both of which produced similar intercepts in our fine-scale study in *Malus domestica* (Fig. 2.7)). Unfortunately, this statistical method is prone to errors (e.g., linear fits that result in negative values) (Ball and Farquhar, 1984; Schulze et al., 1987; Medlyn et al., 2011). Medlyn et al. [*Medlyn et al.*, 2011] provides a prime example of the error influence in a recent effort to reconcile empirical and optimal g_s theories into a simple theoretical framework when they attempt to drop g_0 from a form of the BBL model. The de-emphasis on g_0 was based in part on the conventional optimal g_s theory that $g_s = 0$ when $A_n = 0$ (Cowan and Farquhar, 1977). While g_0 was ultimately retained, this example illustrates, yet again, that using linear extrapolation to derive g_0 neglects to recognize the potential for the g_s-A_n relationship to depart from linearity at lower light levels (Ball, 1988; Collatz et al., 1991). Our measurements in *Malus domestica* show a large departure from linearity at lower light levels (Fig. 2.7), with a lower asymptote to g_s measurements being achieved well above the light compensation point (LCP; horizontal dashed line in Figure 2.7). We note that the measured LCP for *Malus domestica* was low (~10 μmol m^{-2} s^{-1}; data not shown), thus our measurements were unable to provide a high degree of g_s resolution near the LCP. However, this point may be moot because g_s appeared to reach an asymptote well above the LCP (Fig. 2.7). The same departure from linearity was evident in the trees measured in OH,

for which statistical estimates of g_0 in three out of four species were negative and substantially disagreed with observed values.

Small errors in g_0 parameterization can act multiplicatively on transpiration estimates and can compound errors over longer time periods (e.g., Fig. 2.3). To illustrate this we parameterized two versions of MAESTRA for *Malus domestica*, one with observed g_0 (49.7 mmol m^{-2} s^{-1}) and one with statistically estimated g_0 (20.4 mmol m^{-2} s^{-1}, Table 2.2). When parameterized with observed g_0 the model performed with a slight overestimation (~6%) over a four-day period with the majority of overestimation occurring at nighttime. However, when parameterized with g_0 values from statistical estimates, the model did not perform as well, underestimating water use by >40% (Fig. 2.8). We were unable to test the influence of the extrapolated g_0 values from the trees measured in OH because negative g_0 inputs cause a fatal error within the MAESTRA programming. While the influence of g_0 on transpiration estimates is greater under lower light conditions (Fig. 2.5), it is important to note that the mathematical formulation of the BBL equation (e.g. Equation 1) specifies that g_0 will be applied across the entire range of g_s predictions. Hence, in the Ball-Berry family of equations the g_0 parameter independently influences daytime as well as nighttime transpiration estimates.

Our finer scale tests that use observed versus extrapolated g_0 for *Malus domestica* transpiration estimates point to g_0 having a substantial influence on transpiration estimates at night. Published reports show significant levels of nighttime transpiration (up to 25% of daytime) (e.g., Daley and Phillips, 2006; Dawson et al., 2007). In extreme cases, such as well-watered fast-growing *Eucalyptus* species, weekly measurements of nighttime transpiration can approach 80% of daytime (Benyon, 1999). Thus, nighttime estimates of transpiration should be given greater importance in future research. Our data show similar trends in containerized *Malus*

domestica grown under glass house conditions, with nighttime transpiration ranging from 10-25% of average daytime water use (Fig 2.8). We found that observed g_0 improved the predictive accuracy of canopy transpiration estimates versus extrapolated g_0 and the improved accuracy was more pronounced during the daytime periods. However, the slightly lower accuracy of MAESTRA during nighttime periods could be due to our low resolution wind data at nighttime, where intermittent venting in the glass house produces low and variable wind speeds that could influence nighttime transpiration. Additionally, there have been reports that g_0 can vary slightly throughout the nighttime, therefore our measurements 1 h after sunset may not be entirely representative of the dark period (e.g., Howard and Donovan, 2007).

If typical methods of obtaining g_0 through statistical estimation are faulty, yet the BWB and BBL models provide accurate predictions of leaf-level g_s, then other parameters in the g_s or A_n models may be in error. From the standpoint of modeling g_s specifically, this error must be due to the parameterization of one of the other three parameters (Γ, g_1, or D_0). Our full season sensitivity analysis of the coupled g_s-A_n scheme revealed g_1 to be the parameter with the second largest influence on transpiration (~25%) with Γ and D_0 both having <1% influence (data not shown). Like g_0, g_1 has received little attention in the literature. The parameter g_1 is often described, similar to g_0, as a parameter fit to observed data (i.e. the slope of Equation 4 when plotted against observed g_s), even though a physiological significance for g_1 has been described (Xu and Baldocchi, 2003; Medlyn et al., 2011). Currently, it is not agreed upon whether g_1 changes or not in response to environmental factors (Baldocchi, 1997; Xu and Baldocchi, 2003). While there are several methods for calculating g_1 as an index of A_n, CO_2 and VPD (Equation 4, see also: Ball, 1988; Medlyn et al., 2011), these methods rely on statistical extrapolations from a linear regression fit that, like g_0, may not be representative of observed values.

The values for nighttime g_s in the literature come from a broad range of species, ecotypes and PFTs, ranging from 1 to 400 mmol m^{-2} s^{-1} (with a mean of 75.4 mmol m^{-2} s^{-1}) and include only a few instances of a value ≤ 10 mmol m^{-2} s^{-1} (Table 2.3). The reported nighttime g_s values could be useful for parameterizing $g_{0,}$ directly connecting plant physiology studies with ecological modeling efforts. In light of our analyses and the data in the literature, we strongly encourage modeling efforts at all scales to pay more attention to this parameter. For example, the values used in Sellers et al. (1996) (10 mmol m^{-2} s^{-1}) and Oleson et al. (2010) (2 mmol m^{-2} s^{-1}), two prominent large scale land surface schemes, are unrealistically low and also use the same value for all PFT's. While our study does not represent a comprehensive survey, our computed average for four broadleaf deciduous tree species was closer to 40 mmol m^{-2} s^{-1}. An even greater range of values are reported in Table 2.3 that might help provide general PFT g_0 parameterization guidance. We acknowledge the difficulty in species or PFT specific parameterization. However, we find it important to reiterate that species-specific g_0 parameterization in our study greatly improved full season model estimates.

Conclusions

The g_0 parameter in the BBL g_s model has a substantial influence on transpiration estimates at the whole crown level. Historically, little attention has been paid to g_0 and it has typically been parameterized as an empirical fitting coefficient. In this paper we assert that g_0 is a parameter with physiological significance and it can be measured. Knowing this, an additional "mechanistic" attribute may be associated with the BWB family of models. By shifting the current paradigm from g_0 as a linear extrapolation "fitting coefficient" to a basal g_s rate, additional focus can move toward refining measurements of the remaining model parameters.

Although we did not find g_0 to change in response to season or drought, understanding the underlying mechanisms that cause inter- and intraspecific g_0 differences are still warranted, especially given the disagreements found in the literature. Currently, empirical g_0 measurements are easy to obtain with simple hand-held porometers, providing a supplement to data collected with photosynthesis gas-exchange equipment. Finally, models should consider species-specific characterization of g_0 when predicting water flux rather than assume a single value among species or PFTs.

Tables

Table 2.1: Locations and climate characteristics of the Avon, OH and Fort Collins, CO research sites.

	Avon, OH	**Fort Collins, CO**
Latitude/Longitude	41.433, -82.052	40.613, -104.998
Mean annual maximum temperature (°C)	27.0	16.8
Mean annual minimum temperature (°C)	-5.7	1.1
Mean annual precipitation (mm)	1056	383
Mean annual wind speed (m s^{-1})	1.5	3.2

Table 2.2: Species-specific input parameters used in MAESTRA. Observed minimum stomatal conductance ($g_{0\text{-obs}}$), minimum stomatal conductance extrapolated from a least squares fit of the linear net photosynthesis and stomatal conductance relationship ($g_{0\text{-ext}}$), species stomatal response coefficient (g_1), maximum Rubisco mediated rate of photosynthesis (V_{cmax}), maximum electron transport rate (J_{max}), leaf dark respiration (R_d), quantum yield of electron transport (α), CO_2 compensation point (Γ) and leaf width (L_w).

	Units	*Acer rubrum*	*Betula nigra*	*Carpinus betula*	*Cercis canadensis*	*Malus domestica*
$\mathbf{g_{0\text{-obs}}}$	(mmol m^{-2} s^{-1})	42.57 ± 22.1	51.24 ± 14.4	61.78 ± 32.1	26.58 ± 12.5	49.69 ± 3.1
$\boldsymbol{g_{0\text{-ext}}}$	(mmol m^{-2} s^{-1})	15.2 ± 18.2	-14.4 ± 40.5	-29.6 ± 8.2	-29.6 ± 19.3	20.4 ± 10.2
$\boldsymbol{g_1}$	(dimensionless)	7.72 ± 3.7	8.13 ± 3.73	9.53 ± 2.61	8.16 ± 3.55	9.99 ± 0.59
$\boldsymbol{V_{cmax}}$	(μmol m^{-2} s^{-1})	45.55 ± 11.7	56.05 ± 12.9	43.87 ± 7.2	43.58 ± 6.9	22.68 ± 4.1
$\boldsymbol{J_{max}}$	(μmol m^{-2} s^{-1})	131.7 ± 46.6	164.3 ± 50.1	157.7 ± 65.4	120.3 ± 15.9	81.6 ± 22.8
$\boldsymbol{R_d}$	(μmol m^{-2} s^{-1})	1.76 ± 0.9	1.80 ± 0.6	1.71 ± 0.8	2.56 ± 1.2	1.35 ± 0.15
α	(mol e^- mol^{-1} PAR)	0.143 ± 0.06	0.124 ± 0.02	0.116 ± 0.03	0.139 ± 0.04	0.213 ± 0.07
Γ	(ppm)	73.3 ± 45.7	59.8 ± 37.2	54.1 ± 30.4	35.9 ± 28.2	6.78 ± 0.29
$\boldsymbol{L_w}$	(cm)	11.4 ± 0.5	6.4 ± 2.3	3.8 ± 0.3	11.3 ± 1.9	4.7 ± 0.8

Table 2.3: Measurements of nighttime stomatal conductance (g_s) (surrogate for minimum stomatal conductance (g_0)). Values are reported in mmol m^{-2} s^{-1}.

	Species/Functional type	g_0 min	g_0 max	g_0 mean	Reference
Functional type	Seep ecotype	20	120		(Snyder et al., 2003)
	Riparian	40	170		
	Scrub	15	40		
	Warm desert	15	100		
	Conifer trees	20	60		(Caird et al., 2007)
	Broadleaf evergreen	20	180		
	Broadleaf deciduous	20	260		
	Shrubs	20	260		
	Vines	20	140		
	Herbaceous dicots	20	220		
	Perennial grasses	20	140		
Species	*Pinus ponderosa*	10	120		(Misson et al., 2004)
	Pinus ponderosa	1	23		(Grulke et al., 2004)
	Styrax ferrugineus	50	145		(Bucci et al., 2004)
	Roupala Montana	45	125		
	Ouratea hexasperma	35	75		
	Quercus rubra	2	40		(Barbour et al., 2005)
	Ouratea hexasperma	30	60		(Scholz et al., 2007)
	Blepharocalyx salicifolius	77	81		
	Qualea grandiflora	102	158		
	Betula papifera			200	(Daley and Phillips, 2006)
	Quercus rubra			20	
	Acer rubrum			20	
	Helianthus annuus	40	400		(Howard and Donovan, 2007)
	Quercus virginiana			50	(Cavender-Bares et al., 2007)
	Ricinus communis	50	200		(Barbour and Buckley, 2007)
	Picea sitchensis	5	100		(Seibt et al., 2007)
	Fagus sylvatica	5	25		
	Prunus x yedoensis	231	288		(Bowden and Bauerle, 2008)
	Acer rubrum	159	249		
	Acer buergeranum	82	211		
	Prunus serrulata	213	233		
	Platanus x acerifolia	131	210		
	Acer rubrum	35	48		(Bauerle and Bowden, 2011)
	Eucalyptus sideroxylon	15	80		(Zeppel et al., 2011)
	Eucalyptus delegatensis	54	36		(Medlyn et al., 2007)

Figures

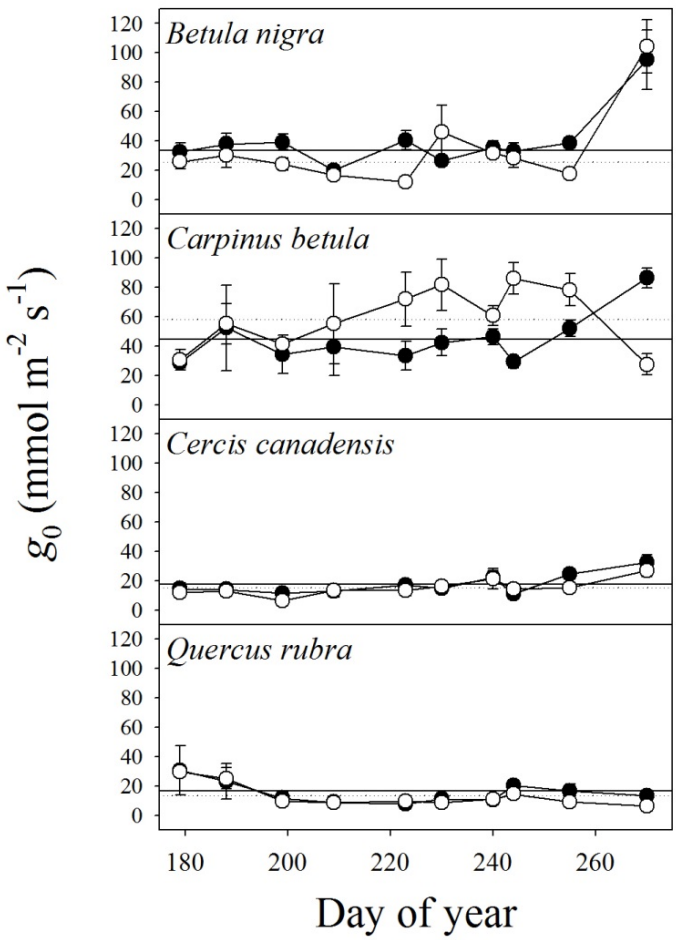

Figure 2.1: Measured values of minimum stomatal conductance (g_0; g_s when $A_n \leq 0$) for the 2011 growing season. Solid circles represent well-watered conditions and open circles represent water stress. The solid horizontal line indicates the whole season g_0 mean for the well-watered treatment and the dotted line represents the whole season mean for the drought treatment. Vertical bars represent one standard error (n = 3). Note: differences between seasonal treatment means were not significant for all species (P > 0.1).

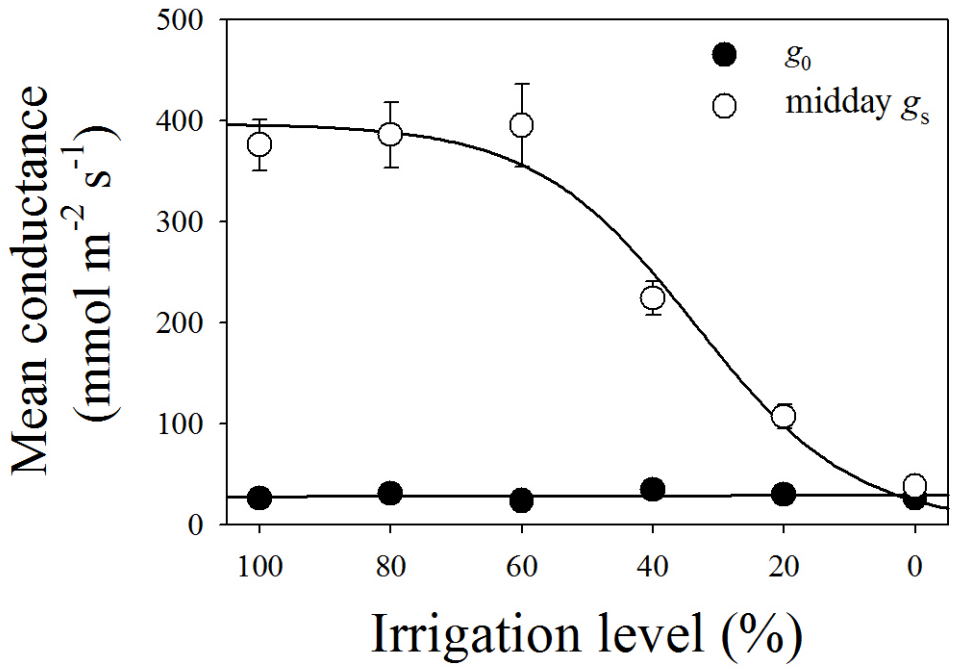

Figure 2.2: Relationship of midday stomatal conductance (g_s) and minimum stomatal conductance (g_0) to increasing levels of water stress (reported as percent of well-watered treatment) as an average of four tree species. The g_s-irrigation level relationship was significant (P = 0.0036, R^2 = 0.97), whereas the g_0-irrigation level relationship was not (P = 0.79, R^2 = 0.02). Vertical bars represent one standard error (n = 36).

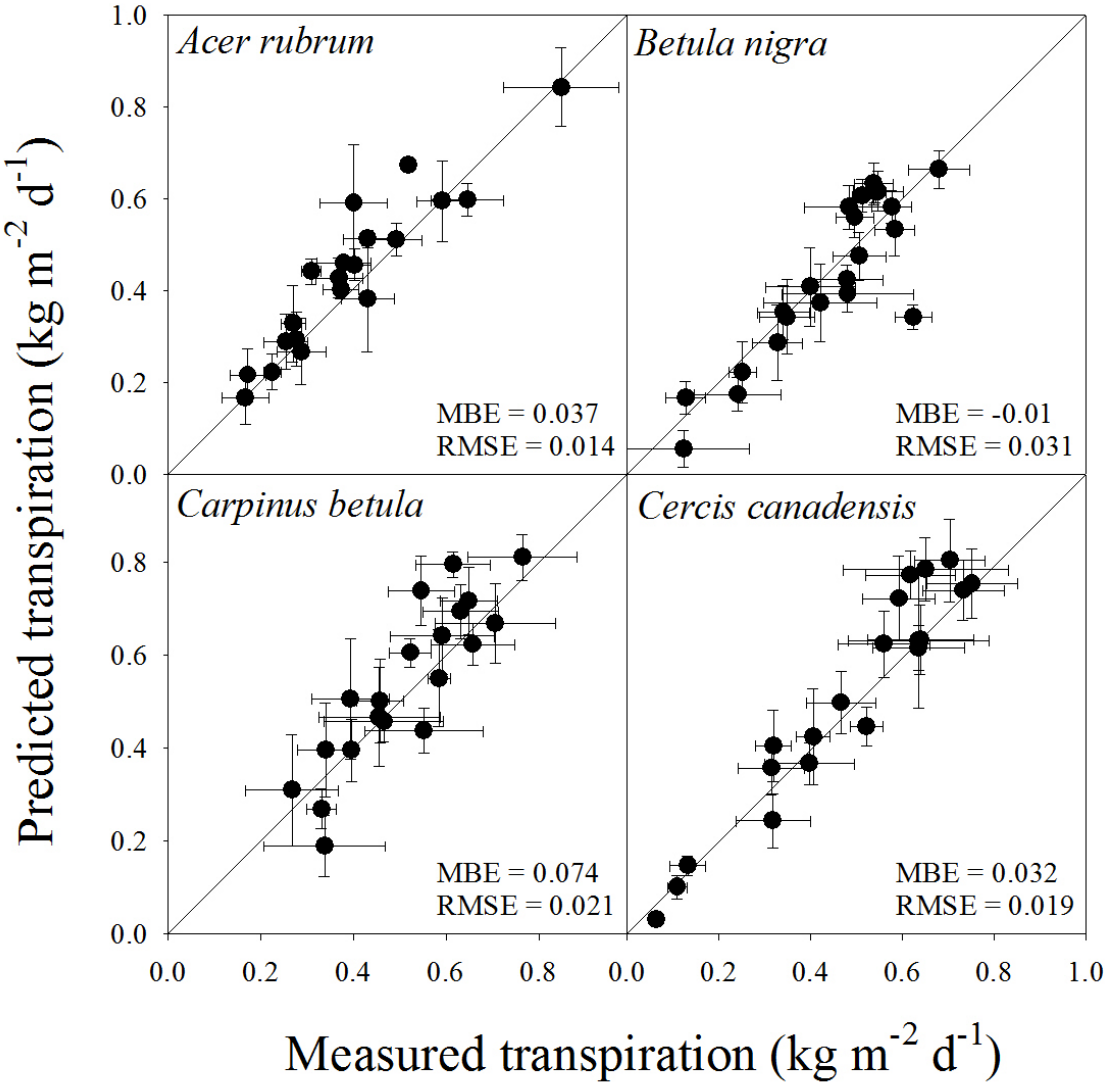

Figure 2.3: Measured versus predicted values of canopy transpiration per m^2 of leaf area for four tree species. Mean bias error (MBE) and root mean square error (RMSE) are reported in kg m^{-2} d^{-1}. Each point represents the mean value of one week of measured versus predicted transpiration. Bars represent one standard error (n = 7).

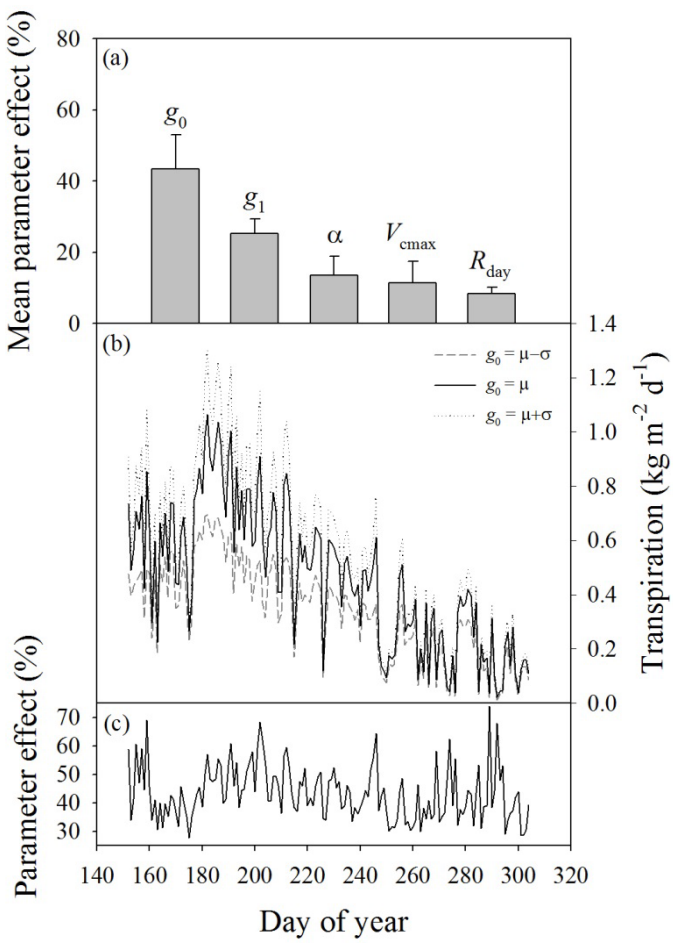

Figure 2.4: Sensitivity of transpiration estimates to five key input parameters. Panel (a) shows the parameter effect for five physiological parameters averaged across the entire season (minimum stomatal conductance (g_0 – mmol H_2O m^{-2} s^{-1}), stomatal response coefficient (g_1 – unit less), quantum yield of electron transport (α – mol e^- mol PAR^{-1}), maximum rate of Rubisco mediated carboxylation (V_{cmax} – μmol CO_2 m^{-2} s^{-1}) and dark respiration (R_d – μmol CO_2 m^{-2} s^{-1}). Panel (b) shows full-season transpiration estimates when MAESTRA was parameterized with the mean measured g_0 (g_0 = μ – solid black line), the mean plus one standard deviation (g_0 = μ+σ – dotted black line) and the mean minus one standard deviation (g_0 = μ-σ – dashed gray line). Panel (c) shows the daily change in the g_0 parameter effect across the season.

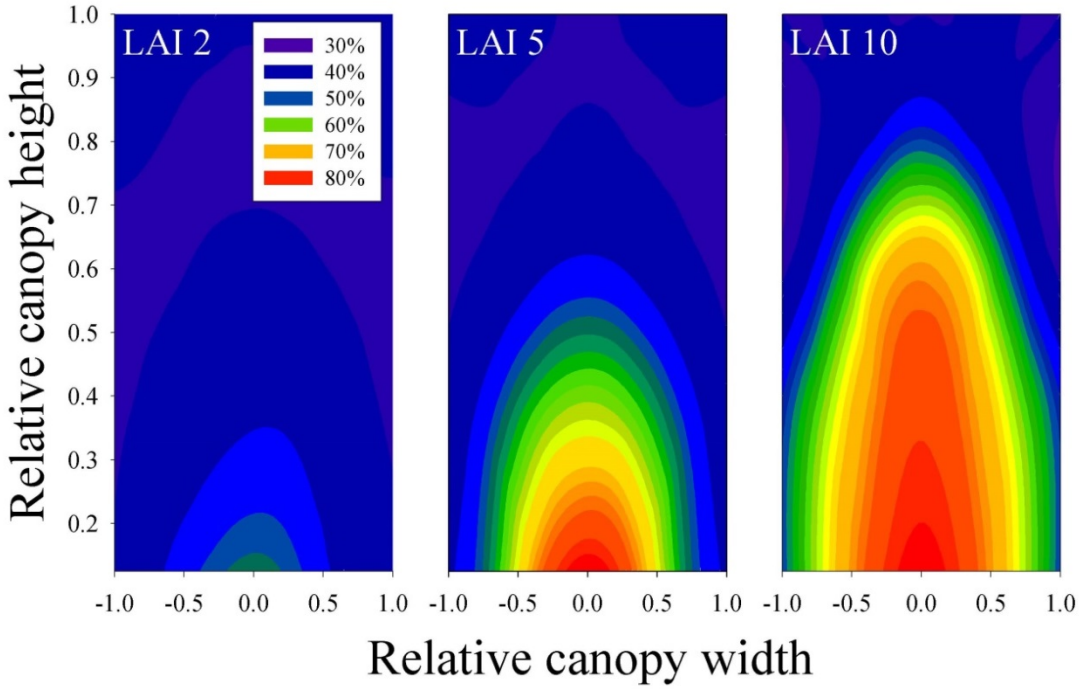

Figure 2.5: The crown spatial minimum stomatal conductance (g_0) parameter effect (%) on transpiration estimates in a simulated crown at a leaf area index (LAI) of 2, 5 and 10. The parameter effect was calculated as the difference in transpiration estimates at the upper (64.67 mmol m^{-2} s^{-1}) and lower (10.47 mmol m^{-2} s^{-1}) range of measured g_0 divided by the mean (42.57 mmol m^{-2} s^{-1}). Contour lines show changes in the g_0 parameter effect (%) at relative canopy height and width.

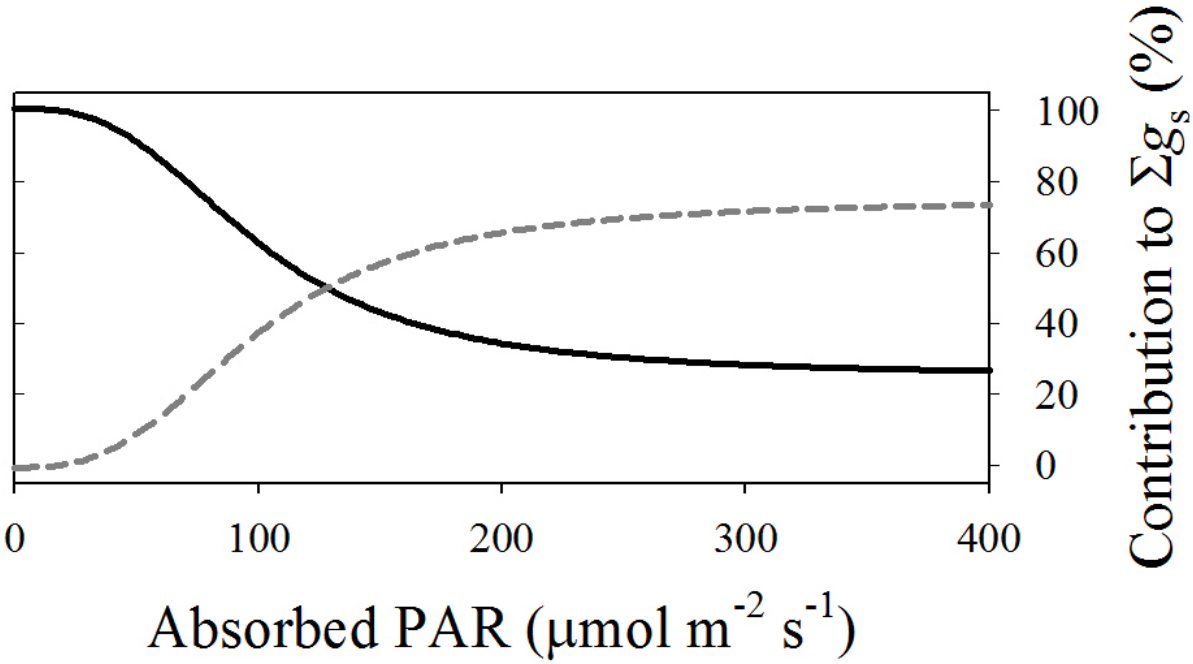

Figure 2.6: A simulated representation of the influence of leaf absorbed photosynthetically active radiation (PAR_L) on components of the Leuning (Leuning, 1995) stomatal conductance (g_s) model – as simplified for this study (refer to Equations 1-3) – where total stomatal conductance (Σg_s) is the sum of the minimum stomatal conductance parameter (g_0) and the portion of the Leuning model driven primarily by photosynthesis (βg_s). The black line represents the percent contribution of g_0 and the grey line represents the βg_s contribution to Σg_s.

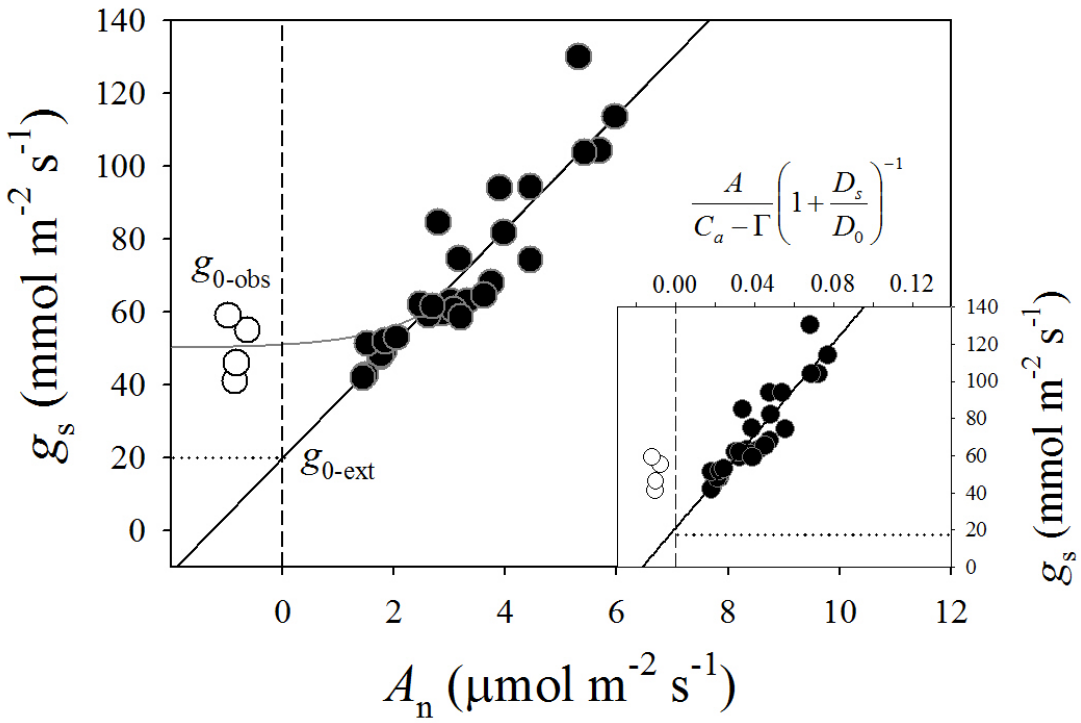

Figure 2.7: Linear relationship between stomatal conductance (g_s) and net photosynthesis (A_n) for *Malus domestica*. The g_0 parameter can be defined as the extrapolated x-y intercept ($A_n = 0$) of a least squares fit to the linear g_s-A_n relationship ($g_{0\text{-ext}}$), however, empirical observations of g_0 ($A_n \leq 0$; $g_{0\text{-obs}}$) from the same leaves show it to be higher, suggesting that the linearity between g_s-A_n becomes non-linear or asymptotic at low light levels. The parameter g_0 can also be defined as the x-y intercept of a linear fit of observed g_s to model output (inset figure) but it is important to note that the g_0 values derived from either fit are not different statistically. See Equation 1 and 4 for description(s) of the model and parameter definitions.

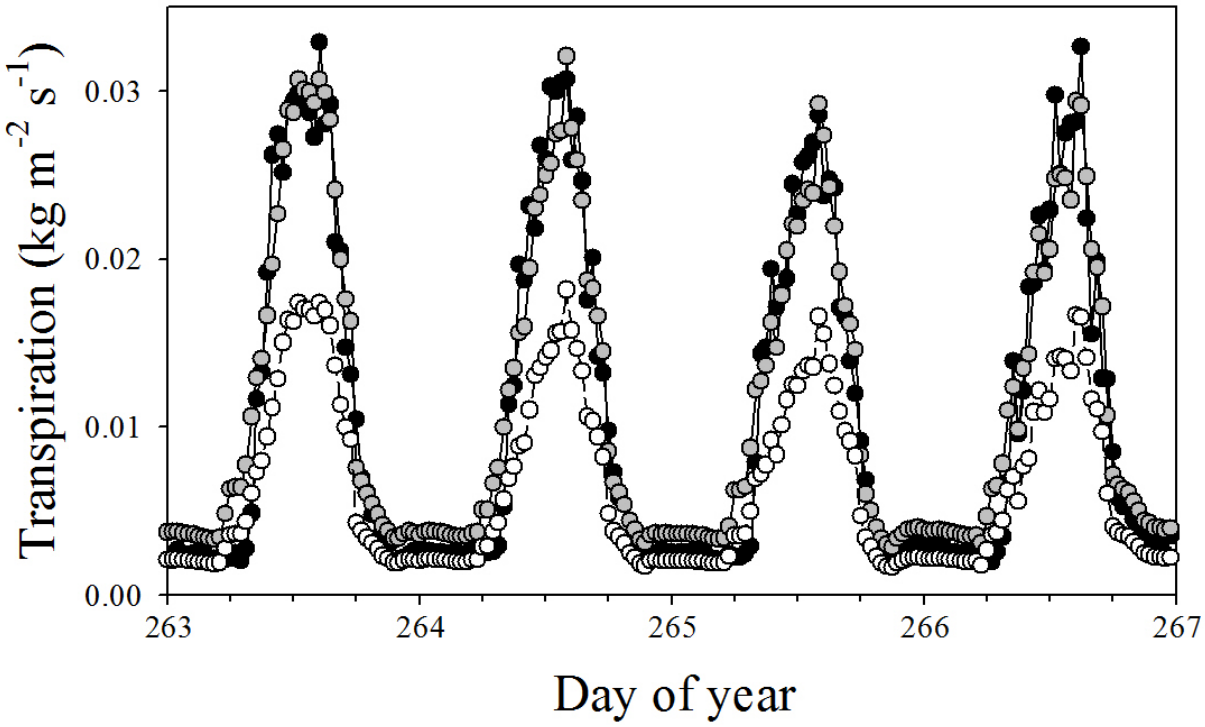

Figure 2.8: Comparison of gravimetric and MAESTRA estimated transpiration for containerized *Malus domestica*. Black circles represent gravimetric measurement values of transpiration, grey circles are transpiration estimates from MAESTRA when parameterized with values of g_0 observed at $A_n \leq 0$ and white circles represent transpiration estimates from MAESTRA when parameterized with g_0 values derived from a least squares estimate of the linear g_s-A_n regression. Each point represents the mean of four individual trees at a 30-minute time step. Root mean square errors of modeled versus measured regressions were 0.0067 and 0.041 g m^{-2} s^{-1} for the observed and least squares fit g_0 respectively. Mean bias errors were 0.0003 and -0.0021 g m^{-2} s^{-1} for the observed and least squares fit g_0 respectively.

References

Allen, M.T. and Pearcy, R.W., 2000. Stomatal behavior and photosynthetic performance under dynamic light regimes in a seasonally dry tropical rain forest. Oecologia, 122(4): 470-478.

Baldocchi, D., 1997. Measuring and modelling carbon dioxide and water vapour exchange over a temperate broad-leaved forest during the 1995 summer drought. Plant, Cell & Environment, 20(9): 1108-1122.

Baldocchi, D. and Meyers, T., 1998. On using eco-physiological, micrometeorological and biogeochemical theory to evaluate carbon dioxide, water vapor and trace gas fluxes over vegetation: a perspective. Agricultural and Forest Meteorology, 90(1-2): 1-25.

Baldocchi, D.D., Wilson, K.B. and Gu, L., 2002. How the environment, canopy structure and canopy physiological functioning influence carbon, water and energy fluxes of a temperate broad-leaved deciduous forest—an assessment with the biophysical model CANOAK. Tree Physiology, 22(15-16): 1065-1077.

Ball, J., Woodrow, I. and Berry, J., 1987. A model predicting stomatal conductance and its contribution to the control of photosynthesis under different environmental conditions. In: J. Biggins (Editor), Progress in Photosynthesis Research. Martinus Niijhoff, Dordrecht, Netherlands, pp. 221-224.

Ball, J.T., 1988. An analysis of stomatal conductance, Stanford University.

Ball, M.C. and Farquhar, G.D., 1984. Photosynthetic and stomatal responses of the grey mangrove, Avicennia marina, to transient salinity conditions. Plant Physiology, 74(1): 7-11.

Barbour, M.M. and Buckley, T.N., 2007. The stomatal response to evaporative demand persists at night in *Ricinus communis* plants with high nocturnal conductance. Plant, Cell & Environment, 30(6): 711-721.

Barbour, M.M. et al., 2005. Nocturnal stomatal conductance and implications for modelling δ18O of leaf-respired CO_2 in temperate tree species. Functional Plant Biology, 32(12): 1107-1121.

Battaglia, M., Sands, P., White, D. and Mummery, D., 2004. CABALA: a linked carbon, water and nitrogen model of forest growth for silvicultural decision support. Forest Ecology and Management, 193(1): 251-282.

Bauerle, W.L. and Bowden, J.D., 2011. Separating foliar physiology from morphology reveals the relative roles of vertically structured transpiration factors within red maple crowns and limitations of larger scale models. Journal of Experimental Botany, 62(12): 4295-4307.

Bauerle, W.L., Bowden, J.D., McLeod, M.F. and Toler, J.E., 2004a. Modeling intra-crown and intra-canopy interactions in red maple: assessment of light transfer on carbon dioxide and water vapor exchange. Tree Physiology, 24(5): 589-597.

Bauerle, W.L., Weston, D.J., Bowden, J.D., Dudley, J.B. and Toler, J.E., 2004b. Leaf absorptance of photosynthetically active radiation in relation to chlorophyll meter estimates among woody plant species. Scientia Horticulturae, 101(1): 169-178.

Benyon, R.G., 1999. Nighttime water use in an irrigated Eucalyptus grandis plantation. Tree Physiology, 19(13): 853-859.

Bowden, J.D. and Bauerle, W.L., 2008. Measuring and modeling the variation in species-specific transpiration in temperate deciduous hardwoods. Tree Physiology, 28(11): 1675-1683.

Bucci, S.J. et al., 2004. Processes preventing nocturnal equilibration between leaf and soil water potential in tropical savanna woody species. Tree Physiology, 24(10): 1119-1127.

Caird, M.A., Richards, J.H. and Donovan, L.A., 2007. Nighttime stomatal conductance and transpiration in C3 and C4 plants. Plant Physiology, 143(1): 4-10.

Cavender-Bares, J., Sack, L. and Savage, J., 2007. Atmospheric and soil drought reduce nocturnal conductance in live oaks. Tree Physiology, 27(4): 611-620.

Christman, M.A. et al., 2008. Genetic variation in *Arabidopsis thaliana* for night-time leaf conductance. Plant, Cell & Environment, 31(8): 1170-1178.

Collatz, G., Ribas-Carbo, M. and Berry, J., 1992. Coupled photosynthesis-stomatal conductance model for leaves of C4 plants. Functional Plant Biology, 19(5): 519-538.

Collatz, G.J., Ball, J.T., Grivet, C. and Berry, J.A., 1991. Physiological and environmental regulation of stomatal conductance, photosynthesis and transpiration: a model that includes a laminar boundary layer. Agricultural and Forest Meteorology, 54(2): 107-136.

Cowan, I. and Farquhar, G.D. (Editors), 1977. Stomatal function in relation to leaf metabolism and environment. Integration of Activity of the Higher Plant. Cambridge University Press, 471-505 pp.

Cox, P., Huntingford, C. and Harding, R., 1998. A canopy conductance and photosynthesis model for use in a GCM land surface scheme. Journal of Hydrology, 212: 79-94.

Daley, M.J. and Phillips, N.G., 2006. Interspecific variation in nighttime transpiration and stomatal conductance in a mixed New England deciduous forest. Tree Physiology, 26(4): 411-419.

Damour, G., Simonneau, T., Cochard, H. and Urban, L., 2010. An overview of models of stomatal conductance at the leaf level. Plant, Cell & Environment, 33(9): 1419-1438.

Dawson, T.E. et al., 2007. Nighttime transpiration in woody plants from contrasting ecosystems. Tree Physiology, 27(4): 561-575.

Dewar, R., 2002. The Ball–Berry–Leuning and Tardieu–Davies stomatal models: synthesis and extension within a spatially aggregated picture of guard cell function. Plant, Cell & Environment, 25(11): 1383-1398.

Donovan, L.A., Richards, J.H. and Linton, M.J., 2003. Magnitude and mechanisms of disequilibrium between predawn plant and soil water potentials. Ecology, 84(2): 463-470.

Farquhar, G.D., Caemmerer, S. and Berry, J., 1980. A biochemical model of photosynthetic CO_2 assimilation in leaves of C_3 species. Planta, 149(1): 78-90.

Franks, P. and Farquhar, G., 1998. A study of stomatal mechanics using the cell pressure probe. Plant, Cell & Environment, 21(1): 94-100.

Franks, P.J. and Farquhar, G.D., 2007. The mechanical diversity of stomata and its significance in gas-exchange control. Plant Physiology, 143(1): 78-87.

Friend, A.D., Geider, R.J., Behrenfeld, M.J. and Still, C.J., 2009. Photosynthesis in global-scale models. Photosynthesis in silico: 465-497.

Grulke, N., Alonso, R., Nguyen, T., Cascio, C. and Dobrowolski, W., 2004. Stomata open at night in pole-sized and mature ponderosa pine: implications for O3 exposure metrics. Tree Physiology, 24(9): 1001-1010.

Hanson, P.J. et al., 2004. Oak forest carbon and water simulations: model intercomparisons and evaluations against independent data. Ecological Monographs, 74(3): 443-489.

Howard, A.R. and Donovan, L.A., 2007. *Helianthus* nighttime conductance and transpiration respond to soil water but not nutrient availability. Plant Physiology, 143(1): 145-155.

Katul, G., Manzoni, S., Palmroth, S. and Oren, R., 2010. A stomatal optimization theory to describe the effects of atmospheric CO2 on leaf photosynthesis and transpiration. Annals of Botany, 105(3): 431-442.

Landsberg, J.J. and Sands, P., 2010. Physiological Ecology of Forest Production: Principles, Processes and Models. Academic Press, San Diego, California.

Leuning, R., 1990. Modelling stomatal behaviour and and photosynthesis of *Eucalyptus grandis*. Functional Plant Biology, 17(2): 159-175.

Leuning, R., 1995. A critical appraisal of a combined stomatal-photosynthesis model for C3 plants. Plant, Cell & Environment, 18(4): 339-355.

Lombardozzi, D., Sparks, J.P., Bonan, G. and Levis, S., 2012. Ozone exposure causes a decoupling of conductance and photosynthesis: implications for the Ball-Berry stomatal conductance model. Oecologia: 1-9.

Matyssek, R., Günthardt-Goerg, M.S., Maurer, S. and Keller, T., 1995. Nighttime exposure to ozone reduces whole-plant production in *Betula pendula*. Tree Physiology, 15(3): 159-165.

Medlyn, B. et al., 2001. Stomatal conductance of forest species after long-term exposure to elevated CO2 concentration: A synthesis. New Phytologist, 149(2): 247-264.

Medlyn, B.E. et al., 2005. Carbon balance of coniferous forests growing in contrasting climates: model-based analysis. Agricultural and Forest Meteorology, 131(1): 97-124.

Medlyn, B.E. et al., 2011. Reconciling the optimal and empirical approaches to modelling stomatal conductance. Global Change Biology, 17(6): 2134-2144.

Medlyn, B.E., Pepper, D.A., O'Grady, A.P. and Keith, H., 2007. Linking leaf and tree water use with an individual-based model. Tree Physiology, 27: 1687-1699.

Meyers, T.P. and Paw U, K.T., 1987. Modelling the plant canopy micrometeorology with higher-order closure principles. Agricultural and forest meteorology, 41(1): 143-163.

Misson, L., Panek, J.A. and Goldstein, A.H., 2004. A comparison of three approaches to modeling leaf gas exchange in annually drought-stressed ponderosa pine forests. Tree Physiology, 24(5): 529-541.

Mott, K.A. and Peak, D., 2010. Stomatal responses to humidity and temperature in darkness. Plant, Cell & Environment, 33(7): 1084-1090.

Nijs, I., Ferris, R., Blum, H., Hendrey, G. and Impens, I., 1997. Stomatal regulation in a changing climate: a field study using free air temperature increase (FATI) and free air CO_2 enrichment (FACE). Plant, Cell & Environment, 20(8): 1041-1050.

Ogle, K. et al., 2012. Differential daytime and night-time stomatal behavior in plants from North American deserts. New Phytologist.

Oleson, K.W. et al., 2010. Technical description of version 4.0 of the Community Land Model (CLM), *NCAR Technical Note NCAR/TN-478+STR*, pp. 257.

Ono, K. et al., 2013. Canopy-scale relationships between stomatal conductance and photosynthesis in irrigated rice. Global Change Biology, In Press.

Pieruschka, R., Huber, G. and Berry, J.A., 2010. Control of transpiration by radiation. Proceedings of the National Academy of Sciences, 107(30): 13372-13377.

Running, S.W., 1976. Environmental control of leaf water conductance in conifers. Canadian Journal of Forest Research, 6(1): 104-112.

Sato, H., Itoh, A. and Kohyama, T., 2007. SEIB–DGVM: A new Dynamic Global Vegetation Model using a spatially explicit individual-based approach. Ecological Modelling, 200(3): 279-307.

Scholz, F.G. et al., 2007. Removal of nutrient limitations by long-term fertilization decreases nocturnal water loss in savanna trees. Tree Physiology, 27(4): 551-559.

Schulze, E., Turner, N., Gollan, T. and Shackel, K., 1987. Stomatal responses to air humidity and to soil drought. Stomatal function, 804713472: 311-321.

Seibt, U., Wingate, L. and Berry, J., 2007. Nocturnal stomatal conductance effects on the δ18O signatures of foliage gas exchange observed in two forest ecosystems. Tree Physiology, 27(4): 585-595.

Sellers, P. et al., 1996. A revised land surface parameterization (SiB2) for atmospheric GCMs. Part I: Model formulation. Journal of Climate, 9(4): 676-705.

Shimono, H. et al., 2010. Diurnal and seasonal variations in stomatal conductance of rice at elevated atmospheric CO2 under fully open-air conditions. Plant, Cell & Environment, 33(3): 322-331.

Snyder, K., Richards, J. and Donovan, L., 2003. Night-time conductance in C_3 and C_4 species: do plants lose water at night? Journal of Experimental Botany, 54(383): 861-865.

Staudt, K., Falge, E., Pyles, R.D., Paw, U. and Foken, T., 2010. Sensitivity and predictive uncertainty of the ACASA model at a spruce forest site. Biogeosciences, 7(11): 3685-3705.

Tuzet, A., Perrier, A. and Leuning, R., 2003. A coupled model of stomatal conductance, photosynthesis and transpiration. Plant, Cell & Environment, 26(7): 1097-1116.

Wang, Y.-P. and Leuning, R., 1998. A two-leaf model for canopy conductance, photosynthesis and partitioning of available energy I: Model description and comparison with a multi-layered model. Agricultural and Forest Meteorology, 91(1): 89-111.

Way, D.A., Oren, R., Kim, H.S. and Katul, G.G., 2011. How well do stomatal conductance models perform on closing plant carbon budgets? A test using seedlings grown under current and elevated air temperatures. Journal of Geophysical Research, 116: G04031.

Wong, S., Cowan, I. and Farquhar, G., 1979. Stomatal conductance correlates with photosynthetic capacity. Nature, 282: 424-426.

Woods, D.B. and Turner, N.C., 2006. Stomatal response to changing light by four tree species of varying shade tolerance. New Phytologist, 70(1): 77-84.

Xu, L. and Baldocchi, D.D., 2003. Seasonal trends in photosynthetic parameters and stomatal conductance of blue oak (Quercus douglasii) under prolonged summer drought and high temperature. Tree Physiology, 23(13): 865-877.

Zeiger, E., 1983. The biology of stomatal guard cells. Annual Review of Plant Physiology, 34(1): 441-474.

Zeppel, M.J.B. et al., 2011. Nocturnal stomatal conductance responses to rising [CO_2], temperature and drought. New Phytologist.

Zhu, H. et al., 2005. A new system to monitor water and nutrient use in pot-in-pot nursery production systems. Journal of Environmental Horticulture, 23(1): 47-53.

Chapter 3: Seasonal canopy aerodynamics varies among species: potential implications for transpiration estimates

Overview

The decline in wind speed with depth into plant canopies is often empirically characterized with an exponential extinction coefficient (α). Aerodynamic properties of the canopy determine α and thus variation among species, vegetation type, and canopy development stage can occur. Error in characterizing α can affect estimates of boundary layer conductance to water vapor (g_{bV}), the canopy decoupling coefficient (Ω), and transpiration. Hence, the goals of the current study were to characterize the change in seasonal aerodynamics in four tree species to compare α calculated from canopy wind profiles to predictions of α from a simple empirical model, determine the influence of α on g_{bV}, Ω, and transpiration, and explain the influence of wind speed on transpiration over a range of environmental conditions using a canopy flux model (MAESTRA). Among species, measured α varied with wind speed above the canopy (U_{3m}) and over the season. Leaf area index (*LAI*) was correlated with α among species and measurement periods (R^2 = 0.78), and the simple empirical model for determining α was well correlated with measurements (R^2 = 0.92). Towards the middle of the season, mean canopy g_{bV} decreased to 20-50% of early season g_{bV}, whereas mean canopy Ω followed a similar but inverted parabolic trend. Mean canopy g_{bV} was strongly correlated with U_{3m} in the lower α/*LAI* canopies and with daily interpolated α in higher α/*LAI* canopies. The influence of a discrete increase in wind speed (0.6 to 2.4 m s^{-1}) resulted in a wide variation of influence on transpiration estimates (-30% to 20%). We conclude that within canopy variation in wind speed can influence transpiration

estimates and Ω, thus accurate characterization of α over the season is integral to preserve transpiration estimate accuracy.

Introduction

Transpiration and energy exchange between vegetation and the atmosphere is regulated by physiological and environmental factors. To estimate the physiological controls on transpiration, photosynthesis (A_n) and stomatal conductance (g_s) are often linked in model formulations that can span multiple scales (e.g., Wang and Jarvis, 1990a; Sellers et al., 1996). The precision of such computations however, depends on an accurate representation of the governing environmental conditions that can vary within the canopy and over the season, e.g., the decrease of wind speed with depth into the canopy. Moreover, seasonal changes in leaf width (L_w) and leaf area index (*LAI*) influences canopy aerodynamics and can alter canopy wind speed attenuation (α), yet this influence has only been quantified for energy exchange (Cammalleri et al., 2010). Hence, an investigation into the seasonal changes in vegetation aerodynamics that effect boundary layer conductance, α, and canopy transpiration estimates is warranted.

Since it was originally introduced, measurement methods for obtaining α have evolved to represent the canopy wind profile with greater resolution. Originally, α was calculated using wind speed above the canopy and at one height within the canopy (Equation 1, see also Inoue, 1963; Cionco, 1966). However, subsequent studies found α to be dependent on the height of the within canopy wind speed measurement and to vary with canopy size and development (Saito, 1964; Cionco, 1978). Regardless of these sources of variation, α is typically reported as a constant value representative of a vegetation type (Wright, 1965; Cionco, 1966; Cionco, 1972; Campbell and Norman, 1998). Neglecting to account for how canopy aerodynamics develop and

their influence on α could be especially detrimental for modeling investigations in vegetation that experience large seasonal changes in canopy size and *LAI* (Westgate et al., 1997; Souch and Stephens, 1998; Trout et al., 2008).

Numerous modeling efforts of varying complexity have been made in an attempt to eliminate the need for within canopy wind speed measurements to characterize canopy wind profiles. For example, Goudriaan (1977) presented a simple sensor-less modeling approach using *LAI*, L_w, and canopy height to estimate α. Limited reports indicate relatively good agreement between measured α and that determined by the Goudriaan model (α_G) (Goudriaan, 1977; Campbell and Norman, 1998). However, comparisons have been mostly limited to densely spaced agronomic crops - leaving some uncertainty as to the effectiveness of the Goudriaan model in other vegetation types. More recently, there have been substantial efforts to characterize the canopy wind profile at a much greater spatial resolution (i.e. 3-dimensions), but complex statistical methods are not practical for larger-scale field studies and often yield substantial modeled-to-measured discrepancies due to turbulence effects (e.g., Grace et al., 1987; Domingo et al., 1996). Simplified 2-dimensional representations of bulk airflow are a more reasonable means to derive α and subsequent calculations of leaf boundary layer conductance at various canopy depths.

Boundary layer conductance regulates the exchange of mass and energy with the atmosphere and is governed by leaf geometry and wind speed (Schuepp, 1993; Nobel, 1999). Hence, accurate estimates of α are important for determining wind speed at different canopy layers for calculations of boundary layer conductance to water vapor (g_{bV}). The ratio between g_s and g_{bV} acts to partition the control of transpiration between bulk incoming radiation (i.e. environmental control) and the physiological control of g_s responses to vapor pressure deficit

(VPD). Jarvis and McNaughton (1986) defined this ratio with a dimensionless coefficient (Ω) ranging from 0 - 1. Lower Ω values (i.e. < 0.4) indicate that g_s is much smaller than g_{bV} and will limit (i.e. control) conductance when determining transpiration rate. Conversely, larger values of Ω (i.e. > 0.6) indicate that g_{bV} will regulate transpiration. Medium range Ω values (i.e. 0.4 - 0.6) indicate intermittent control between g_s and g_{bV}. Nonetheless, a lower g_{bV} indicates that the diffusion of water molecules, evaporated from sub-stomatal cell walls, will be restrained by the boundary layer. This will cause the partial pressure of water vapor at the leaf surface to increase, consequently decreasing the diffusional evaporation gradient. The decline in water loss results in a decrease in g_s (e.g., Bunce, 1985; Aphalo and Jarvis, 1991; Mott and Peak, 2010), effectively decoupling the leaf physiological control of transpiration (i.e. g_s) from atmospheric VPD (Meinzer, 1993).

Increasing wind speed influences several biophysical processes at the leaf level, some of which can lead to an increase in transpiration whereas others can lead to a decrease (Larcher, 2003). For example, if leaf temperature (T_{leaf}) is greater than air temperature (T_{air}), increasing wind speed will lower T_{leaf}, reducing the available kinetic energy for evaporation (the converse would be true if $T_{leaf} < T_{air}$) (Drake et al., 1970). On the other hand, transpiration may be increased by intensifying wind speed as boundary layer conductance increases and evaporative demand is augmented as saturated air in the canopy is exchanged with drier air from aloft (e.g., Schuepp, 1993; Martin et al., 1999; Kim et al., 2014). At the same time, the increased evaporative demand can cause a decline in g_s, potentially reducing transpiration if the canopy is well coupled to the atmosphere (Aphalo and Jarvis, 1991; Meinzer, 1993; Mott and Peak, 2010). Hence, the counter-balancing physiological and environmental interactions may be responsible for the contradictory findings regarding the influence of wind speed on transpiration (for a

summary see Kim et al., 2014). This study had four main goals: (1) to characterize the variation of canopy aerodynamic properties and their influence on α among and within species over a season (2) asses the species and seasonal accuracy of the Goudriaan (1977) model for estimating α (3) to assess the impact of α on estimates of g_{bV} and Ω, and (4) to provide a theoretical assessment of the influence of wind speed on transpiration over a range of environmental conditions using a 3-dimensional canopy flux model.

Materials and methods

Site characteristics and plant material

This study was conducted in the summer of 2011 at a commercial nursery near Avon, OH (41.433°N lat., -82.052°W long.). The research site consisted of four plots, each 11 m wide (east to west) and 75 m long (north to south), separated by a 4 m tractor row. Each plot contained >300 57 L sunken containers (pot-in-pot production) spaced 1.5 m center-to-center. Trees for each plot were grown in 57 L black plastic containers that contained a soil-less substrate mixture consisting of 64% pine bark, 21% peat moss, 7% Haydite ©, and 7% sterilized regrind. The remaining 1% was a 12-0-42 slow release fertilizer (Agrozz Inc., Wooster, OH, USA). The species chosen for this study cover a range of ecological and commercial significance, growth rates and canopy aerodynamic characteristics (*Acer rubrum* 'Franksred', *Betula nigra* 'Cully', *Carpinus betula* 'Columnaris', and *Cercis canadensis*). Trees were irrigated twice daily to container capacity with spray stakes (PC spray stakes, Netafim, Israel). A weather station (Decagon Devices, USA) was installed near the center of each plot at 3 m above the ground to collect measurements of wind speed (U_{3m}) and photosynthetically active radiation (PAR). Air

temperature (T_{air}) and relative humidity (RH) were also collected and used to calculate VPD. Seasonal meteorology is shown in Figure 3.1.

Canopy aerodynamic measurements

To measure α in each plot we constructed a 3 m tall mobile wind tower from 10 cm diameter PVC pipe. Ten cup anemometers (Davis Instruments Corp, Hayward, CA, USA) were attached at 0.33 m intervals and connected to data collection nodes (EM50R, Decagon Devices, Pullman, WA, USA) that recorded a five minute average from one minute measurement intervals. In the center of each plot, an 8 cm diameter steel tube protruded from the ground to a height of 0.5 m - a plumb mount to hold the wind tower. Starting on day of year (DOY) 143 we began to rotate the wind tower among individual plots for measurement periods of >3 days (measurement periods are listed in Table 3.1). At the beginning of each relocation we collected plot *LAI* with a hand-held canopy gap-fraction analyzer (LAI 2000, LiCor Inc., Lincoln NE, USA). These measurements included five separate *LAI* readings in each plot where 270° of the field of view was obscured with a filter. Each reading was taken 10 cm above the ground with the 90° of unobstructed view facing inwards to the plot. All measurements were taken immediately following sundown. We marked the location of the five readings and returned to this location for each subsequent measurement. On the same day *LAI* was collected, we also measured canopy physical characteristics (canopy height, stem height, canopy width in the *x* and *y*-axes, and L_w (Table 3.2). Leaf area density (*LAD*) was calculated as (*LAI* × stem spacing)/canopy volume.

Species-specific characterization of α

Wind speed within plant canopies can be approximated with an exponential equation (Campbell and Norman, 1998) as:

$$U_{\mathrm{z}} = U_{\mathrm{h}} \exp\left[\alpha\left(\frac{z}{h} - 1\right)\right] \tag{1}$$

where U_z is the wind speed at height z within the canopy and U_h is the wind speed at height h above the canopy. Equation 1 can be rearranged to solve for α using measurements of wind speed at two heights. However, α has been determined to vary, depending on the height at which the within-canopy wind speed measurement is collected (Saito, 1964) suggesting that more than one measurement point in the canopy is needed to characterize α with acceptable accuracy. Hence, we tested two different methods for determining α. First, we tested the Goudriaan (1977) model that assumes a uniform distribution of leaf area within a spherical canopy and defines α_G as:

$$\alpha_G = \left(\frac{0.2LAIh}{l_{\mathrm{m}}}\right)^{1/2} \tag{2}$$

where l_m is the mixing length, describing the mean distance between leaves defined as:

$$l_{\mathrm{m}} = \left(\frac{6{L_w}^2 h}{\pi LAI}\right)^{1/3} \tag{3}$$

We calculated α_G using the canopy physical dimensions and *LAI* collected on the first day of each wind tower measurement period. Next, we tested the following equation fit to measurements of wind speed within the canopy to obtain the wind profile fit α (α_F):

$$U_{\mathrm{z}} = 0.5\exp^{\alpha_F U_{3\mathrm{m}}} \tag{4}$$

Our results did indicate that the fit value of α (α_F) varies with U_{3m} (Fig. 3.2). Thus, to normalize α_F for testing and comparisons we fit Equation 4 to wind tower measurements only when U_{3m} was 1.5 m s^{-1} (i.e. seasonal mean: Fig. 3.1) to derive the mean fit α (α_{Fmean}).

Modeling the influence of wind speed on energy exchange, boundary layer conductance and transpiration

In this study, we used the iterative approach of Leuning et al. (1995) executed in the modeling framework of MAESTRA (Wang and Jarvis, 1990a) to determine the influence of wind speed on within- and whole-canopy estimates of g_{bV} and transpiration using a pre-calibrated and validated set of physiological parameters for the four study species (Barnard and Bauerle, 2013). MAESTRA breaks an individual tree crown into a predetermined number of grid cells, each with an associated leaf area that depends on leaf area distribution and canopy shape (e.g., Wang et al., 1990; Baldwin and Peterson, 1997). Radiation conductance (g_{rN}) (Wang and Leuning, 1998) and percentage of sunlit and shaded leaf area is calculated for each grid point (Wang and Jarvis, 1990b). We assumed uniform distribution of leaf area within individual tree crowns.

Initial and subsequent leaf energy balance estimates are based on the assumption that exchanges of sensible heat (H) and latent heat (λE) in a transpiring leaf will balance to equal incoming net solar radiation (R_n) as:

$$R_{\mathrm{n}} = H + \lambda E \tag{5}$$

with H defined as:

$$H = \rho_a C_{\mathrm{p}} (T_{\mathrm{leaf}} - T_{\mathrm{air}}) g_{\mathrm{bH}} \tag{6}$$

Where ρ_a is the density of dry air, C_p is the specific heat of air, and T_{leaf} is leaf temperature. Leaf boundary layer conductance to heat, which in plant canopies is defined by the sum of g_{rN} and free (g_{bHf}) and forced (g_{bHu}) convection as:

$$g_{\mathrm{bH}} = 2(g_{\mathrm{bHf}} + g_{\mathrm{bHu}} + g_{\mathrm{rN}}) \tag{7}$$

with g_{bHf} defined as:

$$g_{\mathrm{bHf}} = \frac{0.5D_{\mathrm{H}}(1.6 \times 10^8 |T_{\mathrm{leaf}} - T_{\mathrm{air}}| {L_w}^3)^{0.25}}{w}\left(\frac{P}{RT_{\mathrm{air}}}\right) \tag{8}$$

where D_H is molecular diffusivity to heat, P is atmospheric pressure, and R is the universal gas constant. Boundary layer forced convection is defined as:

$$g_{\mathrm{bHu}} = 0.003\sqrt{\frac{U_{\mathrm{z}}}{L_w}}\left(\frac{P}{RT_{\mathrm{air}}}\right) \tag{9}$$

Latent heat flux is defined by the Penman-Monteith equation (Monteith, 1965) as:

$$\lambda E = \frac{sR_{\mathrm{n}} + c_{\mathrm{a}} g_{\mathrm{h}} C_{\mathrm{p}} M_{\mathrm{a}}}{s + \gamma({}^{g_{\mathrm{bH}}}/_{g_{\mathrm{V}}})} \tag{10}$$

where s is the slope of the temperature-saturation vapor pressure curve, c_a is the CO_2 concentration of the air, M_a is the molecular mass of air, γ is the psychometric constant, and g_v is total leaf conductance to water vapor which is a combination of g_s and g_{bV} with g_{bV} defined as:

$$g_{\mathrm{bV}} = 1.075 \times 2(g_{\mathrm{bHf}} + g_{\mathrm{bHu}}) \tag{11}$$

and g_s is defined using the Leuning (1995) model as:

$$g_{\mathrm{s}} = g_0 + \frac{g_1 A_{\mathrm{n}}}{(c_s - \Gamma)(1 + \frac{VPD}{D_0})} \tag{12}$$

where g_0 is minimum g_s, g_1 is the marginal cost of water per unit of carbon gain, Γ is the photosynthetic CO_2 compensation point, and D_0 is an empirical coefficient. Net photosynthesis is calculated using the biochemical Farquhar-von Caemmerer model (Farquhar et al., 1980).

Finally, to describe the degree to which the canopy is aerodynamically coupled with the atmosphere, we calculated the Ω coefficient defined by Jarvis and McNaughton (1986) as:

$$\Omega = \frac{s/\gamma + 2}{s/\gamma + 2 + g_{\mathrm{bV}}/g_s} \tag{13}$$

Results and Discussion

Development and characterization of canopy aerodynamics

Values of α_F increased exponentially (by as much as 6x) as concomitant measurements of U_{3m} decreased (Fig. 3.2). Coefficients from power functions fit to U_{3m} versus α_F varied among species and over the season (data not shown). The species that exhibited the most seasonal variation in α_F also had the largest changes in canopy size and *LAI* (e.g. *B. nigra* and *C. canadensis*; Table 3.2). These findings contradict previous studies that report a minor influence of wind speed on α_F in stands with initially low α_F (Cionco, 1972; Cionco, 1978). Instead, α_F was reported to be proportional to canopy characteristics (i.e. $\alpha \propto$ [(element flexibility) × (LAD) × (tree height)]$^{1/3}$ where element flexibility describes leaf, branch, and stem element absorption of wind momentum transfer. Although the variation in the α_F-U_{3m} relationship observed among species in this study supports the influence of crown structure on canopy aerodynamics, our observations show that species differences are most notable at U_{3m} of 1 to 4 m s^{-1}. We note that this observation may be specific to the smaller trees and plots used in this study and that our results may differ from larger forest trees or nursery plots. Due to the variability of α_F in response to U_{3m} and the likelihood of mean U_{3m} varying among measurement periods, we filtered our data set to only include U_{3m} = 1.5 m s^{-1} (mean seasonal U_{3m}) to normalize a mean α (α_{Fmean}) for comparisons. Regardless, this study is the first to quantify the effects of increasing wind velocity on α_F among several tree species which could have implications for studies that collect

α_F values at different time periods or from regions with different native wind speeds (e.g., Campbell and Norman, 1998).

We observed substantial variation in canopy aerodynamic characteristics and α_{Fmean} over the season and among species. Initially, L_w increased in the early season in all species but *C. betula*, whereas α_{Fmean} increased in all species alongside *LAI* (Figs. 3.3 and 3.4). *Acer rubrum* and *C. canadensis* had L_w's that developed at a similar rate and plateaued to roughly the same width at the same time. *Betula nigra* also plateaued at the same time as *A. rubrum* and *C. canadensis* but at a lower L_w (Fig. 3.4). *Cercis canadensis* had the smallest increase in α_{Fmean} (~50%), whereas *C. betula* and *A. rubrum* had closer to a 100% increase. *Betula nigra*, on the other hand, experienced the greatest change in α_{Fmean}, starting out as the lowest of all species (~0.3) then increasing 9x to ~2.7 by the end of the season. The upper value in *B. nigra* (2.7) is particularly noteworthy given that a value of 3 was hypothesized as the maximum canopy α (Cionco, 1978). The seasonal variation we observed is important given that most studies have assumed α to be constant for a given vegetation type regardless of growth stage (Cionco, 1972; Goudriaan, 1977; Inoue and Uchijima, 1979; Sauer et al., 1995; Kim et al., 2014). One exception was Cionco (1978) who reported a counter-intuitive decrease in α with canopy development in corn. Instead, we found α_{Fmean} to increase over the season at variable rates among species in response to the development of *LAI* and L_w. Our findings were similar to Daudet et al. (1999) that found a close correlation between canopy wind attenuation and cumulative *LAI*. For example, *C. canadensis* and *B. nigra* had α_{Fmean}'s that tracked *LAI* relatively closely, whereas the rate of increase of α_{Fmean} outpaced *LAI* in *C. betula*. We observed an increase in α_{Fmean} between the second and third measurement periods in *A. rubrum* and a decrease between the fourth and fifth period that does not correspond to changes in *LAI*. Two potential sources of error may

explain this divergence: (1) seasonal variation in branch, stem and/or, petiole flexibility was not captured by our measurements (Cionco, 1978) and (2) a possible error in gap-fraction *LAI* estimates due to small canopies with high *LAD* (i.e. portions of the crown leaf area may be obscured in the image due to leaf overlap (e.g., Weiss et al., 2004)). Future studies could address these potential error sources with parallel measurements of element flexibility to quantify how this error source changes over the season and the effect it has on canopy aerodynamics.

Regardless of differences in how *LAI* and α_{Fmean} developed over the season, when all species and measurement periods were pooled, *LAI* emerged as a relatively accurate predictor of α_{Fmean} (p <0.0001, R^2 = 0.78; Fig. 3.5a). However, the individual slopes for *A. rubrum* and *C. betula* were higher than that of the pooled regression. The differences in slope may be due to the influence of *LAD* on *LAI* estimates, a result of gap-fraction techniques that do not account for individual crown height or volume. For example, *C. betula* and *A. rubrum* had similar *LAD*'s that were ~3-4x greater than *B. nigra* and 4-6x greater than *C. canadensis* (both species had α_{Fmean}'s that were well characterized by *LAI*: Table 3.3). However, if we assume that there is no error in the gap-fraction *LAI* data, the improved relationship of species-specific α_{Fmean} with α_G would support *LAD* as a source of error because the Goudriaan model distributes *LAI* over a discrete canopy volume - indirectly accounting for canopy density.

The Goudriaan model proved to be a highly accurate method for predicting canopy α (R^2 = 0.92, Fig. 3.5b). While the individual slopes of *C. betula* and *A. rubrum* were higher than the pooled regression, they were more similar than the slopes from the regressions between *LAI* and α_{Fmean}. Hence, the Goudriaan model appears to be an accurate and simple method for determining α from a small set of measurements that are relatively easy to collect (i.e. L_w, tree height, and *LAI*). Our findings are in agreement with a previous assessment which found measured fluxes of

sensible heat to agree well with modeled fluxes when the Goudriaan model was used to characterize α (Cammalleri et al., 2010), however season changes in α were not tested. Hence, our results indicate that intensive sampling of within canopy wind-speeds is not necessary to characterize α on a species basis or to identify seasonal changes. However, it is important to note that the Goudriaan model will not account for the variation of α_{Fmean} with U_{3m}, but will instead provide a general-mean value for that species and canopy size. An alternate benefit of using the Goudriaan model to calculate α is that the equation may be rearranged to solve for *LAI* if α_{Fmean}, canopy height, and L_w are known. This could offer a straightforward real-time method to determine *LAI*, which could be particularly beneficial in vegetation that experiences large changes in *LAI* over a growing season (e.g., agronomic or biomass crops).

Species characteristics affect canopy-to-atmosphere coupling

The evolution of Ω over the growing season varied among species, but generally followed a parabolic increase to a maximum (~DOY 220 to 250), followed by a secondary decrease prior to leaf senescence (Fig. 3.6). An increase in Ω will occur as g_{bV} decreases or as g_s increases. While changes in g_s can be due to a combination of physiological and environmental responses, g_{bV} is generally dependent on the influence of L_w and wind velocity on forced convection and the influence of T_{leaf} *to* T_{air} differences on free convection (i.e. Equations 9 and 10). In this study, modeled mean g_s declined through the season for all species due to A_n declining as the shaded fraction of leaf area increased (Bauerle et al., 2004; Campoe et al., 2013). Despite variable rates of canopy development the rate of seasonal g_s decline was similar among species, but with different early season maximums that corresponded to species-specific $g_{s\text{-}max}$ (Table 3.3). Regardless, the daily variation in g_{bV} (and corresponding variation in Ω) suggests

that wind velocity and canopy aerodynamics are the predominant influences that interact with species-specific physiology (i.e. g_s) to determine the variation in canopy-to-atmosphere coupling. For example, *A. rubrum* and *C. canadensis* had relatively similar seasonal evolution of Ω despite different physiology and α_{Fmean}s. The reason being, *C. canadensis* had lower mean g_{bV} in the early- and mid-season due to lower within canopy wind velocities from higher α_{Fmean} (Fig. 3.2). However, lower α_{Fmean}'s and higher g_{bV} in *A. rubrum* were balanced by higher mean canopy g_s, resulting in similar Ω values to *C. canadensis*. *Carpinus betula* had the second lowest initial g_{bV}, but the second highest $g_{s\text{-}max}$, resulting in the highest initial Ω with the earliest peak. By day of year 220, α_{Fmean} of *B. nigra* was >2.3, and individual crowns had begun to overlap with each other in the canopy (Table 3.2). The resulting decline in wind speed (>70% of above canopy wind speed in the lower ¾ of the canopy) greatly reduced g_{bV}. The highest $g_{s\text{-}max}$ of all three species (*B. nigra*) produced a peak Ω of ~0.6 with minimal decline towards the end of the season. *Cercis canadensis* had the second highest α_{Fmean} at the end of the season and also exhibited the second lowest secondary decline in Ω. *Carpinus betula* showed the strongest secondary decline in Ω despite having an α_{Fmean} not much smaller than *C. canadensis* but with a substantially smaller L_w (3 cm versus 10.5 cm for *C. betula* and *C. canadensis* respectively). Hence, L_w may be more important in determining g_{bV} for tree crowns with high *LAD*. Regardless, our findings clearly point to g_{bV} as the main driver of canopy Ω which is contrary to a previous study that found spatial variability in leaf g_s to dictate variation in Ω (Daudet et al., 1999). It is unlikely that differences in L_w between this study and the Daudet et al. (1999) study because the species we used covered a wide range of L_w's and the species with the smallest L_w (*C. betula*) responded similarly to the other three species.

Figure 3.7 shows that mean daily g_{bV} can be correlated with U_{3m} and/or the daily interpolated value of α_{Fmean}. However, the strength of the correlations between U_{3m} and g_{bV} decreases with α_{Fmean} and *LAI* with the converse being true for the daily interpolated value of α_{Fmean}. As a result, we see a strong correlation between the daily interpolated value of α_{Fmean} and g_{bV} in *C. canadensis* and *B. nigra* ($R^2 > 0.7$), whereas their correlation with U_{3m} is weak ($R^2 < 0.3$). Interestingly, even in the two species with the lowest average seasonal α_{Fmean} (*A. rubrum* and *C. betula*), the correlations with U_{3m} are never > 0.55. Hence, these correlations underscore the importance of accurate characterization of α and its seasonal development in plant canopies. Only measuring above canopy wind speed is not sufficient to adequately characterize the spatial variability of wind speed within a canopy. However, as *LAI* and α_{Fmean} increase U_{3m} has a decreasing influence on g_{bV} which is particularly notable at the end of the season in *B. nigra* and *C. canadensis* and to a lesser extent *A. rubrum* (Fig. 3.6). Mischaracterizing spatial variability in canopy wind speed can skew estimates of g_{bV} and Ω, thus altering estimates of energy and mass exchange (Bunce, 1985; Daudet et al., 1999; Martin et al., 1999). Hence, future studies should focus efforts on accurate characterization of α, especially in canopies that have higher *LAI*.

Theoretical modeling exercises

The modeling framework used in this study provides a theoretical foundation to examine the influence of wind speed on transpiration over a wide range of environmental conditions. We tested 1,000 random combinations of environmental conditions (VPD ranged from 0-4 kPa, PAR from 0-2000 μmol m^{-2} s^{-1}, and T_{air} from 5-40° C) and found that a discrete change in wind speed (i.e. from 0.6 to 2.4 m s^{-1}) resulted in changes in transpiration rates (ΔE_{wind}) that ranged from -30% to +20% (Fig. 3.7). When regressed against individual environmental conditions,

there was a peaked response for PAR (Fig. 3.8a) which identifies that the extreme ends of the range of ΔE_{wind} (i.e. 10 to 20% and -30 to -25%) are most likely to occur in low light conditions. There was a less distinct trend between ΔE_{wind} and T_{air} (Fig. 3.8b) but a clear trend between ΔE_{wind} and VPD (Fig. 3.8c). Overall, ΔE_{wind} is negative or close to zero at the VPD's most often observed in this study (i.e. 0-2 kPa) but becomes positive and asymptotic at higher VPD. Additionally, the more negative end of the range generally coincides with lower T_{air} and the higher end of the range occurs at high T_{air} (Fig. 3.8c). This may be partly due to the fact that lower VPD's are more likely at lower T_{air} with the converse holding true for higher VPDs. Nevertheless, two important conclusions can be drawn from these theoretical exercises. First, in low-light conditions (i.e. $PAR < 250$ μmol m^{-2} s^{-1}) ΔE_{wind} is at the extreme upper and lower ends of the range of influence and were quite negative or positive depending on the other environmental conditions (i.e. VPD). Given that nighttime transpiration can account for a significant portion of total daily transpiration (Benyon, 1999; Dawson et al., 2007) the interactions between wind speed and VPD at low light warrant future investigation under field settings and in larger scale models that use two-stream big-leaf formulations for 24 h estimates (e.g., Sellers et al., 1996; Oleson et al., 2013). Second, the observed relationship between ΔE_{wind} and VPD may isolate the primary indirect influence of wind on transpiration. Currently, there have been numerous studies with contradictory results regarding the influence of wind speed on transpiration. For example, Kim et al. (2014) and Daudet et al. (1999) showed only marginal influence of wind on transpiration whereas Taylor et al. (2001) found a significant positive effect at forest edges and Gutiérrez et al. (1994) found a negative influence in coffee hedgerows. Kim et al. (2014) provided a direct analysis of why wind speed may have positive and negative influences on transpiration. However, their analysis was from big-leaf simulations that account

for one dimension aerodynamic and physiological resistances while not taking into account leaf energy balance. They also filtered their data set to remove the influence of light and VPD, eliminating the ability to see how several environmental parameters interact. There are numerous mechanisms by which wind speed can influence leaf-level properties and the vegetation and site specific (e.g., α and Ω) characteristics will all interact to dictate wind influence. Out modeling simulations, however, indicate a more substantial role of the leaf energy balance and suggest that increasing wind speed will reduce the leaf-to-air temperature difference (T_{dif}) by increasing H, g_{bV}, and (if $T_{leaf} > T_{air}$) λE. However, as ambient VPD decreases, the diffusional driving force for transpiration declines causing λE to decrease. The resulting decrease in T_{dif} will lower g_{bH} and then total leaf H. Figure 3.9 describes this relationship between H and λE, as they must balance with incoming net radiation (i.e. Equation 4), to show that the Bowen Ratio (i.e. H: λE) approaches zero at high VPD. This indicates that almost all heat transfer is convective in saturated air conditions due to the marginal humidity gradient reducing transpiration..

Conclusions

In this study we provided descriptions of the seasonal development of canopy aerodynamics and their influence on α in four broadleaf tree species. In addition, we showed that the empirical Goudriaan (1977) model for predicting α was highly predictive among species and over the season. By accurately characterizing α we were able to improve the understanding of the influence of within canopy wind speed on g_{bV} and Ω - showing how they work in unison to partition the control of transpiration between environment and physiology. Most importantly, we have identified the role of leaf energy balance in determining the influence of wind speed on transpiration which has not been previously considered (e.g., Kim et al., 2014). Further, this

study has identified a connection between the meteorological conditions and the influence of wind speed on transpiration, suggesting future wind speed studies disseminate their results within the context of environmental interactions.

Tables

Table 3.1: Day(s) of year that the wind tower was placed in the plots of each species that comprised each measurement period. The wind tower was left in each plot for >3 days or longer depending on average wind conditions and time needed to complete additional data collection. Note: no Period 5 data was collected in *Cercis canadensis* due to early leaf senescence.

	Period 1	**Period 2**	**Period 3**	**Period 4**	**Period 5**
Acer rubrum	147-151	166-176	198-201	218-222	237-242
Betula nigra	143-147	163-166	195-198	214-218	233-237
Carpinus betula	151-154	176-180	201-206	222-225	242-248
Cercis canadensis	154-157	180-185	206-210	225-228	

Table 3.2: Physical dimensions of the four study species (n = 12) at the beginning of the five measurement periods used to calculate the wind extinction coefficient from the Goudriaan (1977) model. Leaf area index (*LAI*) was estimated for each species at the plot scale. Note: Period 5 *LAI* data was not collected for Period 5 in *Cercis canadensis* due to early leaf senescence.

Species	**Period**	**Tree height (m)**	**Stem height (m)**	**Canopy width (m)**	**Stem caliper (mm)**	***LAI* (m^2 m^{-2})**
Acer rubrum	1	1.87	0.74	0.25	22.4	0.34
	2	2.12	1.21	0.43	27.5	0.48
	3	2.23	1.21	0.75	30.2	0.62
	4	2.34	1.20	0.81	33.4	0.65
	5	2.37	1.20	0.86	34.7	0.64
Betula nigra	1	0.61	0	0.27	38.4	0.25
	2	1.14	0	0.89	50.3	0.8
	3	1.71	0	1.33	66.8	1.21
	4	2.19	0	1.64	79.0	2.05
	5	2.25	0	1.73	85.5	2.99
Carpinus betula	1	1.51	0.43	0.36	26.1	0.57
	2	1.82	0.40	0.51	30.1	0.65
	3	2.02	0.39	0.55	32.5	0.67
	4	2.07	0.38	0.56	33.4	0.66
	5	2.06	0.38	0.57	33.6	0.7
Cercis canadensis	1	2.12	1.01	0.80	25.5	0.49
	2	2.41	0.98	1.17	28.1	0.74
	3	2.72	0.98	1.41	31.2	1.08
	4	2.68	0.98	1.64	32.4	1.45
	5	2.68	0.97	1.70	32.5	

Table 3.3: Seasonal mean crown leaf area density (LAD), mean maximum leaf width (L_w), maximum theoretical stomatal conductance ($g_{s\text{-}max}$), and photosynthesis (A_{max}) at 400 ppm CO_2.

	LAD (m^2 m^{-3})	L_w (cm)	$g_{s\text{-}max}$ (mol m^{-2} s^{-1})	A_{max} (μmol m^{-2} s^{-1})
Acer rubrum	0.33	8.9	0.489	10.38
Betula nigra	0.12	4.7	0.801	13.72
Carpinus betula	0.46	3.3	0.601	10.81
Cercis canadensis	0.08	9.6	0.443	9.44

Figures

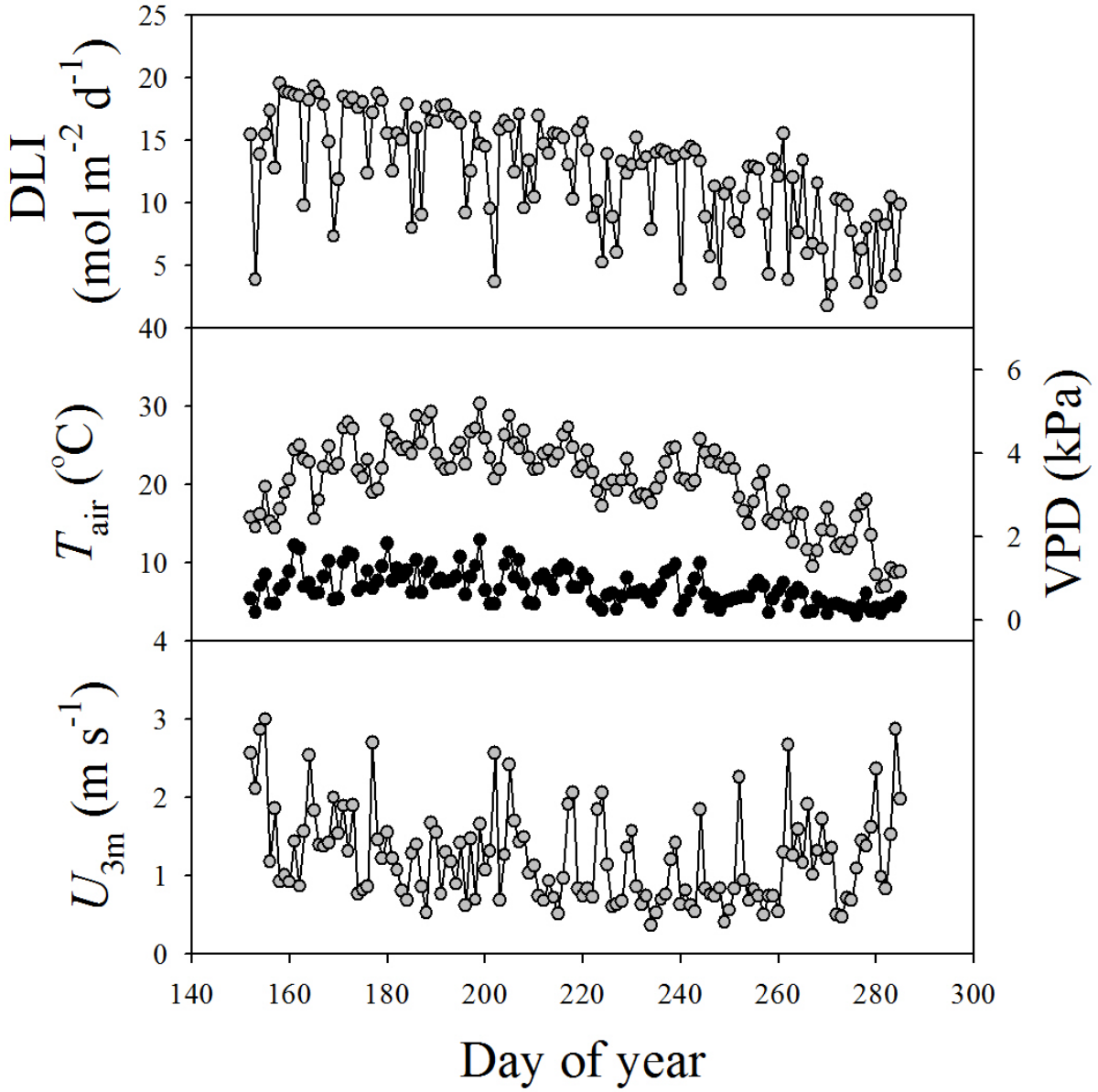

Figure 3.1: Seasonal daily light integral (DLI), mean daily air temperature (T_{air}), vapor pressure deficit (VPD), and wind speed at 3 m (U_{3m}).

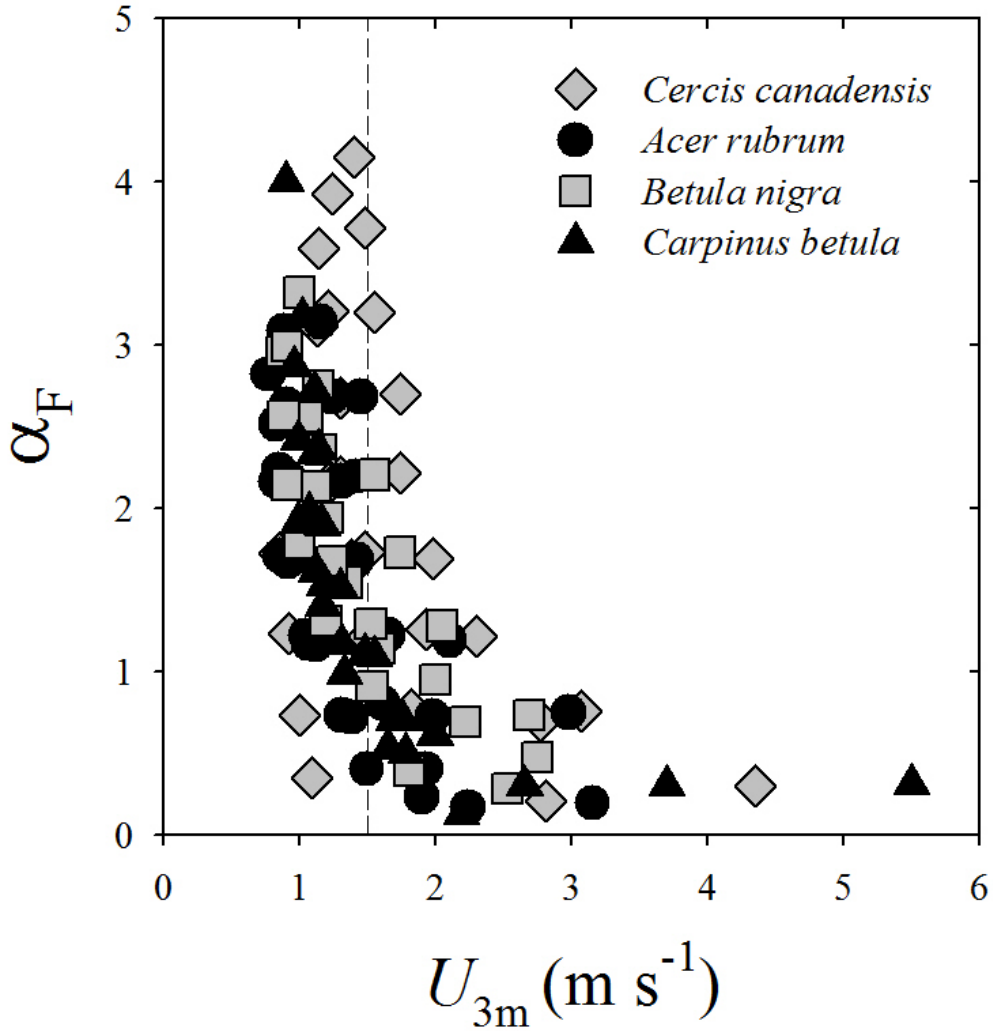

Figure 3.2: Values of α fit to within canopy wind speed (α_F) are dependent on wind speed at 3 m (U_{3m}). Dashed vertical line represents the mean seasonal U_{3m} (1.5 m s^{-1}). Points for each species include 4-5 measurement periods (cf. Table 3.1) and 3-6 measurement points within the canopy depending on canopy height (cf. Table 3.2).

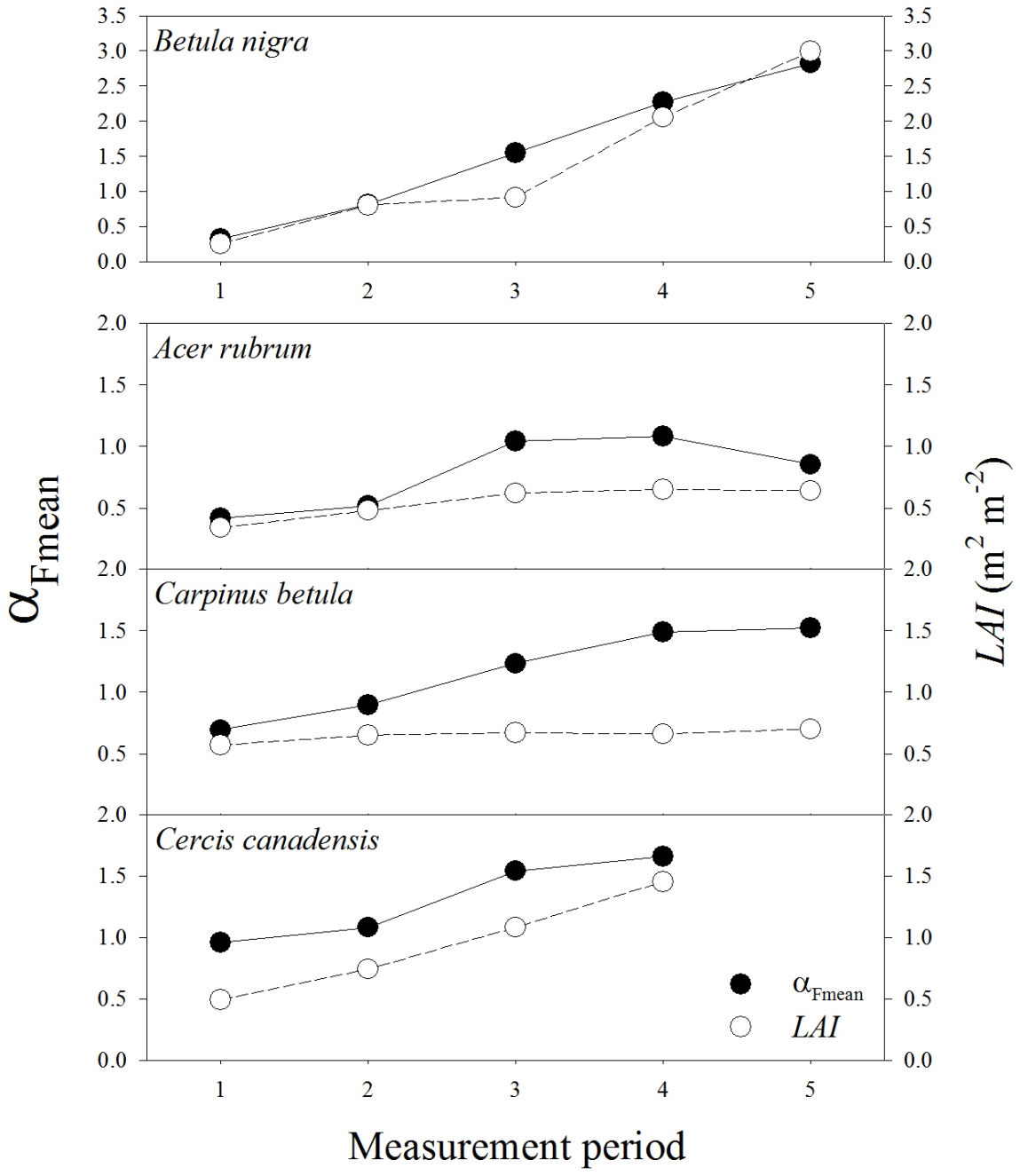

Figure 3.3: Canopy wind extinction coefficient values fit to within canopy wind speed at mean seasonal daytime wind speed at 3 m (α_{Fmean}) and canopy leaf area index (*LAI*) over the season. Measurement periods are listed in Table 3.2.

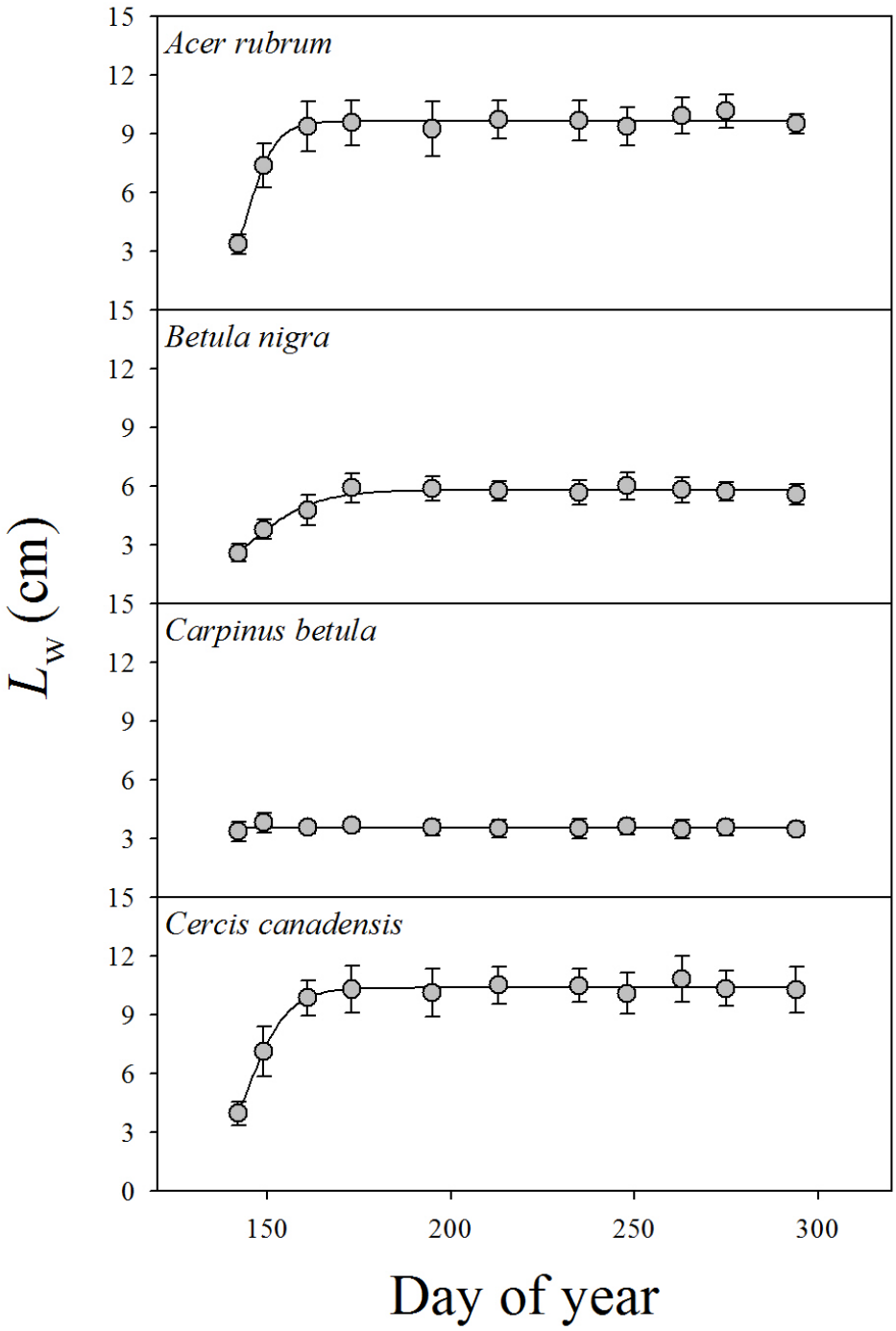

Figure 3.4: Mean canopy leaf width (L_w) increases in the initial portion of the season before reaching a canopy maximum in three of the four species. Seasonal variation in L_w was not evident in *C. betula*. Bars represent one standard deviation (n = 14).

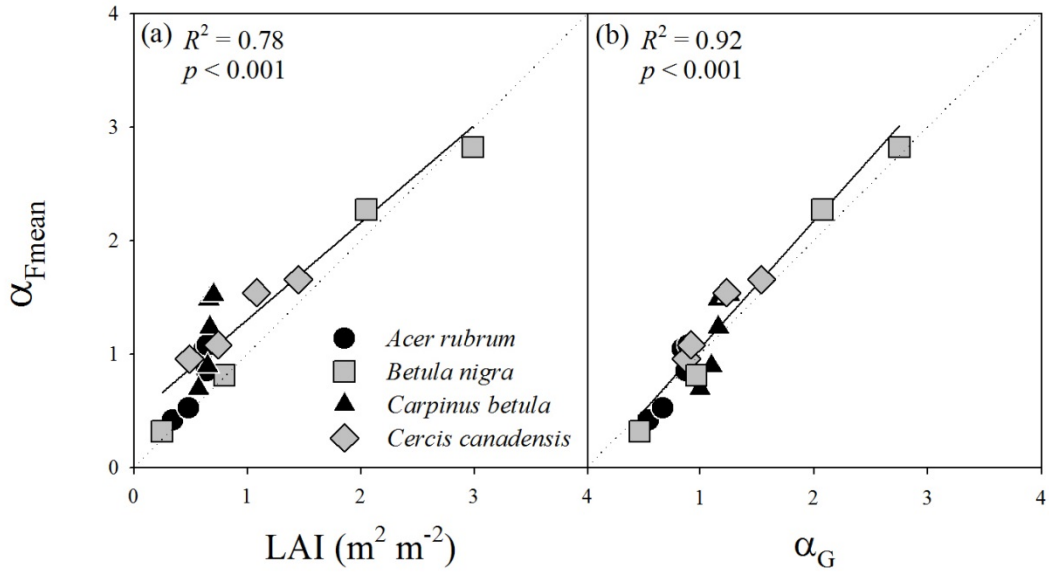

Figure 3.5: Leaf area index (*LAI*) and Goudriaan (1977) model estimates of canopy wind extinction coefficient (α_G) regressed against canopy wind extinction coefficient values as fit to wind tower data at mean seasonal daytime wind speed at 3 m (α_{Fmean}).

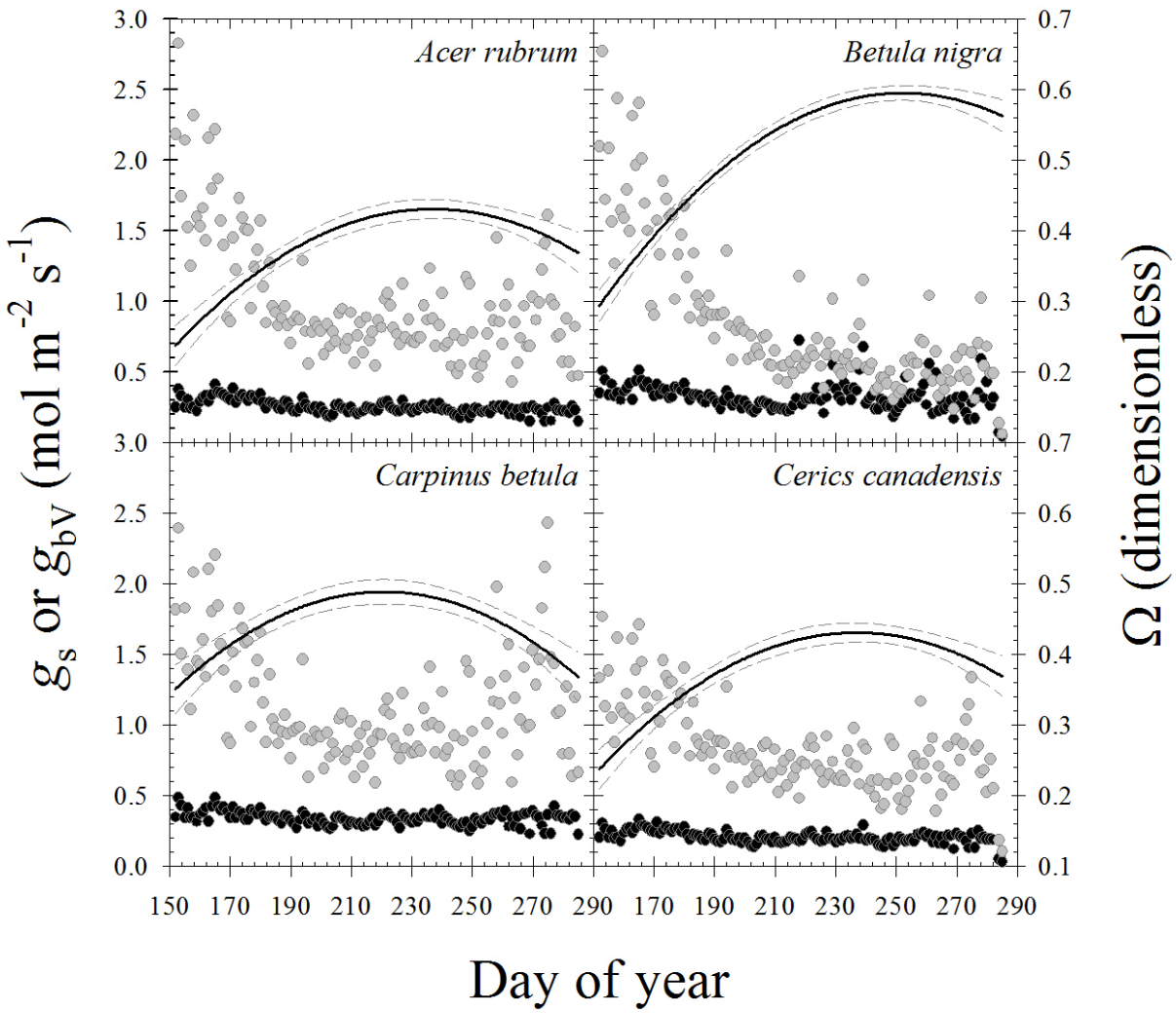

Figure 3.6: Seasonal evolution of stomatal conductance (g_s – black circles), leaf boundary layer conductance to water vapor (g_{bV} – grey circles) and the least squares parabolic fit of the canopy decoupling coefficient (Ω - black line). Dashed grey lines represent 95% confidence interval.

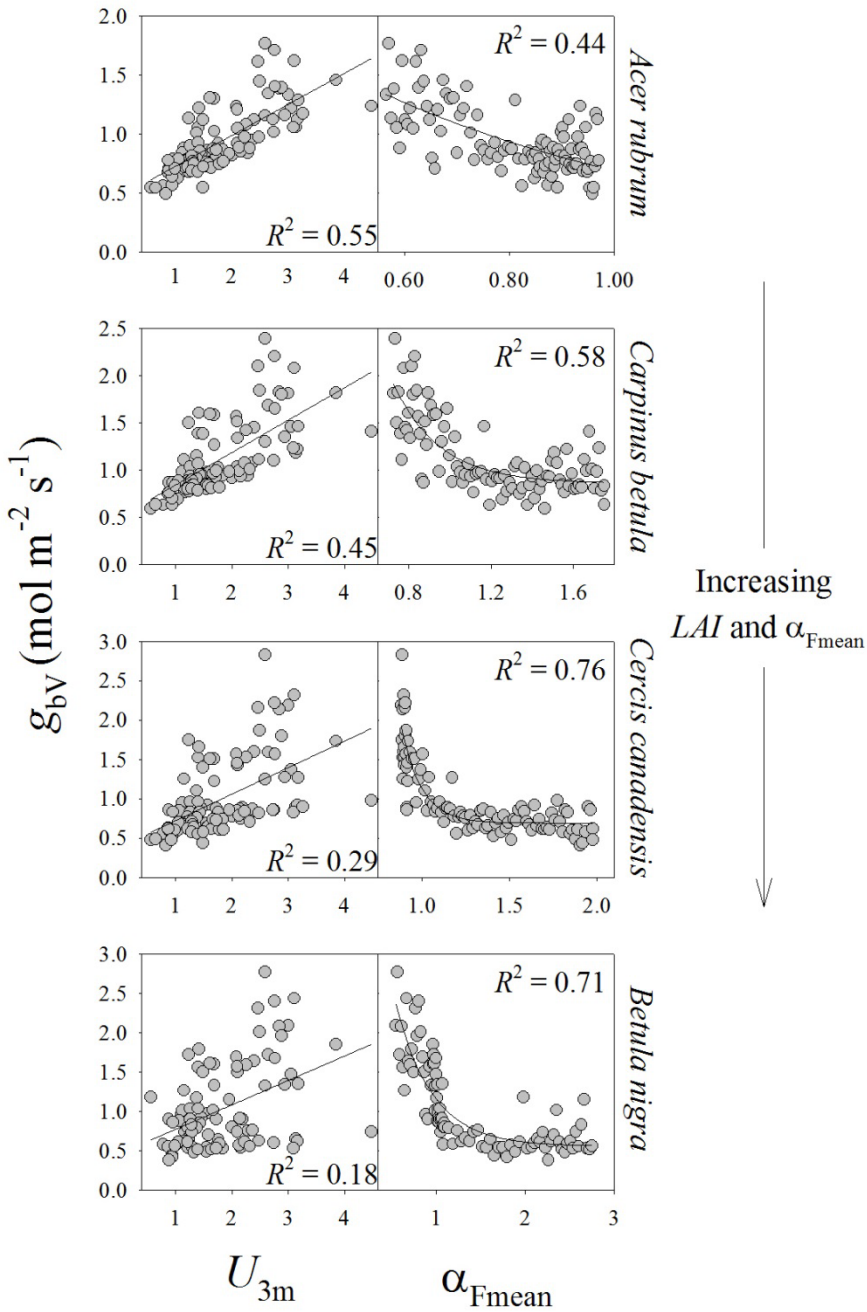

Figure 3.7: The correlation between leaf boundary layer conductance to water vapor (g_{bV}) and wind speed measured at 3 m (U_{3m}) and mean seasonal canopy wind extinction coefficient ($\alpha_{Fseason}$). The correlation between g_{bV} and α_{Fmean} increases as mean seasonal α_{Fmean} and *LAI* increase. Panels are arranged from top to bottom in increasing order of measured α (cf. Figure 3.2). Note: *y*-axis scales differ among the four species.

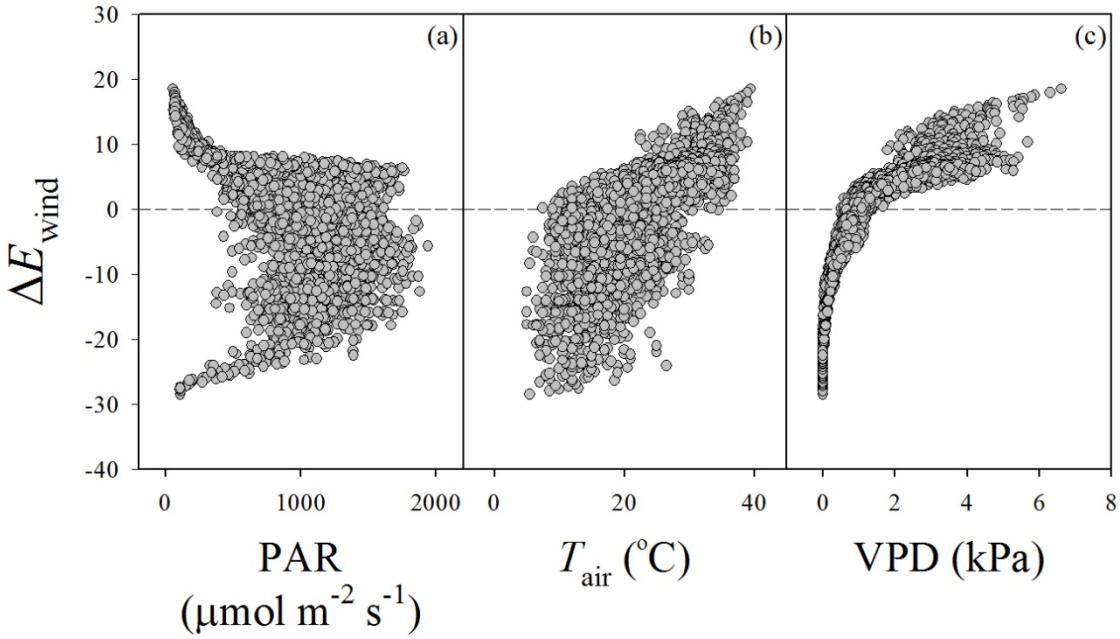

Figure 3.8: The influence of a discrete increase in wind speed (0.6 – 2.4 m^{-1}: Table 3.1) on transpiration rates (ΔE_{wind}) at 1000 random combinations of air temperature (T_{air}), photosynthetically active radiation (PAR) and vapor pressure deficit (VPD). Each panel represents a regression of the influence of wind speed plotted against the value of an individual meteorological parameter within the random combinations.

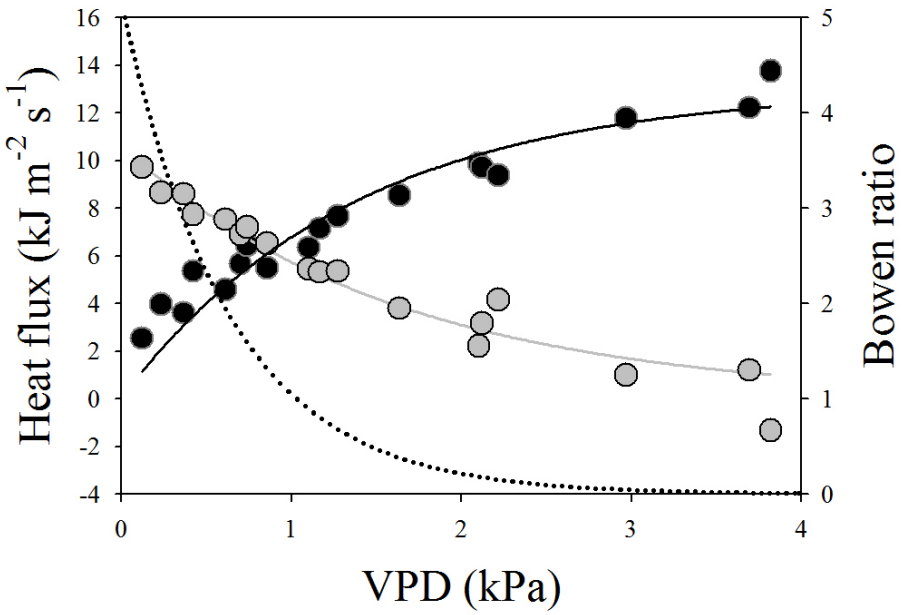

Figure 3.9: Sensible (grey circles) and latent (black circles) heat flux and the Bowen ratio (sensible to latent heat ratio; dotted line) response to increasing vapor pressure deficit (VPD). Photosynthetically active radiation was held steady at 1500 µmol m^{-2} s^{-1} while wind speed varied from 1-5 m s^{-1}.

References

Aphalo, P. and Jarvis, P., 1991. Do stomata respond to relative humidity? Plant, Cell & Environment, 14(1): 127-132.

Baldwin, J., V Clark and Peterson, K.D., 1997. Predicting the crown shape of loblolly pine trees. Canadian Journal of Forest Research, 27(1): 102-107.

Barnard, D. and Bauerle, W., 2013. The implications of minimum stomatal conductance on modeling water flux in forest canopies. Journal of Geophysical Research: Biogeosciences, 118(3): 1322-1333.

Bauerle, W.L., Bowden, J.D., McLeod, M.F. and Toler, J.E., 2004. Modeling intra-crown and intra-canopy interactions in red maple: assessment of light transfer on carbon dioxide and water vapor exchange. Tree Physiology, 24(5): 589-597.

Benyon, R.G., 1999. Nighttime water use in an irrigated *Eucalyptus grandis* plantation. Tree Physiology, 19(13): 853-859.

Bunce, J., 1985. Effect of boundary layer conductance on the response of stomata to humidity. Plant, Cell & Environment, 8(1): 55-57.

Cammalleri, C. et al., 2010. The impact of in-canopy wind profile formulations on heat flux estimation in an open orchard using the remote sensing-based two-source model. Hydrology and Earth System Sciences, 14(12): 2643-2659.

Campbell, G.S. and Norman, J.M., 1998. An Introduction to Environmental Biophysics. Springer.

Campoe, O.C. et al., 2013. Stem production, light absorption and light use efficiency between dominant and non-dominant trees of *Eucalyptus grandis* across a productivity gradient in Brazil. Forest Ecology and Management, 288: 14-20.

Cionco, R.M., 1966. A mathematical model for air flow in a vegetative canopy, DTIC Document.

Cionco, R.M., 1972. A wind-profile index for canopy flow. Boundary-Layer Meteorology, 3(2): 255-263.

Cionco, R.M., 1978. Analysis of canopy index values for various canopy densities. Boundary-Layer Meteorology, 15(1): 81-93.

Daudet, F., Le Roux, X., Sinoquet, H. and Adam, B., 1999. Wind speed and leaf boundary layer conductance variation within tree crown: consequences on leaf-to-atmosphere coupling and tree functions. Agricultural and Forest Meteorology, 97(3): 171-185.

Dawson, T.E. et al., 2007. Nighttime transpiration in woody plants from contrasting ecosystems. Tree Physiology, 27(4): 561-575.

Domingo, F., Van Gardingen, P. and Brenner, A., 1996. Leaf boundary layer conductance of two native species in southeast Spain. Agricultural and Forest Meteorology, 81(3): 179-199.

Drake, B., Raschke, K. and Salisbury, F., 1970. Temperature and transpiration resistances of *Xanthium* leaves as affected by air temperature, humidity, and wind speed. Plant Physiology, 46(2): 324-330.

Farquhar, G.D., Caemmerer, S. and Berry, J., 1980. A biochemical model of photosynthetic CO_2 assimilation in leaves of C_3 species. Planta, 149(1): 78-90.

Goudriaan, J., 1977. Crop micrometeorology: a simulation study. Pudoc, Center for Agricultural Publishing and Documentation.

Grace, J., Jarvis, P. and Norman, J., 1987. Modelling the interception of solar radiant energy in intensively managed stands. New Zealand Journal of Forestry Science, 17(2-3): 193-209.

Gutiérrez, M., Meinzer, F. and Grantz, D., 1994. Regulation of transpiration in coffee hedgerows: covariation of environmental variables and apparent responses of stomata to wind and humidity. Plant, Cell & Environment, 17(12): 1305-1313.

Inoue, E., 1963. On the turbulent structure of airflow within crop canopies. Journal of the Meteorological Society of Japan, 41: 317-326.

Inoue, K. and Uchijima, Z., 1979. Experimental study of microstructure of wind turbulence in rice and maize canopies. Bulletin of the National Institute of Agricultural Sciences. Series A. Physics and Statistics.

Jarvis, P.G. and McNaughton, K., 1986. Stomatal control of transpiration: scaling up from leaf to region. Advances in Ecological Research, 15(1): 49.

Kim, D. et al., 2014. Sensitivity of stand transpiration to wind velocity in a mixed broadleaved deciduous forest. Agricultural and Forest Meteorology, 187: 62-71.

Larcher, W., 2003. Physiological Plant Ecology: Ecophysiology and Stress Physiology of Functional Groups. Springer, NY.

Leuning, R., 1995. A critical appraisal of a combined stomatal-photosynthesis model for C3 plants. Plant, Cell & Environment, 18(4): 339-355.

Leuning, R., Kelliher, F., Pury, D.D. and Schulze, E.D., 1995. Leaf nitrogen, photosynthesis, conductance and transpiration: scaling from leaves to canopies. Plant, Cell & Environment, 18(10): 1183-1200.

Martin, T.A., Hinckley, T.M., Meinzer, F.C. and Sprugel, D.G., 1999. Boundary layer conductance, leaf temperature and transpiration of *Abies amabilis* branches. Tree Physiology, 19(7): 435-443.

Meinzer, F.C., 1993. Stomatal control of transpiration. Trends in Ecology & Evolution, 8(8): 289-294.

Monteith, J., 1965. Evaporation and environment, Symposium of the Society for Experimental Biology, pp. 4.

Mott, K.A. and Peak, D., 2010. Stomatal responses to humidity and temperature in darkness. Plant, Cell & Environment, 33(7): 1084-1090.

Nobel, P.S., 1999. Plant Physiology: Park S. Nobel. Academic press.

Oleson, K. et al., 2013. Technical description of version 4.5 of the Community Land Model (CLM), NCAR Technical Note NCAR/TN-503+STR, pp. 420.

Saito, T., 1964. On the wind profile within plant communities. Bulletin of the National Institute of Agricultural Sciences, 11: 7.

Sauer, T., Norman, J., Tanner, C. and Wilson, T., 1995. Measurement of heat and vapor transfer coefficients at the soil surface beneath a maize canopy using source plates. Agricultural and Forest Meteorology, 75(1): 161-189.

Schuepp, P., 1993. Tansley review No. 59. Leaf boundary layers. New Phytologist: 477-507.

Sellers, P. et al., 1996. A revised land surface parameterization (SiB2) for atmospheric GCMs. Part I: Model formulation. Journal of Climate, 9(4): 676-705.

Souch, C. and Stephens, W., 1998. Growth, productivity and water use in three hybrid poplar clones. Tree Physiology, 18(12): 829-835.

Taylor, P.J., Nuberg, I.K. and Hatton, T., 2001. Enhanced transpiration in response to wind effects at the edge of a blue gum (*Eucalyptus globulus*) plantation. Tree Physiology, 21(6): 403-408.

Trout, T.J., Johnson, L.F. and Gartung, J., 2008. Remote sensing of canopy cover in horticultural crops. HortScience, 43(2): 333-337.

Wang, Y.-P. and Leuning, R., 1998. A two-leaf model for canopy conductance, photosynthesis and partitioning of available energy I: Model description and comparison with a multi-layered model. Agricultural and Forest Meteorology, 91(1): 89-111.

Wang, Y. and Jarvis, P., 1990a. Description and validation of an array model—MAESTRO. Agricultural and Forest Meteorology, 51(3): 257-280.

Wang, Y. and Jarvis, P., 1990b. Influence of crown structural properties on PAR absorption, photosynthesis, and transpiration in Sitka spruce: application of a model (MAESTRO). Tree Physiology, 7: 297-316.

Wang, Y., Jarvis, P. and Benson, M., 1990. Two-dimensional needle-area density distribution within the crowns of *Pinus radiata*. Forest Ecology and Management, 32(2): 217-237.

Weiss, M., Baret, F., Smith, G., Jonckheere, I. and Coppin, P., 2004. Review of methods for in situ leaf area index (*LAI*) determination: Part II. Estimation of *LAI*, errors and sampling. Agricultural and Forest Meteorology, 121(1): 37-53.

Westgate, M., Forcella, F., Reicosky, D. and Somsen, J., 1997. Rapid canopy closure for maize production in the northern US corn belt: Radiation-use efficiency and grain yield. Field Crops Research, 49(2): 249-258.

Wright, J.L., 1965. Evaluating Turbulent Trasfer Aero-Dynamically within the Microclimate of a Cornfield, Cornell University, Ithaca, NY, 174 pp.

Chapter 4: Species-specific irrigation scheduling with a spatially explicit biophysical model: a comparison to substrate moisture sensing with insight into simplified physiological parameterization

Overview

Biophysical models that spatially characterize the photosynthesis-stomatal conductance (A_n-g_s) linkage offer a predictive approach to determining species-specific transpiration for irrigation scheduling. However, due to the complexity of physiological parameterization, biophysical models have been impractical for nursery implementation. An alternative to predictive irrigation scheduling is substrate moisture sensing, controlling irrigation based on measured volumetric water content. Substrate moisture sensing to aid irrigation scheduling is increasingly being adopted in nurseries thus a comparison with predictive control is warranted. This study had two primary goals: first, we compared the growth (crown leaf area and stem caliper) and irrigation application efficiency (e_a) of a predictive scheduling method to a substrate moisture sensing-based method in five deciduous tree species that were grown in a containerized pot-in-pot production system. The predictive method applied 18-56% more water than the sensing-based method in four species and 6% less in the fifth. Mean e_a, was 80.1 and 89.5% for predictive and sensing-based treatments respectively. Across species, predictive scheduling yielded 11-53% greater leaf area and 3.4-11% more caliper growth than sensing-based scheduling. Our second goal was to quantify the loss of transpiration estimate accuracy per species when key species-specific physiology parameter values in the A_n-g_s scheme were replaced with multi-species means. We found the accuracy of transpiration estimates to depend largely on two parameters: g_0 the minimum stomatal conductance and g_1 the marginal water cost

per unit carbon gain. When only these two parameters were characterized on a species-specific basis transpiration estimates were within 10% error >65% of the time and within 20% error >95% of the time. We conclude that the parameters g_0 and g_1 in the A_n-g_s scheme are critical to accurate species-specific transpiration estimates and that most other physiology parameters may be generalized, potentially eliminating the need for extensive A_n-g_s gas exchange experiments to parameterize individual species or varieties.

Introduction

Water resource availability for agricultural use is in decline (Vörösmarty et al., 2000), leading producers to carefully evaluate irrigation efficiency. A variety of plant monitoring, substrate moisture sensing and predictive water use methods are available to refine irrigation scheduling decisions (Jones and Tardieu, 1998; Jones, 2004). However, spatially explicit biophysical models that couple within-canopy photosynthesis-stomatal conductance (A_n-g_s) have received less attention for irrigation scheduling (Bauerle et al., 2002; Kim et al., 2008). One reason for this is the complexity involved in parameterizing and validating the species-specific physiology sub-models. Recent studies indicate that the accuracy of the A_n-g_s scheme for estimating transpiration may largely depend on two parameters however, potentially simplifying species-specific model parameterization (Bauerle and Bowden, 2011; Barnard and Bauerle, 2013). Moreover, biophysical models are relevant to predictive irrigation scheduling in containerized crops that have limited substrate volumes and likely require multiple daily irrigation events (e.g., Beeson and Haydu, 1995). Thus, an irrigation scheduling comparison between a predictive method and a substrate moisture sensing-based method is warranted,

including an assessment of the influence of physiologically-based parameters on transpiration prediction accuracy.

Substrate moisture sensing-based methods have been successful for scheduling irrigation in containerized crops (e.g., Sammons and Struve, 2008; Lea-Cox, 2012; Bayer et al., 2013; Chappell et al., 2013). However, implementation at nursery scales is limited by the need for numerous sensors to capture variation in volumetric water content (VWC) within and among containers as well as variation among species (Daniels et al., 2012; Bauerle et al., 2013). Sensing-based methods also require *a priori* analyses to determine lower and upper VWC set-points (unique to each substrate type) to serve as irrigation prompts. Alternative plant monitoring methods for irrigation scheduling have been successful (e.g., canopy temperature) but face similar limitations when moving across scales (e.g., Jones, 2004). Thus, a scalable real-time predictive method for determining crop water needs may provide a more efficient and effective way to schedule irrigation if it can reduce labor and system hardware (Romero et al., 2012; McCarthy et al., 2013).

Coupling a photosynthesis model (e.g., Farquhar et al., 1980) to a g_s model (e.g., Ball et al., 1987) is a method frequently used to predict transpiration at a variety of scales (Sellers et al., 1996; Baldocchi and Meyers, 1998; Hanson et al., 2004; Landsberg and Sands, 2010; Oleson et al., 2013). The benefit of linking a form of the Ball-Berry g_s model to A_n as opposed to an entirely empirical g_s model (e.g., Jarvis, 1976) is that it contains some parameters that are physiologically-based (Leuning, 1990; Barnard and Bauerle, 2013). In addition, substantial environmental variation within heterogeneous canopies requires spatially explicit estimates and physiological feedback to preserve the accuracy of the A_n-g_s model prediction (Bauerle et al.,

2009; Yuan et al., 2014). Such hierarchical schemes have been previously tested, validated and implemented (Wang and Jarvis, 1990b; Medlyn et al., 2007; Bowden and Bauerle, 2008).

A recent study has shown transpiration estimates derived from a Ball-Berry type g_s model to be largely dependent on two key parameters (g_0; the minimum g_s when $A_n \leq 0$ and g_1; the marginal cost of water per unit of carbon gain) (Barnard and Bauerle, 2013). The g_0 parameter has received less attention, and has typically been assumed to be unrealistically low or statistically extrapolated from A_n-g_s data collected under well-lit conditions (Barnard and Bauerle, 2013). In other studies that included sensitivity analyses, four additional physiology-based parameters have been shown to have a > 5% effect on transpiration (Bowden and Bauerle, 2008; Bauerle and Bowden, 2011), suggesting that the accuracy of transpiration estimates may largely depend on a subset of model parameters. Building upon these findings, we designed this study to accomplish two primary goals. First, we compared the growth and irrigation application efficiency (e_a) among five container grown deciduous tree species that were irrigated to maintain substrate moisture within a preset VWC range to a treatment irrigated by predictive physiologically-based transpiration estimates. Second, we assessed how much species-specific physiology is required to accurately estimate transpiration by comparing *post-hoc* parameter set simulations of generalized physiology (i.e. multi-species averages) with species-specific characterization of six key physiology parameters.

Materials and methods

Site characteristics and plant material

This study was conducted during the summer of 2012 near Avon, OH (41.433°N lat., -82.052°W long.). Zhu et al. (2005) provides a full description of the research site. Briefly, the

site consists of six plots, each containing 25 subsurface 57 L socket containers (a pot-in-pot production system). Each plot was sub divided into five rows of five sockets per row. Irrigation was controlled by a solenoid valve connected to 2.54 cm black tubing. Two pressure (137 kPa) compensated emitters with 160° spray angles (PC Spray Stake, Netafim USA, Fresno, USA) placed 10 cm from the container wall - one directly north and one south of the stem – applied irrigation at a combined flow rate of 24 L h^{-1}. Emitters were Three replicate rows of five deciduous tree species (*Acer rubrum* L. 'Red Sunset', *Betula nigra* 'Cully', *Carpinus betula* 'Columnaris', *Cercis canadensis* and *Quercus rubra*) were randomly assigned to predictive and sensing-based irrigation treatments (three plots per treatment with a replicate species row per plot). Trees were one-year-old bare-root whips planted into 57 L containers with a soil-less organic substrate consisting of a mixture of 64% pine bark, 21% peat moss, 7% Haydite© and 7% sterilized regrind. The remaining 1% was slow release fertilizer 12-0-42 (Agrozz Inc., Wooster, OH, USA). To measure leachate per species, the five sockets within a row were connected in series by subterranean PVC that channeled leachate into a tipping bucket (FC525, Texas Electronics Inc., Dallas, TX, USA). Counted tips (10 mL per tip) were recorded at one minute intervals (model CR23X, Campbell Scientific, Logan, UT, USA). A Theta Probe measured substrate moisture (model ML2x, Dynamax Corp. Houston, TX, USA). It was positioned in the eastern side of the container, halfway between the trunk and the container wall (~15 cm) with the prongs at 45° beginning 20 cm below the substrate surface. Moisture readings were logged once per minute to determine substrate dielectric permittivity (ε_a), which is converted to VWC using sensor-to-substrate specific calibration curves. Environmental conditions (temperature, wind speed, relative humidity and incident photosynthetically active

radiation (PAR)) were measured every minute and averages stored at five minute intervals (model EM50R, Decagon Devices Inc., USA) (Fig. 4.1).

Substrate moisture sensing-based irrigation

Irrigation for the sensing-based treatment was controlled within a set pre-determined well-watered VWC range of 35-42% (Model CR23X integrated with the model SDM-CD16AC 16 channel controller; Campbell Scientific, USA). If the measured VWC went below 35%, a 5-second pulse of irrigation (14 mL) was commanded every minute until substrate VWC readings became > 42%. We note that replicate rows of species in different plots were irrigated independently. A detailed description of the sensing-based system can be found in Zhu et al. (2005).

Predictive model irrigation

The predictive irrigation treatment was designed to replace water lost according to transpiration estimates. MAESTRA (Wang and Jarvis, 1990a; Medlyn, 2004), a spatially explicit and semi mechanistic flux model was parameterized with leaf-level physiology (Table 4.1) and used to calculate transpiration on a 15-minute time step from weather data collected on site (Decagon Environmental Monitoring System, Decagon, USA). A description of MAESTRA's leaf to crown transpiration linkage can be found in Medlyn et al. (2007). Software developmental issues delayed the deployment of real-time predictive irrigation until DOY 205. Prior to this date (DOY 157-204); we completed simulations once every 1-2 days to estimate average daily water use. This water use estimate was divided into six equal irrigation events, applied at 2 hour intervals between 0800 and 2000.

Irrigation application use efficiency

To determine irrigation application use efficiency (e_a), we summed the volumes of precipitation, irrigation, and leachate and calculated treatment specific efficiency as:

$$e_a = \left(\frac{V_s}{V_f}\right) \times 100 \tag{1}$$

where V_f is the volume of water applied to the substrate (both precipitation and irrigation) and V_s is the volume available in the substrate - defined as:

$$V_s = V_f - V_l \tag{2}$$

where V_l is the leached volume. The volume of precipitation for the V_f parameter was measured by a tipping bucket rain gauge (FC525, Texas Electronics Inc., USA) located in the center of the plots at a height of 3 m.

Predictive model description

Essential to solving for a discontinuous canopy MAESTRA provides a hierarchical computational-framework that divides the crown into sub-volumes and integrates multiple sub-models that are solved iteratively. The leaf area associated with each grid point was based on empirical measurements of crown leaf area, leaf optical properties, and crown shape (described below). Direct and diffuse beam radiation and within-canopy light scattering are spatially accounted for and used in leaf energy balance and temperature calculations. Leaf temperature estimates are input into a mechanistic biochemical photosynthesis model (Farquhar et al., 1980) to determine grid point A_n for sun exposed and shaded leaves calculated as:

$$A_n = \min\left(A_c, A_j, A_p\right) - R_d \tag{3}$$

where A_n is limited by Rubisco limited CO_2 assimilation rate (A_c), the Ribulose 1-5 bisphosphate regeneration (RuBP) rate of CO_2 assimilation (A_j) or the triose phosphate utilization (TPU) limiting CO_2assimilation rate (A_p) minus leaf dark respiration (R_d). The A_c limitation is calculated as:

$$A_c = V_{cmax}\left[\frac{C_C - \Gamma}{C_C + K_C(1 + O/K_O)}\right] - R_d \tag{4}$$

where V_{cmax} is the maximum rate of Rubisco carboxylation, C_c is the partial pressure at the sites of carboxylation, Γ is the CO_2 compensation point, K_c is the Michaelis-Menten constant of Rubisco for CO_2, O is the partial pressure of oxygen at the site of carboxylation and K_O is the inhibition constant of Rubisco for oxygen. The A_j limitation is calculated as:

$$A_j = J_{max}\frac{C_C - \Gamma}{4C_C + 8\Gamma} - R_d \tag{5}$$

where J_{max} is the rate of electron transport, and the A_p limitation is calculated as:

$$A_P = 3TPU - R_d \tag{6}$$

Calculated A_n is input into the semi-empirical g_s model (Leuning, 1995) for grid point specific g_s calculated as:

$$g_s = g_0 + \frac{g_1 A_n}{(C_a - \Gamma)\left(1 + \frac{VPD}{D_0}\right)} \tag{7}$$

where C_a is the CO_2 concentration of ambient air, VPD is the air vapor pressure deficit and D_0 is an empirical coefficient. Grid point g_s and canopy aerodynamics are used to determine the canopy conductance parameter in an isothermal version of the Penman-Monteith evapotranspiration equation (Monteith, 1965) calculated as:

$$E = \frac{SR_n + \rho_a C_p VPD g_k}{\lambda\left[S + \gamma\left({}^{g_k}/_{g_v}\right)\right]} \tag{8}$$

where E is transpiration, S is the slope of the saturation VPD versus air temperature, R_n is isothermal net radiation, ρ_a is dry air density, C_p is the specific heat capacity of air, λ is the latent heat of evaporation of water, γ is the psychrometric constant, g_h is leaf conductance to heat and g_v is the leaf conductance to water vapor. Because latent heat loss from evaporation (determined by grid point E) alters the leaf energy balance the process is repeated with an updated estimate until the iterations reach convergence. Within canopy point estimates are then summed for whole crown estimates.

Predictive model parameterization and growth measurements

MAESTRA integrates physiological, morphological, site (plant spacing, slope, aspect etc.), and canopy aerodynamic parameters. Bauerle and Bowden (2011) report a sensitivity analysis that identified five physiological parameters, each having > 5% influence on canopy transpiration estimates. Of the five, three were from the Farquhar et al. (1980) photosynthesis model (V_{cmax}, R_d and α; the quantum yield of photosynthesis) and two were from the Ball-Berry family of g_s models (e.g., Ball et al., 1987; Leuning, 1995; Medlyn et al., 2011) (g_0 and g_1). To characterize each of these parameters accurately and to capture potential seasonal dynamics (e.g., Bauerle et al., 2012) we collected CO_2 and light response curves (AC_i and AQ curves respectively) from identical plant material four times throughout season on one south facing, sun exposed leaf from mid canopy height (n = 4 per species) with a portable gas exchange system (Ciras-II, PP Systems, Amesburry, MA, USA). We calculated V_{cmax}, J_{max}, and g_1 (and others) from the AC_i curve (Sharkey et al., 2007) and α and R_d (and others) from AQ curves (Ögren and Evans, 1993) (Table 4.1). The g_0 parameter, which is recently thought to be the most significant Ball-Berry model parameter for accurate transpiration estimates (Barnard and Bauerle, 2013),

was measured four times throughout the season at one hour after sunset with a hand-held porometer (Model SC-1, Decagon Devices Inc., USA). Leaf absorptance, reflectance and transmittance were calculated from hand-held SPAD meter (Model SPAD-502Plus, Konica-Minolta, Tokyo, Japan) readings as per Bauerle et al. (2004b). Key physiological and morphological parameters are reported in Table 4.1.

Canopy physical dimensions (canopy height and width in the X and Y axes), trunk caliper, leaf area and leaf morphological characteristics (i.e. L_w) were measured every 14 days during the study on n = 9 trees per species per treatment. To measure leaf area we randomly sampled n = 30 leaves from each species within a treatment, photographed the leaves and determined average area per leaf using image analysis software (ImageJ, National Institutes of Health, Washington D.C., USA). We then counted the total number of leaves on n = 6 trees per species per treatment and multiplied that number by the average area per individual leaf.

Within container substrate moisture distribution

To characterize the spatial distribution of substrate moisture within the containers we deployed an array of 12 substrate moisture sensors (Model 5TM, Decagon Devices Inc. USA) in one container of four different species in the sensing-based treatment. Four sensors were placed in each of three vertical layers at 10, 20 and 30 cm below the substrate surface (one in each cardinal direction) inserted horizontally 15 cm inward from the container wall through holes drilled in the container side. All substrate moisture sensors in the array were connected to a wireless data collection node (EM50R, Decagon Devices Inc., USA) to measure sensor output and record a five-minute average. We were unable to collect these measurements in *Q. rubra* due to numerous sensor failures throughout the season.

MAESTRA performance with generalized physiology parameters

To test the accuracy of transpiration estimates when parameterized with generalized multi-species means in place of species-specific measured values we combined the validated physiological parameter set (Barnard and Bauerle, 2013) with the observed canopy dimensions and leaf area (from this study) to calculate daily benchmark transpiration estimates for each of the five study species. Generalized multi-species parameter values were calculated as the mean of nine deciduous hardwood tree species (the five species used in this study plus four additional species – Table 4.1). All together, these nine trees species were chosen to represent a variety of species of ecological and commercial significance that would also be representative of the temperate broadleaf deciduous tree functional type used in large scale land surface schemes (Oleson et al., 2013). We then compared that benchmark model estimate to *post-hoc* model estimates in which one or more of the input parameters were generalized to determine parameter specific influence on seasonal transpiration estimates. Because V_{cmax} and J_{max} parameters both display seasonal responses to day length (which can be estimated for any day of the year given the target day and a measurement of V_{cmax} or J_{max} at the summer solstice (Bauerle et al., 2012) we used interspecific means of V_{cmax} and J_{max} collected on the summer solstice (V_{cmax}* and J_{max}*, Table 4.1) to estimate these parameter values at six time points through the growing season (day of year 153, 172, 198, 224, 250 and 283).

Results

Tree water use and irrigation application efficiency

In terms of total volume of applied irrigation, about 1.4x more water was applied to the predictive treatment versus the sensing-based treatment across all species (Table 4.2). In both

scheduling treatments, *B. nigra* was provided with the largest total volume of irrigation (1197 and 770 L tree^{-1} for predictive and sensing-based treatments respectively). For the predictive treatment, *Q. rubra* received the least total irrigation (303 L tree^{-1}), whereas *C. betula* received the least amount in the sensing-based treatment (238 L tree^{-1}). However, *C. betula* had the second greatest volume of irrigation (516 L tree^{-1}) in the predictive treatment.

When normalized by leaf area, differences in irrigation application volumes were not much different with an average of 1.33x irrigation applied to the predictive treatment (1.57 L m^{-2} d^{-1}) than to the sensing-based treatment (1.18 L m^{-2} d^{-1}) (Table 4.2). Despite the total volume of water applied being greater in the predictive treatment of *A. rubrum*, the volume applied per m^2 of leaf area was less. In the other four species, the predictive treatment had both the greater total volume applied and volume applied per leaf area with C. *betula* receiving the most water per day (2.19 L m^{-2} d^{-1}) and *Q. rubra* receiving the least (1.09 L m^{-2} d^{-1}). In the sensing-based treatment, *B. nigra* received the most irrigation (1.33 L m^{-2} d^{-1}) and *C. betula* the least (1.06 L m^{-2} d^{-1}). Differences in applied irrigation between the two treatments, using MAESTRA estimates as the benchmark, varied daily, ranging from ~6 L m^{-2} d^{-1} to near zero (Fig. 4.2). *Carpinus betula* had the largest average difference in applied water between treatments (0.91 L m^{-2} d^{-1}) and *B. nigra* had the second largest difference (0.65 L m^{-2} d^{-1}). The average difference between treatments for *A. rubrum* and *C. canadensis* was 0.04 and 0.17 L m^{-2} d^{-1} respectively. *Quercus rubra* was the opposite of other species with 0.04 L m^{-2} d^{-1} more water applied in the sensing based treatment.

Across all species, total leachate was 2.6x greater in the predictive treatment than the sensing-based treatment, with a total of 583 and 219 L tree^{-1} leached respectively (Table 4.2). Among all species and treatments, predictive *C. betula* had the largest total leachate volume (211 L tree^{-1}) and sensing-based *A. rubrum* had the lowest (16 L tree^{-1}).

Normalizing total leachate volume by the amount of water applied (i.e. precipitation and irrigation) yields e_a's that were greater in the sensing-based treatment than the predictive treatment (Table 4.2). On a species basis, the predictive treatment e_a was linearly correlated with e_a in the sensing-based treatment (R^2 = 0.63; data not shown) but irrigation was overall ~9% more efficient in the sensing-based treatment (80.1% versus 89.5%). Sensing-based irrigation for *A. rubrum* was the most efficient (~95%) with *B. nigra* also performing at >90% e_a. *Carpinus betula* had the lowest e_a of all five species in both treatments (58.9 and 73.8% for predictive and sensing-based treatments respectively).

When normalized by leaf area, all predictive treatment species except *A. rubrum* transpired more water per day (Table 4.2). Within the predictive treatment, *B. nigra* had the highest daily water use (1.73 L m^{-2} d^{-1}) and *Q. rubra* had the lowest (1.04 L m^{-2} d^{-1}). Within the sensing-based treatment *A. rubrum* had the highest daily water use (1.12 L m^{-2} d^{-1}) and *C. betula* had the lowest (0.94 L m^{-2} d^{-1}). The predictive treatment typically transpired 1.2 - 1.7x more water per m^2 of leaf area than the sensing-based treatment.

Seasonal tree growth and container VWC

Trees from the predictive irrigation treatment plots had greater caliper growth by the end of the season (Fig. 4.3). The species with the largest difference in caliper growth between predictive and sensing-based treatments was *B. nigra* with ~11% greater caliper in the predictive irrigation treatment, whereas the other four tree species ranged from 3.4% (*Q. rubra*) to 8% (*C. betula*) (Fig. 4.3).

Canopy leaf area accumulation was also greater in trees irrigated with the predictive method (Fig. 4.4). Maximum canopy leaf area was the greatest in *B. nigra* with ~7 m^2 of leaf

area in the predictive treatment, whereas sensing-based trees developed ~6 m^2 of canopy leaf area (i.e. ~15% difference in canopy leaf area between treatments, the second smallest difference between treatments). *Carpinus betula* had the largest difference in maximum leaf area between treatments (53%). The predictive treatment of *A. rubrum* had the second largest maximum leaf area (~4.7 m^2) and the second largest difference of leaf area between treatments (44%). *C. canadensis* and *Q. rubra* had the third and fifth smallest difference in leaf area between treatments with a 23% and 11% difference respectively.

Between treatment and spatial variation in within container substrate moistures

Over a representative period of ten days that consisted of high, medium and low transpiration rates (Fig. 4.5a), the mean container VWC for the predictive treatment of *A. rubrum* was 42.8% with a coefficient of variation of 2.9%. The mean VWC in the sensing-based treatment was slightly lower (40.1%) with a coefficient of variation >2x higher than the predictive treatment (6.4%) (Fig. 4.5b).

Container VWC varied along a vertical height gradient, increasing linearly with depth. Sensors in the middle layer of the container (i.e. 20 cm) were more characteristic of mean container VWC than other depths (Table 4.3). The east sensor at the 20 cm depth (which corresponded with the Theta Probe sensor locations in the sensing-based treatment) was commonly the first or second best sensor to represent bulk container VWC. The exception to this was *C. canadensis* in which the east sensor at 20 cm was the fourth least representative sensor and the sensor at the 30 cm depth was the most representative. The east sensor at 20 cm was more representative of bulk container VWC more than 90% of the time in *A. rubrum* and *C. betula*, while only being representative 65.8% of the time in *B. nigra*.

MAESTRA simulations and performance with a generalized parameter set

By generalizing one physiology parameter at a time, it was clear that individual parameter influence on daily transpiration estimates varied from day to day and within species (Table 4.4). Overall, g_0 and g_1 were the two parameters with the greatest daily influence, averaging 12.8 and 15.2% respectively. The one exception was *C. betula*, where α was the parameter with the second highest influence. Regardless, J_{max} was consistently the least influential parameter (1.16%); R_d and V_{cmax} were both ~1.4% and α had a 1.92% influence. Across species R_d, J_{max}, V_{cmax}, and α could all be generalized without having >10% influence on daily transpiration estimates. Both g_0 and g_1 emerged as reliable predictors of measured water use in the predictive treatment as evidence from a strong linear relationship with transpiration (Fig. 4.6).

When we generalized R_d, J_{max}, V_{cmax}, and α but retained species-specific g_0 and g_1, all five species were within 10% of the benchmark species-specific transpiration estimates on >65% of the days during the experimental period and within 20% of the benchmark more than 95% of the days (Table 4.5). When species-specific g_1's were replaced with interspecific means, *C. betula* and *B. nigra* were still within 10% of the benchmark estimates >90% of the time and were within 20% for all days of the study. *Acer rubrum* was only within 10% of the benchmark ~50% of the time but within 20% of the benchmark every day. Both *Q. rubra* and *C. canadensis* where within 10% of the benchmark <25% of the days, but were within 20% of the benchmark for ~40% of the days. When both species-specific g_0 and g_1 were replaced with generalized interspecific means, *A. rubrum*, *B. nigra*, and *C. betula* were all within 20% of the benchmark >98% of the time (with *B. nigra* being within 10% over 90% of the time). *Cercis canadensis* and *Q. rubra* were within 20% <6% and were never within 10% of the benchmark.

For g_0 and g_1, the percent difference between transpiration estimates when the model was run with species-specific values for these two parameters versus the generalized multi-species mean was correlated with the difference between the species-specific value and the generalized value (Fig. 4.7). The correlation was stronger for g_0 (R^2 = 0.99) than it was for g_1 (R^2 = 0.91).

Error accumulation over the entire season was the greatest when g_0 and g_1 were generalized (ranging from -200% up to 600% error accumulation) (Fig. 4.8a). *Quercus rubra* was the most heavily influenced by the generalization of these two parameters with >400% error per parameter. The remaining four parameters (R_d, J_{max}, V_{cmax}, and α) had variable but much smaller transpiration influences than g_0 and g_1 (Fig. 4.8b).

Discussion

Higher growth rates in the predictive treatment were mostly the result of greater irrigation volumes. However, *Q. rubra* had higher growth in the predictive treatment as well, but with less water applied - a difference that may be due in part to the more frequent irrigations in the predictive method. Previous studies have reported greater plant growth in containerized plants when daily irrigation volume is applied in smaller quantities several times per day instead of receiving the same volume all at once (Ruter, 1998; Beeson and Keller, 2003). It is important to note that the sensing-based treatment had fewer irrigation events because the difference between the lower and upper VWC set-points (i.e. 35 and 42% respectively) was large enough that only 2-4 irrigation events occurred each day, resulting in a lower mean VWC. Prior to beginning this study, we chose the 35-42% range using two criteria: first, for the upper set-point, our sensor calibrations with this substrate indicated that 43% VWC was container capacity and preliminary work showed that setting the upper set-point at 43% would result in almost continuous irrigation,

but 42% did not. Second, for the lower set-point, studies using similar potting mediums reported a loss of water use efficiency at VWC <35% (Bayer et al., 2013). We did observe that VWC could go above 43% during large precipitation events (cf. arrow in Fig. 4.5b), but note that overall the predictive method maintained a higher average VWC than the sensing-based treatment. Nevertheless, had we chosen a smaller window *a priori* (in particular using a higher VWC for the low-end set-point) the sensing-based treatment would have applied water more frequently, achieved a higher mean VWC and would have potentially produced more growth. Hence, it is difficult to conclude that the predictive method is superior to sensor-based control given growth and irrigation efficiency in this study alone. Future studies would benefit from testing various substrate moisture ranges and mean VWC levels to identify which proves optimal for a given substrate and/or species. The research in this area has thus far been restricted to field grown crops (e.g., Dabach et al., 2013)

There was variation in e_a among species and between treatments due to substrate hydraulic properties and species-specific traits that affect water uptake. On average, e_a was ~10% greater in the sensing-based treatment than the predictive treatment with greater irrigation volumes being coupled with greater leachate. However, high leachate may not be due entirely to greater irrigation volumes. More frequent irrigation events in the predictive treatment likely led to the development of preferential water flow pathways within the substrate (Bacci et al., 2003) which would result in water channeling towards container drainage holes. In the sensing-based method, however, the less frequent irrigation events allowed the substrate to dry down to a lower VWC, potentially priming the substrate to absorb more of the irrigation dosage (Naasz et al., 2005).

On a species basis however, the correlation between treatment e_a's suggest that variation in e_a may be determined by species-specific root system characteristics. For example, a higher proportion of fine uptake roots to coarse transport roots or the presence of larger first-order (i.e. fine uptake) roots can result in greater bulk root water uptake and potentially higher e_a (Gardner, 1964; Andreu et al., 1997; Amato and Ritchie, 2002). While we did not collect root measurements in this study, Bauerle et al. (2013) investigated within container root characteristics in six tree species (including the five used in this study) of comparable age and grown in the same containers and substrate. We observed a positive linear trend between mean species e_a and the surface area of first-order roots from the Bauerle et al. (2013) study but no significant relationship between mean species e_a and mean root diameter or mean root length. We believe this relationship may identify one potential causative factor determining species differences in water uptake and variation in e_a.

Excess irrigation is sometimes applied to leach fertilizer salts that accumulate in containerized substrates (Yeager et al., 1997; Jacobs and Timmer, 2005; Sammons and Struve, 2010). Previous studies suggest that leaching fractions (100 - e_a) between 10-20% can reduce salt buildup (Moratiel and Martínez-Cob, 2013; Stanley, 2013) and best management practices recommend a 20% leaching fraction (Yeager et al., 1997) - although even higher leaching fractions have been reported in irrigation comparison studies (~35%; Incrocci et al., 2014). In this study, we observed a wide range of leaching fractions from 4.2% up to 41.1%. The average leaching fraction for the predictive treatment was ~20% and in agreement with best management practices (Yeager et al., 1997). The average leaching fraction in the sensing-based treatment was closer to 10% with two species at ~5%. Lower leaching fractions in the sensing-based treatment did accrue water savings, but they came at the cost of reduced growth from salt and/or water

stress (Sammons and Struve, 2010). Thus, growers using a moisture sensing-based method might need to monitor substrate salt content so they can manually command irrigation events to leach salts.

Container grown plants are often widely-spaced to create an open canopy for maximum light interception (Papadopoulos and Pararajasingham, 1997; Bauerle et al., 2004). The resulting canopy structure has relatively high aerodynamic roughness and is well-coupled to the atmosphere - lending the majority of transpiration control to species-specific stomatal regulation (Jarvis and McNaughton, 1986; Meinzer, 1993). We confirmed stomatal control of transpiration in this study with the observation of different transpiration rates among species and between treatments on a m^2 of leaf area basis. In addition to species differences in water use we also observed a strong linear relationship between measured transpiration rates and stomatal parameters in the predictive treatment (e.g., g_0 and g_1). Recent studies have identified the importance of these two parameters in predicting transpiration rates in linked A_n-g_s schemes (Xu and Baldocchi, 2003; Bauerle and Bowden, 2011; Medlyn et al., 2011; Barnard and Bauerle, 2013), but this is the first study to identify a direct relationship between g_s model parameters and measured whole-plant transpiration. However, the relationship between g_s model parameters and measured transpiration was less clear in the sensing-based treatment, suggesting that less frequent irrigation and lower water volumes may have resulted in marginal water stress (Beeson and Keller, 2003). Nevertheless, given the identical environmental conditions of the shared plots in this study, transpiration rates were lower in four of the five species in the sensing-based treatment, indicating that g_s was constrained. Future studies would benefit from coupled measurements of A_n-g_s and leaf and substrate water potential when comparing irrigation scheduling methods to determine the effect of irrigation frequency on whole plant water status.

While potentially easier to apply at the plot scale, farm scale deployment of sensing-based irrigation scheduling would be labor and hardware intensive and involve numerous logistical difficulties. First, while the cost of substrate moisture sensors has continually declined, the need for numerous sensors (and subsequent data loggers) to characterize species-specific moisture status marginalizes decreases in costs per-sensor (Daniels et al., 2012; McCarthy et al., 2013). Second, moisture sensors have a limited life span under field conditions and can be difficult to remove from containers following a season or more of root growth. Moreover, in the case of emerging wireless sensors, they could accidentally be shipped with the container at the time of sale. Sensors also require a substrate specific calibration to account for the physical differences in water holding capacity – creating a barrier to adoption for nurseries that customize substrates for different species. Finally, the spatial variability of substrate moisture and root distribution within a container necessitates that sensors be placed in the identical position among containers (Daniels et al., 2012; Bauerle et al., 2013). Similar to Bauerle et al. (2013), we observed the middle of the container to represent bulk container VWC >90% of the time.

The complexity of integrating various technologies in order to operate biophysical models in real-time could prove to be problematic over large ornamental production sites that contain hundreds of species and cultivars. However, predictive control may offer the most robust irrigation scheduling tool in the future given its ability to operate for long periods of time without expert intervention, minimal hardware requirements and because of its stability due to the potential for season long calibration (Romero et al., 2012; McCarthy et al., 2013). Predictive control has had few agricultural applications in the past due to lack of user friendly open-source models (Romero et al., 2012). The model formation used in this study (MAESTRA), while complex, is open source and well documented. Hence, the second of our primary goals in this

study was to identify methods in which the complexity of MAESTRA could be simplified to improve species or cultivar based implementation at the farm scale.

Two possibilities that could reduce the complexity of MAESTRA would be (1) to identify key physiological transpiration parameters and focus efforts towards their characterization with less effort placed on the parameters that have less influence on model output (discussed below) or (2) to categorize species into transpiration functional groups based on an easily measurable physiological characteristic that relates to water use. In the latter, we propose using the g_s model parameter g_0 to determine functional group classification. Not only did we observe a strong relationship between measured transpiration and g_0 in this study (Fig. 4.6) but g_0 has been shown to be the most influential parameter for predicting transpiration and it can be easy to measure with a hand-held porometer (Barnard and Bauerle, 2013).

To minimize the amount of species-specific physiology parameters we compared *post hoc* the decrease in model accuracy as species-specific physiological parameters were substituted for generalized multi-species averages (c.f. Table 4.1). The multi-species averages were analogous to plant functional type values (i.e. identical physiology parameter values that are representative of a plant functional type e.g. deciduous hardwoods) (Oleson et al., 2013). We acknowledge that generalizing parameters among species can be perceived as a contradiction to modeling species-specific transpiration. However, a tradeoff exists between the complexity of model formulation and accuracy. The collective error from species-specific gas exchange measurements combined with non-linear statistical analyses used to obtain parameter values from that data may cancel out greater process representation (Reynolds and Acock, 1985). However, we found that all but two of the species-specific parameters in the A_n-g_s scheme could be replaced with a general multi-species mean value while encountering limited loss of

transpiration estimate accuracy. The parameters that we found to be generalizable were all from the photosynthetic sub-model: J_{max}, V_{cmax}, R_d, and α. The amount of time and labor involved in characterizing J_{max}, V_{cmax}, R_d, and α on a species (let alone cultivar) basis is substantial. At the expense of a 5-10% reduction in transpiration prediction accuracy for the species in this study, gas exchange experiments could be substantially reduced. We note that our parameter influence findings are lower than previously published studies that report J_{max}, V_{cmax}, R_d, and α as having a greater effect on transpiration estimates (Bauerle and Bowden, 2011; Barnard and Bauerle, 2013). However, it is important to compare methods. Both Bauerle and Bowden (2011) and Barnard and Bauerle (2013) tested the influence of individual parameters by observing the change in model output over a range of observed intraspecific variation (i.e. a species mean ± standard deviation). In this study, we took a different approach and tested how model output changed when a generalized value was used in place of a species-specific value for a given parameter. Using a single parameter value to represent a group of species is equivalent to the method used in larger-scale terrestrial models that characterize vegetation on a plant functional type basis. In fact, they often times use the same values for multiple plant functional types (e.g., Oleson et al., 2013). We found strong non-linear relationships between the deviation from a species-specific physiology parameter value and its influence on transpiration in g_0 and g_1 (i.e. Fig. 4.6) and weaker relationships with other parameters (data not shown). Hence, using identical values across physiologically diverse sub-groups may present a substantial source of error in transpiration estimates. We note that the hierarchy of influence we report for A_n parameters pertains specifically to transpiration estimates and A_n would likely be more influential for carbon flux predictions (e.g., Bauerle et al., 2014).

Unlike the photosynthetic parameters that may be generalized with a minimal loss of transpiration predictive accuracy, g_s model parameters (i.e. g_0 and g_1) require species-specific characterization. The influence of these parameters for predicting transpiration has been reported elsewhere (e.g., Baldocchi et al., 2002; Bauerle and Bowden, 2011; Medlyn et al., 2011), but this is the first study to identify the percent loss in predictive accuracy when generalized among several deciduous species. We found that g_0 and g_1 were the two most influential parameters in determining transpiration predictive accuracy in all species except *C. betula* (α was higher than g_1; Table 4.5). In all five species, daily irrigation estimates could be within 20% accuracy >95% of the time when only g_0 and g_1 were parameterized on a species-specific basis and within 10% on >65% of the days during the study period (with >96% of the days in three of the five species; Table 4.5). Once species-specific characterization of g_1 is removed the *post-hoc* model runs become unreliable in *C. canadensis* and *Q. rubra* >50% of the time. When all parameters are generalized only *A. rubrum*, *B. nigra* and *C. betula* maintain accuracy within 20% on most days. Studies indicate that although the range of g_0 and g_1 across all species can be large, they can often be categorized into smaller ranges per plant functional type (Caird et al., 2007; Medlyn et al., 2011).

Conclusions

Irrigation scheduling has developed into a mature field (Jones, 2004). However, few studies have directly compared the performance of irrigation scheduling methods in real-time and no study to our knowledge has used a spatially explicit biophysical model to schedule irrigation in real time. Greater water application volumes and/or more frequent irrigation events resulted in the predictive method producing greater canopy leaf area development and stem

caliper, at the expense of slightly lower e_a than the substrate moisture sensor-based method. While the predictive method was superior in terms of producing more plant growth in this study, both it and sensing-based methods provided realistic avenues for improving nursery-level water use. We observed a marginal loss of transpiration estimate accuracy when photosynthetic parameters where generalized, but g_0 and g_1 in the A_n-g_s scheme must remain characterized on a species-specific basis to maintain predictive accuracy. The ability to generalize multiple physiology parameters in biophysical models represents a step forward in making such model formulations applicable across species. Furthermore, the influence of these parameters on the accuracy of transpiration predictions will help to inform larger scale modeling efforts that use the A_n-g_s sub model scheme.

Tables

Table 4.1: Species-specific physiology parameters (mean ± standard deviation) used in this study. Minimum stomatal conductance (g_0), marginal water cost per unit of carbon gain (g_1), seasonal mean maximum-Rubisco mediated rate of carboxylation (V_{cmax}), maximum-Rubisco mediated rate of carboxylation measured on the summer solstice (V_{cmax}*), seasonal mean maximum electron transport rate (J_{max}), maximum electron transport rate measured on the summer solstice (J_{max}*), leaf dark respiration (R_d) and quantum yield of electron transport (α). Reported mean and standard deviation calculated from four time points throughout the season (DOY 140, 182, 215 and 288) where each time point included n = 4 replicate trees. The mean value in the far right column is calculated from the nine species.

	Units	*Acer rubrum*	*Betula nigra*	*Carpinus betula*	*Cercis canadensis*	*Quercus rubra*	*Acer saccharum*	*Magnolia stellata*	*Gelditsia triacanthos*	*Platanus acerifolia*	**Mean**
g_0	(mmol m^{-2} s^{-1})	32.6 ± 22	51.2 ± 14	61.8 ± 32	26.6 ± 13	18.9 ± 6	29.5 ± 4	38.2 ± 11	21.4 ± 6	42.9 ± 9	**35.9 ± 14**
g_1	(dimensionless)	7.7 ± 3.7	8.1 ± 3.7	9.5 ± 2.6	8.2 ± 3.6	7.1 ± 4.7	11.3 ± 1.6	9.9 ± 4.3	5.6 ± 2.6	7.9 ± 0.7	**8.49 ± 3.9**
V_{cmax}	(µmol m^{-2} s^{-1})	45.6 ± 11.7	56.1 ± 12.9	43.9 ± 7.2	43.6 ± 6.9	44.7 ± 12.3	40.7 ± 9.8	34.7 ± 8.7	23.9 ± 3.4	52.0 ± 10.1	**42.8 ± 9.3**
V_{cmax}*	(µmol m^{-2} s^{-1})	59.7 ± 2.4	71.58 ± 4.5	51.65 ± 4.5	41.03 ± 2.8	58.53 ± 6.9	68.55 ± 4.2	53.70 ± 3.7	36.60 ± 2.5	76.9 ± 8.7	**56.2 ± 13.4**
J_{max}	(µmol m^{-2} s^{-1})	131.7 ± 46.6	164.3 ± 50.1	157.7 ± 65.4	120.3 ± 15.9	152.3 ± 47.4	140.3 ± 34.9	106.3 ± 29.4	79.5 ± 19.3	178.5 ± 65.1	**141.4 ± 33.9**
J_{max}*	(µmol m^{-2} s^{-1})	205.1 ± 21	222.7 ± 53	249.4 ± 61	138.5 ± 34	243.2 ± 67	244.5 ± 45	198.1 ± 39	127.5 ± 21	273.3 ± 82	**208.1 ± 48**
R_d	(µmol m^{-2} s^{-1})	1.76 ± 0.9	1.80 ± 0.6	1.71 ± 0.8	2.56 ± 1.2	1.75 ± 0.9	1.42 ± 0.4	1.42 ± 0.7	1.96 ± 0.5	2.52 ± 1.1	**1.88 ± 0.4**
α	(mol e$^-$ mol^{-1} PAR)	0.143 ± 0.06	0.124 ± 0.02	0.116 ± 0.03	0.139 ± 0.04	0.131 ± 0.02	0.101 ± 0.03	0.139 ± 0.02	0.253 ± 0.06	0.128 ± 0.04	**0.138 ± 0.04**

Table 4.2: Species-specific total volume of water applied (irrigation and precipitation) and leached, irrigation application efficiency (e_a), mean daily water applied per m^2 of leaf area (does not include precipitation) and mean daily water transpired per m^2 of leaf area for predictive and sensing-based irrigation treatments for the five study species.

	Predictive	**Sensing-based**
Acer rubrum		
Total volume water applied/leached (L $tree^{-1}$)	470 / 86	389 / 16
e_a (%)	81.7	95.8
Mean daily water applied (L m^{-2} d^{-1})	1.21	1.24
Mean daily water transpired (L m^{-2} d^{-1})	1.11	1.12
Betula nigra		
Total volume water applied/leached (L $tree^{-1}$)	1197 / 185	777 / 43
e_a (%)	84.5	94.4
Mean daily water applied (L m^{-2} d^{-1})	2.01	1.33
Mean daily water transpired (L m^{-2} d^{-1})	1.73	1.04
Carpinus betula		
Total volume water applied/leached (L $tree^{-1}$)	516 / 211	238 / 62
e_a (%)	58.9	73.8
Mean daily water applied (L m^{-2} d^{-1})	2.19	1.06
Mean daily water transpired (L m^{-2} d^{-1})	1.58	0.94
Cercis canadensis		
Total volume water applied/leached (L $tree^{-1}$)	453 / 49	372 / 38
e_a (%)	89.3	89.8
Mean daily water applied (L m^{-2} d^{-1})	1.34	1.12
Mean daily water transpired (L m^{-2} d^{-1})	1.34	1.10
Quercus rubra		
Total volume water applied/leached (L $tree^{-1}$)	303 / 52	321 / 60
e_a (%)	82.7	81.5
Mean daily water applied (L m^{-2} d^{-1})	1.09	1.13
Mean daily water transpired (L m^{-2} d^{-1})	1.04	0.96
Total irrigation applied/leached (L $tree^{-1}$)	2939 / 583	2097 / 219
Mean e_a (%)	80.1	89.5

Table 4.3: Container moisture sensor locations and their relation to bulk container moisture content (calculated as the average of 12 sensors). Sensors were installed at depths of 10, 20 and 30 cm below the substrate surface and the container was placed within the socket such that sensor locations within a vertical layer corresponded to the four cardinal directions. The east sensor at 20 cm (denoted with a *) corresponds to the location of the Theta-probe in the sensing-based irrigation treatment. The three most representative sensors of bulk container moisture are indicated by bold font with their rank in parentheses.

Sensor depth	Sensor location	*Acer rubrum*	*Betula nigra*	*Carpinus betula*	*Cercis canadensis*
10 cm	North	8.3	21.1	3.9	56.7
	East	7.8	40.3	2.8	49.7
	South	9.9	26.6	4.0	25.4
	West	2.2	17.7	2.1	14.8
20 cm	North	37.6	**84.1 (1)**	**93.7 (1)**	**58.4 (3)**
	East*	**97.5 (1)**	**65.8 (2)**	**90.4 (2)**	27.9
	South	**85.6 (3)**	**64.2 (3)**	**85.7 (3)**	**59.1 (2)**
	West	**85.7 (2)**	58.7	76.3	36.5
30 cm	North	8.3	21.1	3.9	31.2
	East	7.8	40.3	2.8	32.2
	South	9.9	26.6	4.1	**60.1 (1)**
	West	2.3	27.8	2.0	9.1

Table 4.4: The influence of physiological parameters on daily transpiration estimates when the species-specific measured value is replaced with a multi-species generalized mean. Within a species the parameters are ranked top-to-bottom in order of their percent influence on model output (second column) and the percent influence is reported in the individual parameter influence column. The additive influence column shows how, starting with the parameter with the lowest influence, the influence of generalizing additional parameters (individually) is cumulative on model output. The final bolded number per species indicates the total error that would be encountered if all six parameters were generalized. Generalized parameter values were calculated as the interspecific mean of nine deciduous hardwood tree species (cf. Table 4.1).

Species	**Parameter**	**Individual parameter influence (%)**	**Additive parameter influence (%)**
Acer rubrum	J_{max}	0.45	0.45
	R_d	0.67	1.12
	α	0.87	1.99
	V_{cmax}	1.99	3.98
	g_0	3.03	7.01
	g_1	16.98	**23.99**
Betula nigra	R_d	0.65	0.65
	J_{max}	0.74	1.39
	V_{cmax}	1.18	2.57
	α	2.54	5.11
	g_1	9.87	14.98
	g_0	11.25	**26.23**
Carpinus betula	V_{cmax}	0.42	0.42
	J_{max}	0.55	0.97
	R_d	0.78	1.75
	g_1	2.11	3.86
	α	4.35	8.16
	g_0	16.66	**24.82**
Cercis canadensis	α	0.25	0.25
	J_{max}	1.95	2.20
	V_{cmax}	2.49	4.69
	R_d	4.29	8.98
	g_0	11.22	20.20
	g_1	14.55	**34.70**

Quercus rubra	R_d	0.84	0.84
	V_{cmax}	1.31	2.15
	α	1.59	3.74
	J_{max}	2.14	5.88
	g_0	21.95	27.83
	g_1	32.61	**60.44**

Table 4.5: Model performance with and without generalized parameterization of g_0 and g_1. Values were calculated as the interspecific mean of nine deciduous hardwood tree species (cf. Table 4.1). The second column indicates the parameters generalized (i.e. species-specific parameterization). Mean, maximum (Max.) and minimum (Min.) daily departures are calculated with the validated species-specific output as the benchmark against which generalized model runs were compared. The final two columns report the percentage of days (out of 153 days) that result in water use predictions within 10% and 20% of the validated species-specific model estimates when generalized parameters are used as input.

	Parameters not generalized	**Mean daily departure (%)**	**Max. daily departure (%)**	**Min. daily departure (%)**	**% of days within 10%**	**% of days within 20%**
Acer rubrum	g_0 and g_1	-5.8	-10.7	-4.1	98.7	100
	g_0	9.8	3.3	12.9	50.3	100
	none	12.6	8.2	15.9	9.8	100
Betula nigra	g_0 and g_1	-3.6	-14.0	0.03	96.7	100
	g_0	5.2	12.9	0.05	94.1	100
	none	-5.8	-16.8	-0.03	91.5	100
Carpinus betula	g_0 and g_1	1.4	5.9	0.05	100	100
	g_0	3.8	8.6	-0.03	100	100
	none	-12.2	-25.3	-3.6	27.5	98.0
Cercis canadensis	g_0 and g_1	7.2	14.4	-0.01	67.3	100
	g_0	22.5	10.7	34.5	0	41.8
	none	31.9	16.6	46.5	0	2.6
Quercus rubra	g_0 and g_1	-7.4	-22.2	-0.07	66.7	95.4
	g_0	22.2	47.9	1.1	20.3	46.4
	none	43.0	80.7	12.8	0	5.2

Figures

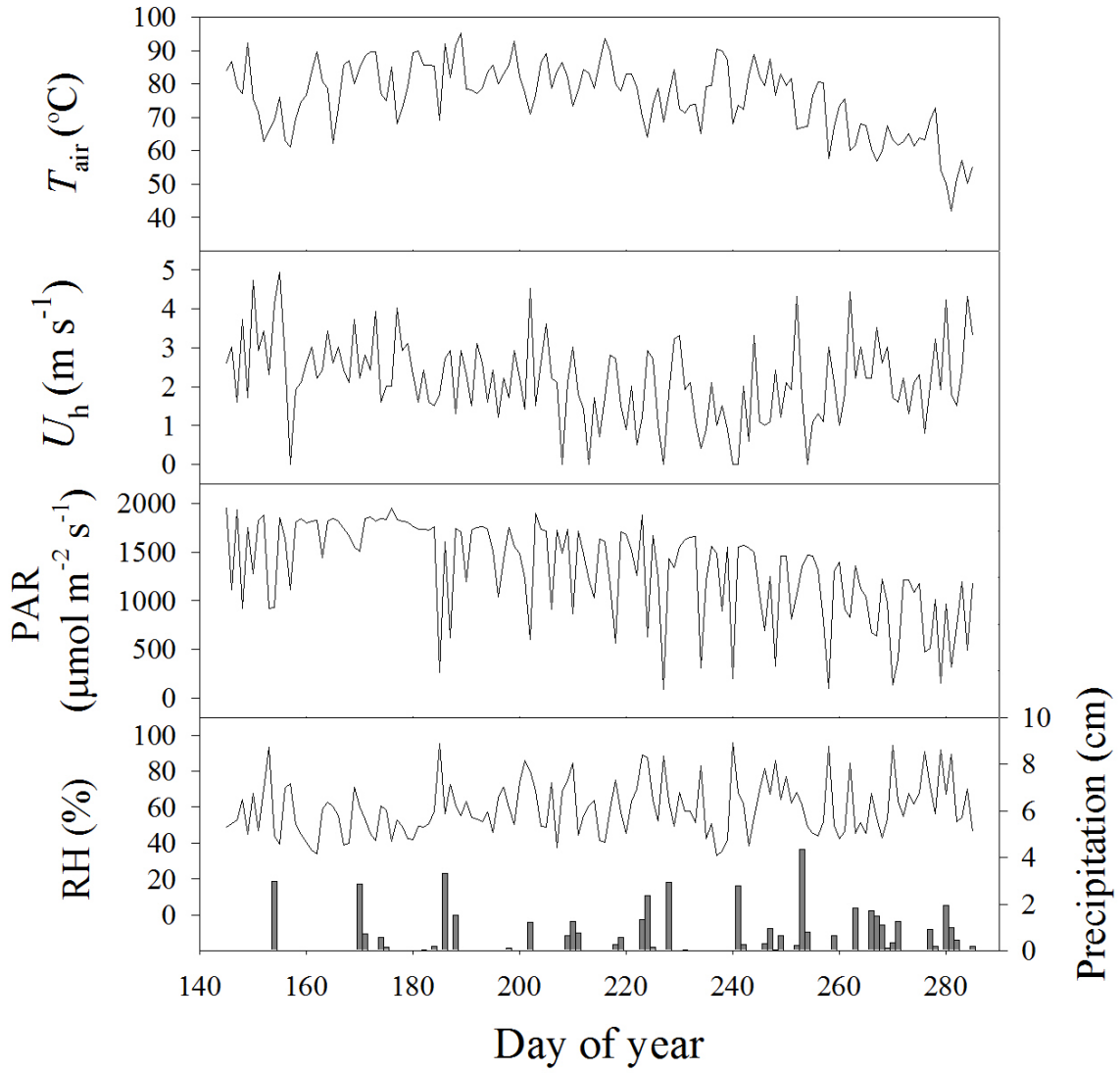

Figure 4.1: Daily meteorological measurements at the research site. Air temperature and wind speed at 3m (T_{air} and U_h respectively), photosynthetically active radiation (PAR), relative humidity (RH) and precipitation.

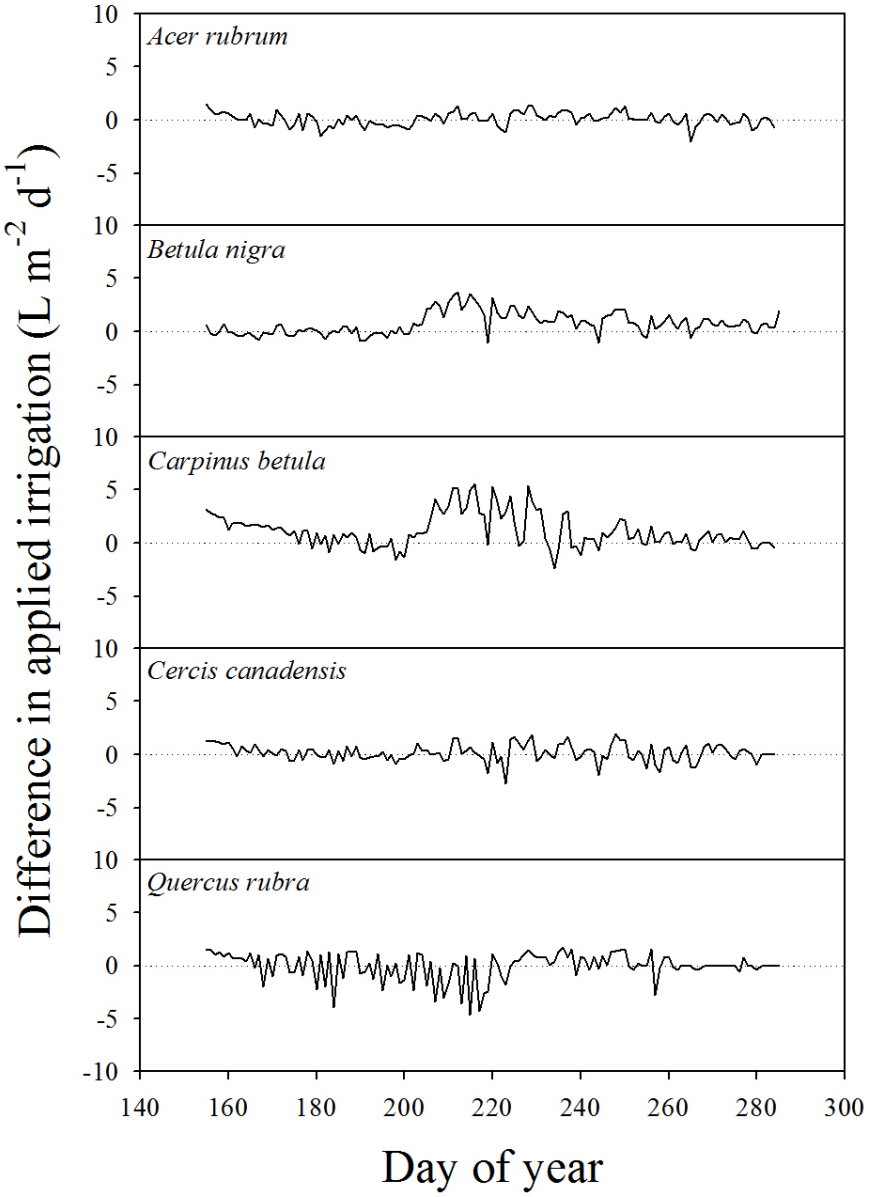

Figure 4.2: Daily difference in applied irrigation between predictive and sensing-based treatments. Positive values indicate higher predictive treatment versus sensor-based water application volumes and negative values indicate lower.

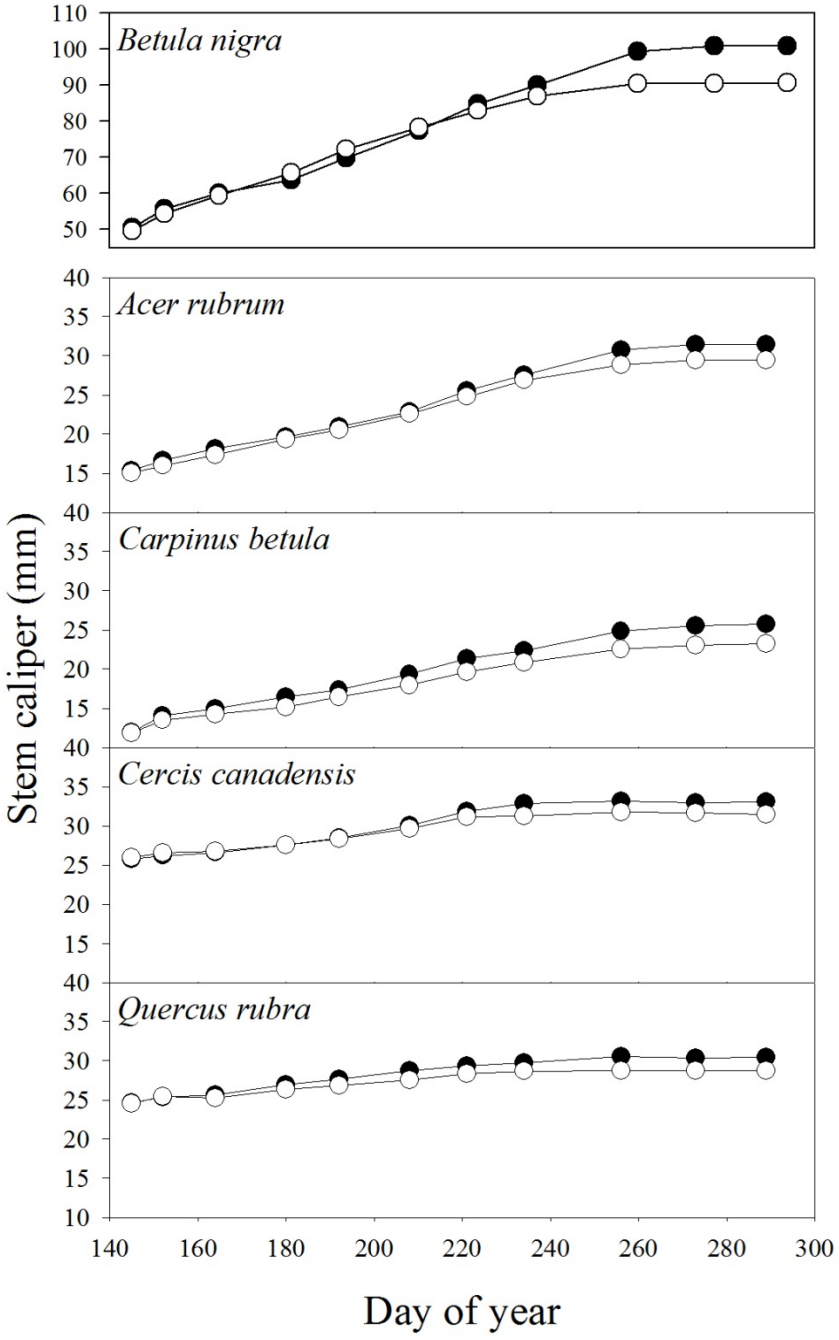

Figure 4.3: Seasonal accumulation of stem growth measured at 10 cm above the ground. The predictive treatment is represented by black circles and the sensing-based treatment by white circles. Note: *y*-axis scale differs for top panel (*Betula nigra*).

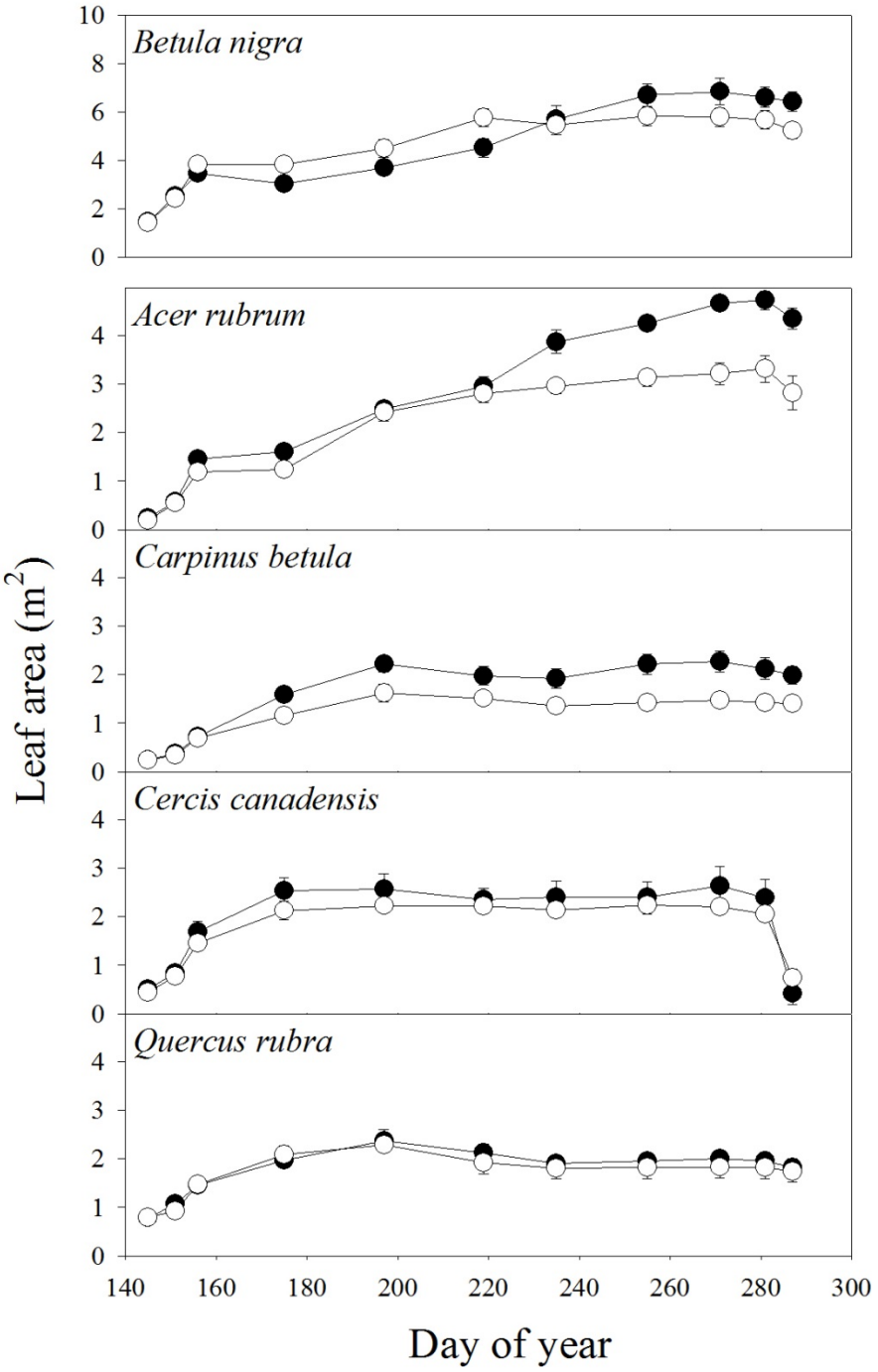

Figure 4.4: Seasonal development of canopy leaf area. The predictive treatment is represented by black circles and the sensing-based treatment by white circles. Note: *y*-axis scale differs for top panel (*Betula nigra*).

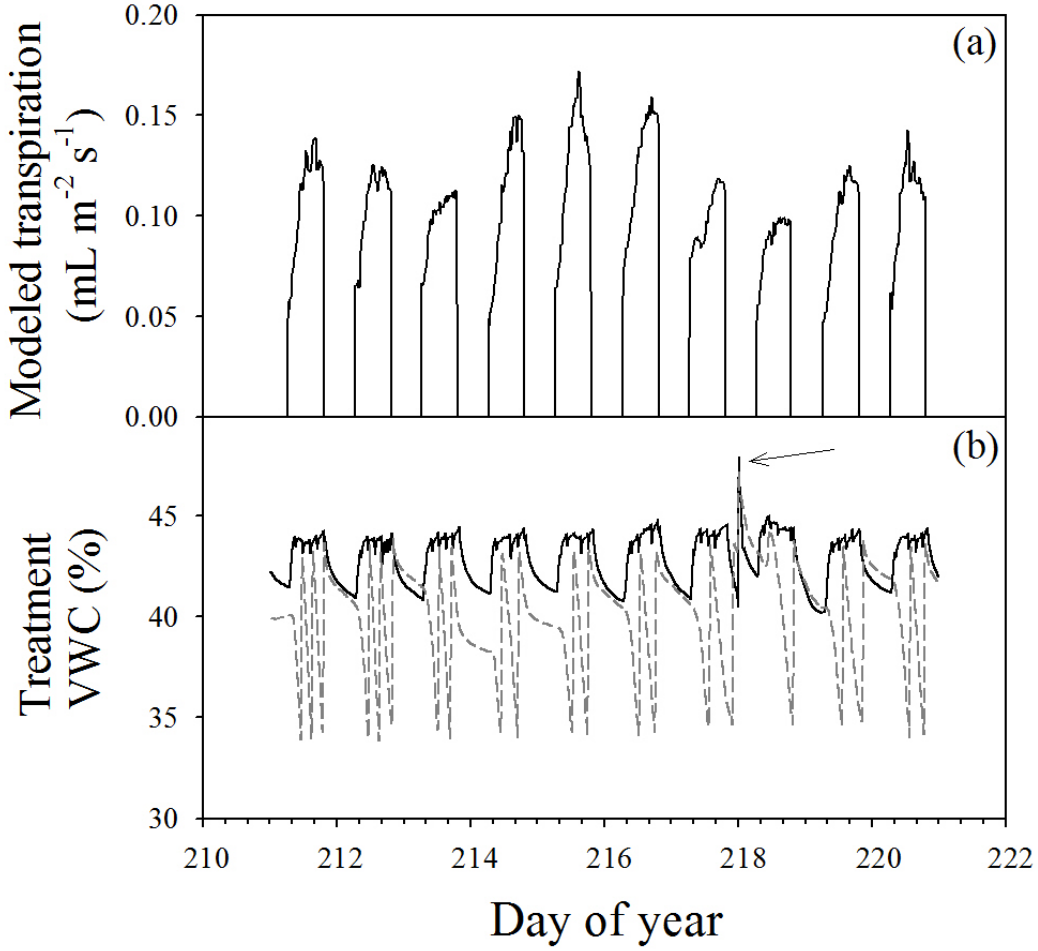

Figure 4.5: a) Ten consecutive days of transpiration estimates and b) variation in container substrate volumetric water content (VWC) in the predictive (solid black line) and sensing-based (dashed gray line) treatments for *Acer rubrum*. Arrow points to a precipitation even that occurred in the evening on day of year 217.

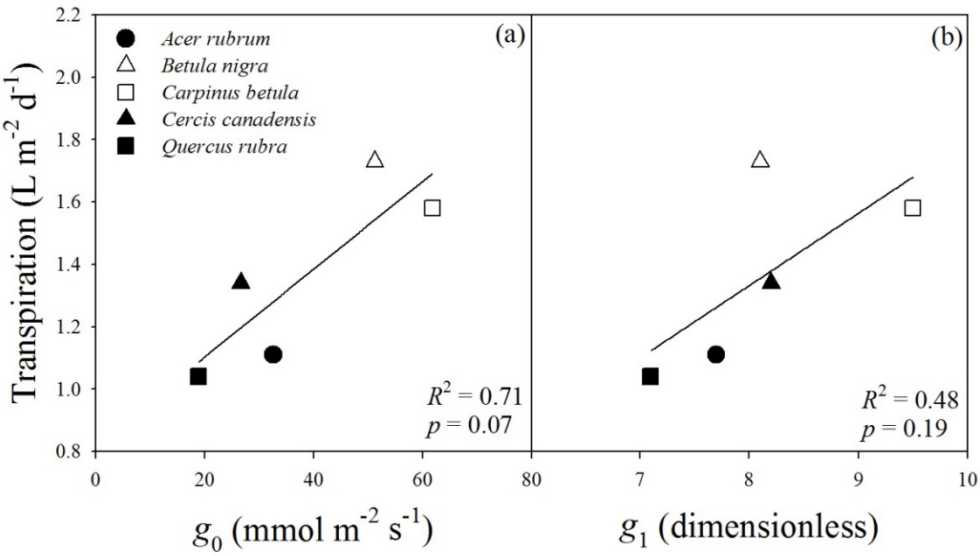

Figure 4.6: Measured transpiration linear correlation with two key input parameters of the Ball-Berry-Leuning g_s model, g_0 (panel (a) - minimum stomatal conductance) and g_1 (panel (b) - marginal water cost per unit of carbon gain).

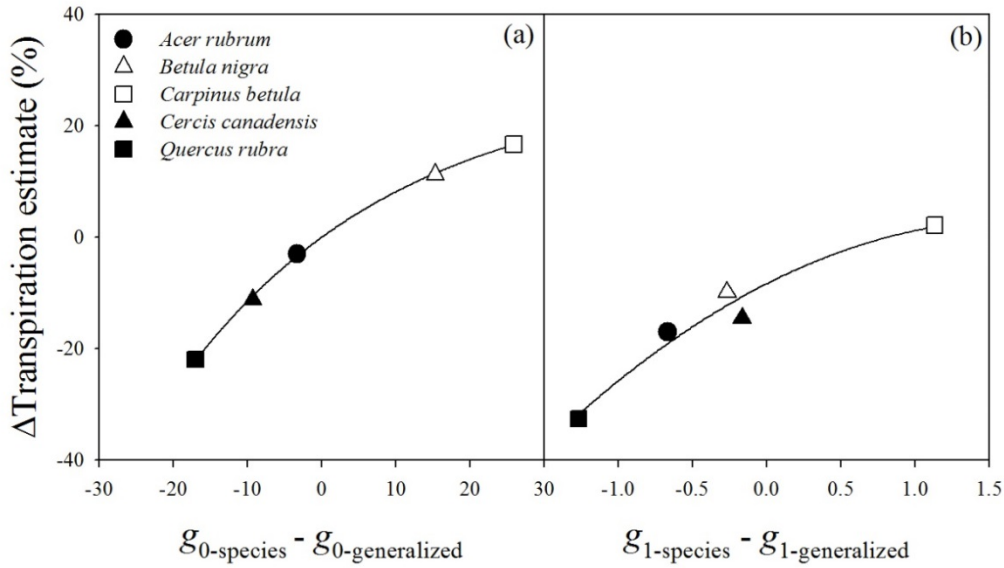

Figure 4.7: The percent influence of generalizing parameters with multi-species means substituted for species-specific values correlates with the difference between the species-specific parameter values and the generalized multi-species means for g_0 (panel (a) - minimum stomatal conductance when net photosynthesis < 0) and g_1 (panel (b) - marginal water cost per unit of carbon gain). X-axis indicates the difference between the species-specific value (e.g., $g_{0\text{-species}}$) and the generalized multi-species value (e.g., $g_{0\text{-generalized}}$)

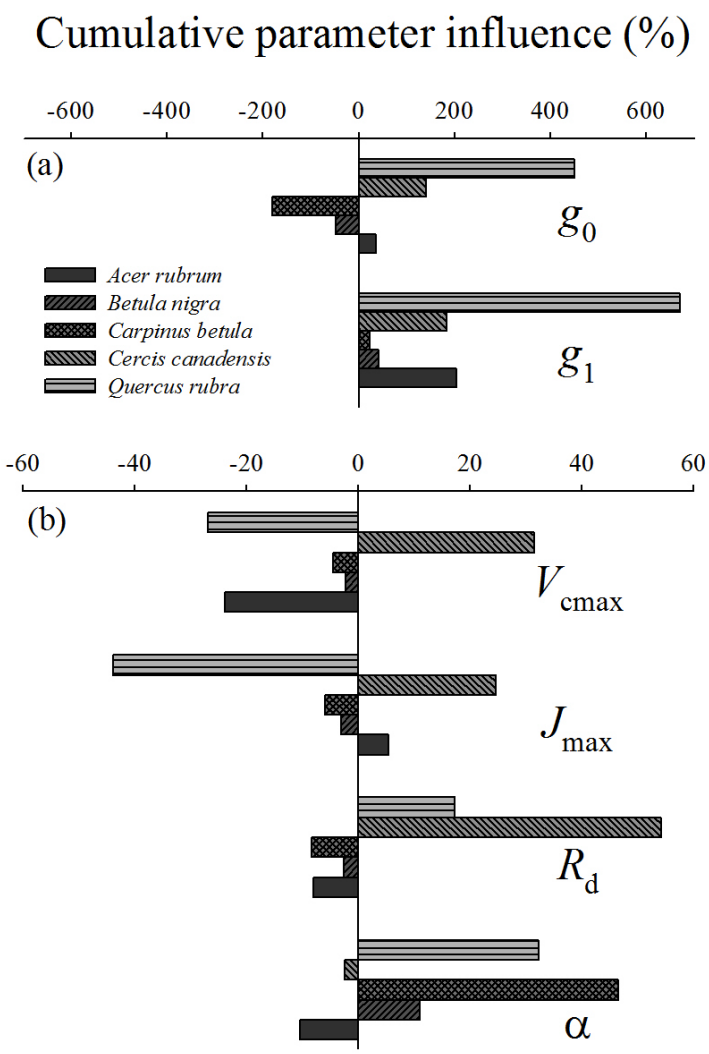

Figure 4.8: The seasonal cumulative influence of six key physiological parameters on seasonal transpiration estimates when replaced with multispecies means (cf. Table 4.1). Parameter abbreviations: g_0; the minimum stomatal conductance when $A_n \leq 0$, g_1; the marginal water cost per unit of carbon gain, V_{cmax}; the maximum rate of carboxylation, J_{max}; the maximum rate of electron transport, R_d; leaf dark respiration and α; the quantum efficiency of photosynthesis. Note, the scale between the panel (a) and panel (b) differ by over an order of magnitude.

References

Amato, M. and Ritchie, J.T., 2002. Spatial distribution of roots and water uptake of maize (L.) as affected by soil structure. Crop Science, 42(3): 773-780.

Andreu, L., Hopmans, J. and Schwankl, L., 1997. Spatial and temporal distribution of soil water balance for a drip-irrigated almond tree. Agricultural Water Management, 35(1): 123-146.

Bacci, L., Battista, P., Rapi, B., Sabatini, F. and Checcacci, E., 2003. Irrigation control of container crops by means of tensiometers, International Symposium on Managing Greenhouse Crops in Saline Environment 609, pp. 467-474.

Baldocchi, D. and Meyers, T., 1998. On using eco-physiological, micrometeorological and biogeochemical theory to evaluate carbon dioxide, water vapor and trace gas fluxes over vegetation: a perspective. Agricultural and Forest Meteorology, 90: 1-25.

Baldocchi, D.D., Wilson, K.B. and Gu, L., 2002. How the environment, canopy structure and canopy physiological functioning influence carbon, water and energy fluxes of a temperate broad-leaved deciduous forest—an assessment with the biophysical model CANOAK. Tree Physiology, 22(15-16): 1065-1077.

Ball, J., Woodrow, I. and Berry, J., 1987. A model predicting stomatal conductance and its contribution to the control of photosynthesis under different environmental conditions. In: J. Biggins (Editor), Progress in Photosynthesis Research. Martinus Niijhoff, Dordrecht, Netherlands, pp. 221-224.

Barnard, D. and Bauerle, W., 2013. The implications of minimum stomatal conductance on modeling water flux in forest canopies. Journal of Geophysical Research: Biogeosciences, 118(3): 1322-1333.

Bauerle, T.L., Bauerle, W.L., Goebel, M. and Barnard, D.M., 2013. Root system distribution influences substrate moisture measurements in containerized ornamental tree species. HortTechnology, 23(6): 754-759.

Bauerle, W.L. and Bowden, J.D., 2011. Separating foliar physiology from morphology reveals the relative roles of vertically structured transpiration factors within red maple crowns and limitations of larger scale models. Journal of Experimental Botany, 62(12): 4295-4307.

Bauerle, W.L., Bowden, J.D., McLeod, M.F. and Toler, J.E., 2004. Modeling intra-crown and intra-canopy interactions in red maple: assessment of light transfer on carbon dioxide and water vapor exchange. Tree Physiology, 24(5): 589-597.

Bauerle, W.L., Bowden, J.D., Wang, G.G. and Shahba, M.A., 2009. Exploring the importance of within-canopy spatial temperature variation on transpiration predictions. Journal of Experimental Botany, 60(13): 3665-3676.

Bauerle, W.L., Daniels, A.B. and Barnard, D.M., 2014. Carbon and water flux responses to physiology by environment interactions: a sensitivity analysis of variation in climate on photosynthetic and stomatal parameters. Climate Dynamics, 42: 2539-2554.

Bauerle, W.L. et al., 2012. Photoperiodic regulation of the seasonal pattern of photosynthetic capacity and the implications for carbon cycling. Proceedings of the National Academy of Sciences, 109(22): 8612-8617.

Bauerle, W.L., Post, C.J., McLeod, M.F., Dudley, J.B. and Toler, J.E., 2002. Measurement and modeling of the transpiration of a temperate red maple container nursery. Agricultural and Forest Meteorology, 114(1): 45-57.

Bauerle, W.L., Weston, D.J., Bowden, J.D., Dudley, J.B. and Toler, J.E., 2004b. Leaf absorptance of photosynthetically active radiation in relation to chlorophyll meter estimates among woody plant species. Scientia Horticulturae, 101(1): 169-178.

Bayer, A., Mahbub, I., Chappell, M., Ruter, J. and van Iersel, M.W., 2013. Water use and growth of *Hibiscus acetosella* 'Panama Red'grown with a soil moisture sensor-controlled irrigation system. HortScience, 48(8): 980-987.

Beeson, R. and Haydu, J., 1995. Cyclic microirrigation in container-grown landscape plants improves plant growth and water conservation. Journal of Environmental Horticulture, 13(1): 6-11.

Beeson, R. and Keller, K., 2003. Effect of cyclic irrigation on growth of magnolias produced using five in-ground systems. Journal of Environmental Horticulture, 21(3): 148-152.

Bowden, J.D. and Bauerle, W.L., 2008. Measuring and modeling the variation in species-specific transpiration in temperate deciduous hardwoods. Tree Physiology, 28(11): 1675-1683.

Caird, M.A., Richards, J.H. and Donovan, L.A., 2007. Nighttime stomatal conductance and transpiration in C_3 and C_4 plants. Plant Physiology, 143(1): 4-10.

Chappell, M., Dove, S.K., van Iersel, M.W., Thomas, P.A. and Ruter, J., 2013. Implementation of wireless sensor networks for irrigation control in three container nurseries. HortTechnology, 23(6): 747-753.

Dabach, S., Lazarovitch, N., Šimůnek, J. and Shani, U., 2013. Numerical investigation of irrigation scheduling based on soil water status. Irrigation Science, 31(1): 27-36.

Daniels, A.B., Barnard, D.M., Chapman, P.L. and Bauerle, W.L., 2012. Optimizing substrate moisture measurements in containerized nurseries. HortScience, 47(1): 98-104.

Farquhar, G.D., Caemmerer, S. and Berry, J., 1980. A biochemical model of photosynthetic CO_2 assimilation in leaves of C_3 species. Planta, 149(1): 78-90.

Gardner, W., 1964. Relation of root distribution to water uptake and availability. Agronomy Journal, 56(1): 41-45.

Hanson, P.J. et al., 2004. Oak forest carbon and water simulations: model intercomparisons and evaluations against independent data. Ecological Monographs, 74(3): 443-489.

Incrocci, L. et al., 2014. Substrate water status and evapotranspiration irrigation scheduling in heterogenous container nursery crops. Agricultural Water Management, 131: 30-40.

Jacobs, D.F. and Timmer, V.R., 2005. Fertilizer-induced changes in rhizosphere electrical conductivity: relation to forest tree seedling root system growth and function. New Forests, 30(2-3): 147-166.

Jarvis, P., 1976. The interpretation of the variations in leaf water potential and stomatal conductance found in canopies in the field. Philosophical Transactions of the Royal Society of London. B, Biological Sciences, 273(927): 593-610.

Jarvis, P.G. and McNaughton, K., 1986. Stomatal control of transpiration: scaling up from leaf to region. Advances in Ecological Research, 15(1): 49.

Jones, H. and Tardieu, F., 1998. Modelling water relations of horticultural crops: a review. Scientia Horticulturae, 74(1): 21-46.

Jones, H.G., 2004. Irrigation scheduling: advantages and pitfalls of plant-based methods. Journal of Experimental Botany, 55(407): 2427-2436.

Kim, H.-S., Oren, R. and Hinckley, T.M., 2008. Actual and potential transpiration and carbon assimilation in an irrigated poplar plantation. Tree physiology, 28(4): 559-577.

Landsberg, J.J. and Sands, P., 2010. Physiological Ecology of Forest Production: Principles, Processes and Models. Academic Press, San Diego, California.

Lea-Cox, J.D., 2012. Using wireless sensor networks for precision irrigation scheduling. Problems, perspectives and challenges of agricultural water management. InTech Press, Rijeka, Croatia: 233-258.

Leuning, R., 1990. Modelling stomatal behaviour and and photosynthesis of *Eucalyptus grandis*. Functional Plant Biology, 17(2): 159-175.

Leuning, R., 1995. A critical appraisal of a combined stomatal-photosynthesis model for C3 plants. Plant, Cell & Environment, 18(4): 339-355.

McCarthy, A.C., Hancock, N.H. and Raine, S.R., 2013. Advanced process control of irrigation: the current state and an analysis to aid future development. Irrigation Science, 31(3): 183-192.

Medlyn, B., 2004. A maestro retrospective. Forests at the Land–Atmosphere Interface. CAB International: 105-121.

Medlyn, B.E. et al., 2011. Reconciling the optimal and empirical approaches to modelling stomatal conductance. Global Change Biology, 17(6): 2134-2144.

Medlyn, B.E., Pepper, D.A., O'Grady, A.P. and Keith, H., 2007. Linking leaf and tree water use with an individual-based model. Tree Physiology, 27: 1687-1699.

Meinzer, F.C., 1993. Stomatal control of transpiration. Trends in Ecology & Evolution, 8(8): 289-294.

Monteith, J., 1965. Evaporation and environment, Symposium of the Society for Experimental Biology, pp. 4.

Moratiel, R. and Martínez-Cob, A., 2013. Evapotranspiration and crop coefficients of rice (*Oryza sativa* L.) under sprinkler irrigation in a semiarid climate determined by the surface renewal method. Irrigation Science, 31(3): 411-422.

Naasz, R., Michel, J.-C. and Charpentier, S., 2005. Measuring hysteretic hydraulic properties of peat and pine bark using a transient method. Soil science society of America Journal, 69(1): 13-22.

Ögren, E. and Evans, J., 1993. Photosynthetic light-response curves. Planta, 189(2): 182-190.

Oleson, K. et al., 2013. Technical description of version 4.5 of the Community Land Model (CLM), NCAR Technical Note NCAR/TN-503+STR, pp. 420.

Papadopoulos, A. and Pararajasingham, S., 1997. The influence of plant spacing on light interception and use in greenhouse tomato (*Lycopersicon esculentum* Mill.): A review. Scientia Horticulturae, 69(1): 1-29.

Reynolds, J.F. and Acock, B., 1985. Predicting the response of plants to increasing carbon dioxide: a critique of plant growth models. Ecological Modelling, 29(1): 107-129.

Romero, R., Muriel, J., García, I. and Muñoz de la Peña, D., 2012. Research on automatic irrigation control: State of the art and recent results. Agricultural Water Management, 114: 59-66.

Ruter, J.M., 1998. Pot-in-pot production and cyclic irrigation influence growth and irrigation efficiency of'Okame'cherries. Journal of Environmental Horticulture, 16: 159-162.

Sammons, J.D. and Struve, D.K., 2008. Monitoring effective container capacity: a method for reducing over-irrigation in container production systems. Journal of Environmental Horticulture, 26(1): 19.

Sammons, J.D. and Struve, D.K., 2010. The effects of near-zero leachate irrigation on growth and water wse efficiency and nutrient uptake of container grown baldcypress (*Taxodium distichum* (L.) Rich.) plants. Journal of Environmental Horticulture, 28(1): 27.

Sellers, P. et al., 1996. A revised land surface parameterization (SiB2) for atmospheric GCMs. Part I: Model formulation. Journal of Climate, 9(4): 676-705.

Sharkey, T.D., Bernacchi, C.J., Farquhar, G.D. and Singsaas, E.L., 2007. Fitting photosynthetic carbon dioxide response curves for C3 leaves. Plant, Cell & Environment, 30(9): 1035-1040.

Stanley, J., 2013. Using Leaching Fractions to Maximize Irrigation Efficiency. Proceedings of the International Plant Propagators' Society, 1014: 331-334.

Vörösmarty, C.J., Green, P., Salisbury, J. and Lammers, R.B., 2000. Global water resources: vulnerability from climate change and population growth. Science, 289(5477): 284-288.

Wang, Y. and Jarvis, P., 1990a. Description and validation of an array model—MAESTRO. Agricultural and Forest Meteorology, 51(3): 257-280.

Wang, Y. and Jarvis, P., 1990b. Influence of crown structural properties on PAR absorption, photosynthesis, and transpiration in Sitka spruce: application of a model (MAESTRO). Tree Physiology, 7: 297-316.

Xu, L. and Baldocchi, D.D., 2003. Seasonal trends in photosynthetic parameters and stomatal conductance of blue oak (*Quercus douglasii*) under prolonged summer drought and high temperature. Tree Physiology, 23(13): 865-877.

Yeager, T. et al., 1997. Best management practices guide for producing container-grown plants. Southern Nursery Association. Atlanta, GA.

Yuan, H. et al., 2014. A 3D Canopy Radiative Transfer Model for Global Climate Modeling: Description, Validation, and Application. Journal of Climate, 27(3).

Zhu, H. et al., 2005. A new system to monitor water and nutrient use in pot-in-pot nursery production systems. Journal of Environmental Horticulture, 23(1): 47-53.

Chapter 5: Conclusions

Modeling provides a representation of vegetation biophysical processes that are otherwise difficult to measure directly with equipment. However, it is essential that these processes be accurately represented in modeling frameworks in order to accurately depict interactions between physiology and environment. Hence, the purpose of this dissertation was to improve upon the robust modeling framework of MAESTRA by expanding the understanding of individual parameters, how they interact with the environment, how the model reacts to environmental change, and to ultimately test the predictive ability of the model by applying it in a real-time irrigation system for container grown trees.

The second chapter of this dissertation investigated the role of g_0 and its sizeable influence on transpiration estimates over a range of environmental conditions. Typically, g_0 has received little attention and is often assumed as an unrealistically low value or characterized by statistical extrapolation. Instead, I found that g_0 is not well characterized by extrapolation in trees and that using the same values assumed in large scale modeling efforts (e.g., Sellers et al., 1996; Oleson et al., 2013) would result in gross underestimation of transpiration. I found that the g_0 parameter can be well characterized with a hand-held porometer by measuring leaf g_s 1 h after sunset, providing a simple method to observe the response of g_0 to season, drought or other stimuli. Thus, the main implications of this chapter are (1) that g_0 is a parameter with physiological significance and can be measured directly - circumventing potential errors obtained by using statistical extrapolations or assumed values and (2) that the lack of drought or seasonal response of g_0 in broadleaf trees indicates that temporal or drought response functions are not needed for this parameter. Given the significant influence of g_0 in modeling transpiration,

coupled with the ease of obtaining field estimates, future studies and modeling efforts would be greatly improved by an increased focus on characterizing this parameter more accurately.

The species and seasonal variation in α and its subsequent influence on g_{bV}, Ω, and transpiration were the focus of the third chapter. Contrary to previous studies, I found α to be dynamic in response to U_{3m} and canopy development stage (i.e. *LAI*). These findings are important because α is typically assumed to be environmentally static and a single value is often used to represent a vegetation type regardless of growth stage (e.g., Cionco, 1966; Kim et al., 2014). In conjunction with canopy development and subsequent changes to α, L_w also increased in the early season, resulting in seasonal variation in g_{bV} and Ω. Similar to α, Ω is often assumed to be static for the representation of vegetation-type coupling to the atmosphere. I found that canopy development led to substantial shifts in Ω and in one species (*B. nigra*) increasing to ~0.6 (i.e. roughly the point at which physiological control of transpiration becomes secondary). These findings underscore the importance of characterizing seasonal development of canopy structure and aerodynamics when modeling transpiration.

There has been disagreement among studies that quantified the response of transpiration to increases in wind speed (see: Kim et al., 2014). However, it was common among these studies to isolate the influence of wind speed by removing variation in other environmental parameters, perhaps occluding true biophysical responses at the leaf level. I tested the influence of a discrete increase in wind speed over 1000 random combinations of environmental parameters (PAR, VPD and T_{air}) and found ΔE_{wind} to vary predictably with VPD but less so with T_{air} or PAR. This theoretical exercise has significant implications at a variety of scales by assigning VPD as a cofactor in determining the influence of wind speed on transpiration - a connection which had not been previously identified.

The fourth chapter of my dissertation presented the results of a comparison between a substrate moisture and predictive technique (i.e. MAESTRA) for scheduling irrigation in container grown trees. This is the first study of its type to use a complex model to schedule irrigation. I found that MAESTRA-controlled irrigation produced greater tree growth by determining plant water needs more accurately than the moisture sensing technique. As agricultural water resources decline, these findings will have industry implications for improving irrigation scheduling as growers struggle to improve crop growth efficiency. I also found that, despite the complexity of MAESTRA, a close focus on two key parameters (g_0 and g_1) can yield accurate transpiration estimates while minimizing the need for the measurement of extraneous parameters. Hence, other transpiration model parameters for MAESTRA may be simplified with default values, increasing the ease of MAESTRA application in research and commercial settings.

References

Cionco, R.M., 1966. A mathematical model for air flow in a vegetative canopy, DTIC Document.

Kim, D. et al., 2014. Sensitivity of stand transpiration to wind velocity in a mixed broadleaved deciduous forest. Agricultural and Forest Meteorology, 187: 62-71.

Oleson, K. et al., 2013. Technical description of version 4.5 of the Community Land Model (CLM), NCAR Technical Note NCAR/TN-503+STR, pp. 420.

Sellers, P. et al., 1996. A revised land surface parameterization (SiB2) for atmospheric GCMs. Part I: Model formulation. Journal of Climate, 9(4): 676-705.